QUADRUPOLE ION TRAP MASS SPECTROMETRY OF PEPTIDES

Thesis by

Karen R. Jonscher

In Partial Fulfillment of the Requirements

for the Degree of

Doctor of Philosophy

California Institute of Technology

Pasadena, California

1997

(Submitted September 30, 1996)

To Peter, Spencer, and Raleigh and in loving memory of my grandmother, Sally Fried.

Acknowledgments

I feel grateful that my mentors, Dr. Lee Hood and Dr. John Yates, provided me with a supportive atmosphere throughout my graduate career. I have been fortunate to have 2.8 children and continue my graduate work. Dr. Hood's vision and enthusiasm excited my imagination and sparked my interest in molecular biology. Dr. John Yates provided insightful comments and helpful discussions. He has made the last few years challenging and stimulating and as a result, I have developed a keen interest in the field of biological mass spectrometry.

I have had a great deal of help from a number of people over the past several years. Dr. Jae Schwartz built the ion trap mass spectrometer that was used for most of the work presented in this dissertation. His technical expertise was much appreciated. Jon DeGnore and Richard Yost from the University of Florida provided the wonderful ion trap renderings found in Chapters One and Two. These can be accessed on their web page at http://analytic15.chem.ufl.edu/anim1.html. Sendai virus P Protein samples were graciously provided by Dr. K.C. Gupta at Rush Presbyterian St. Luke's Medical Center, Chicago, IL. Bill Loyd gave unstintingly of his technical expertise and his friendship. The guys in the machine shop: Tom, Eric, Brian, Doug, and Norm were incredibly helpful with designs and often manufactured things for me while I waited. The people in our lab provided helpful discussions in addition to their friendship. Thank you to Dave, Andy, Lara, Edwin, Ashok and Tina. A special word of thanks to Dr. Ashley McCormack who shared her mass spectrometry experience and friendship. In addition, she was an excellent editor.

Finally, I would like to thank my family. My parents and in-laws have been rooting for me throughout. My husband, Peter, should be nominated for sainthood. My children Spencer (age 4), Raleigh (age 2) and ??? (due 11/11/96) have made it all worthwhile. Their unconditional love has helped me to believe in myself.

Abstract

Biological mass spectrometry addresses the challenging unsolved structural issues surrounding biopolymers of fundamental importance to the biomedical sciences. Key to this discipline is the ability to extract useful information from complex peptide mixtures. Several approaches were developed to analyze peptides utilizing the unique capabilities of the quadrupole ion trap mass spectrometer. An external matrix-assisted laser desorption ionization source was constructed. Detection of peptides in the mid-femtomole range and of proteins in the low-femtomole range was reported. Singly-charged molecules with molecular weights in excess of 34,000 u were observed. Peptides generated by enzymatic digestion of the P protein of Sendai virus were separated by HPLC and the technique was successfully applied to locate phosphorylation sites.

A hybrid quadrupole mass filter/quadrupole ion trap mass spectrometer was assembled. Peptide mixtures were separated by sequentially transmitting one value of *m/z* into the ion trap for mass analysis. The sequential injection technique served to significantly reduce space charge-induced suppression effects and improved resolution and fragmentation efficiency when compared to results obtained using an ion trap. A novel method of scanning afforded the ability to perform neutral loss experiments for the identification of phosphopeptides in a mixture. A long duty cycle, due to acquisition hardware, limited the utility of this approach for continuous ionization techniques.

A low flowrate ionization source was constructed and interfaced to the hybrid and to an ion trap. A unique needle configuration provided a detection limit of 75 attomole of a peptide mixture infused into the source. A new type of liquid junction was developed to

apply voltage to the sample consisting of a platinum wire inserted into the sidewall of a length of Teflon tubing. The junction was versatile, robust, and easy to use and performance compared well with other types of junctions. Capillary electrophoresis and hydrophobic membranes were used to separate peptide mixtures. Detection limits of the techniques were 1 femtomole and 10 femtomoles, respectively, for angiotensin. Differential release of peptides using step elutions from the hydrophobic membrane was demonstrated, providing a sensitive, high throughput means of mixture simplification prior to separation by capillary electrophoresis.

Table of Contents

List of Tables and Schemes

List of Figures

Chapter 1

Introduction

1.1 Thesis Overview

The work presented in this dissertation involves the development of a number of independent methods to analyze biological molecules by ion trap mass spectrometry. Chapter One (below) historically presents the development of ion trap technology from a reactor used to trap isolated ions to a versatile mass spectrometer capable of sophisticated analysis of many different types of molecules. The particular advantages of mass spectrometry as a means of protein sequencing are discussed and the different ionization modes appropriate for biomolecular analysis are delineated. Strategies for protein sequencing by ion trap mass spectrometry (1) are addressed.

Chapter Two provides a practical description of the theoretical considerations involved in ion trap operation and serves to illustrate the versatility of the instrument and how it may be employed. Chapter Three addresses the development of a matrix-assisted laser desorption ionization source and its use for the determination of phosphorylation sites on the P protein of Sendai virus. A hybrid instrument composed of a quadrupole mass filter and the quadrupole ion trap was assembled and applied to the analysis of simple mixtures of peptides. Results are presented in Chapter Four. Membrane chromatography techniques at high sensitivity were investigated in Chapter Five for the analysis of mixtures

of peptides using the ion trap. A summary of results and future prospects are given in Chapter Six.

1.2 Role of Mass Spectrometry in Biological Research

Mass spectrometry is developing into an essential technique for biochemical and biological research. The range of problems that mass spectrometry is currently being applied to includes the analysis of post-translational modifications of proteins (2); non-covalent protein-protein, protein-DNA, and protein-RNA interactions (3-6); study of peptides implicated in the functioning of the immune system (7-9); and the study of proteins involved in signal transduction pathways (10-12). The study of these processes by mass spectrometry is significantly facilitated by information produced from genomic sequence analysis. Model organisms are used in the study of prokaryotic and eukaryotic cell biology, cell differentiation, and developmental biology. The information derived from genome sequences of these organisms will aid in identifying the function, structure, and regulation of the gene products. Identification of the functional elements involved in a biological process will entail correlating the sequence of proteins observed in a process to genomic sequence information contained in databases. Post-translational modifications, especially phosphorylation, serve to regulate pathways in cell processes. Mass spectrometry is well-suited for the identification of gene products and covalent modifications.

A sensitive and versatile analytical system, capable of detecting both large and small molecules and determining aspects of molecular structure, is required to address the

complex mixtures of molecules found in these types of biological problems. Developments over the last ten years have made the quadrupole ion trap mass spectrometer an excellent tool for biomolecular analysis. A quadrupole ion trap is an instrument roughly the size of a tennis ball whose size is inversely proportional to its versatility. Three hyperbolic electrodes, consisting of a ring and two endcaps, form the core of this instrument (Figure 1.1). Using theory to drive instrument development, the nominal mass range of the instrument has been extended from *m/z* 650 to *m/z* 70,000 (13); up to 12 stages of tandem mass spectrometry (MS^{12}) have been performed (14); and mass resolution that can allow the separation of ions of *m/z* 10^6 and *m/z* $10^6 + 1$ has been implemented (15). Quadrupole ion trap mass spectrometers are also exquisitely sensitive. Molecular weight information has been recorded with as few as 1.5 million peptide molecules (16). Although not all of these features can be applied simultaneously, a judicious choice of parameters can afford sensitive molecular weight measurements and structural analyses of biopolymers.

1.3 History of the Development of Ion Traps

In the early 1950's, Wolfgang Paul and co-workers invented two instruments that could be used to determine mass-to-charge (*m/z*) ratios of ions (17, 18). The first was the quadrupole mass filter that rapidly was applied to a wide range of analytical problems (19). The second was the quadrupole ion trap, consisting of a ring electrode and two endcap electrodes with hyperbolic surfaces. As is shown in Table 1.1 (20), the quadrupole ion trap was primarily used by the physics community, notably Hans Dehmelt at the University of

Figure 1.1 Rendering of the ion trap electrode assembly showing the two endcaps and the ring electrode.

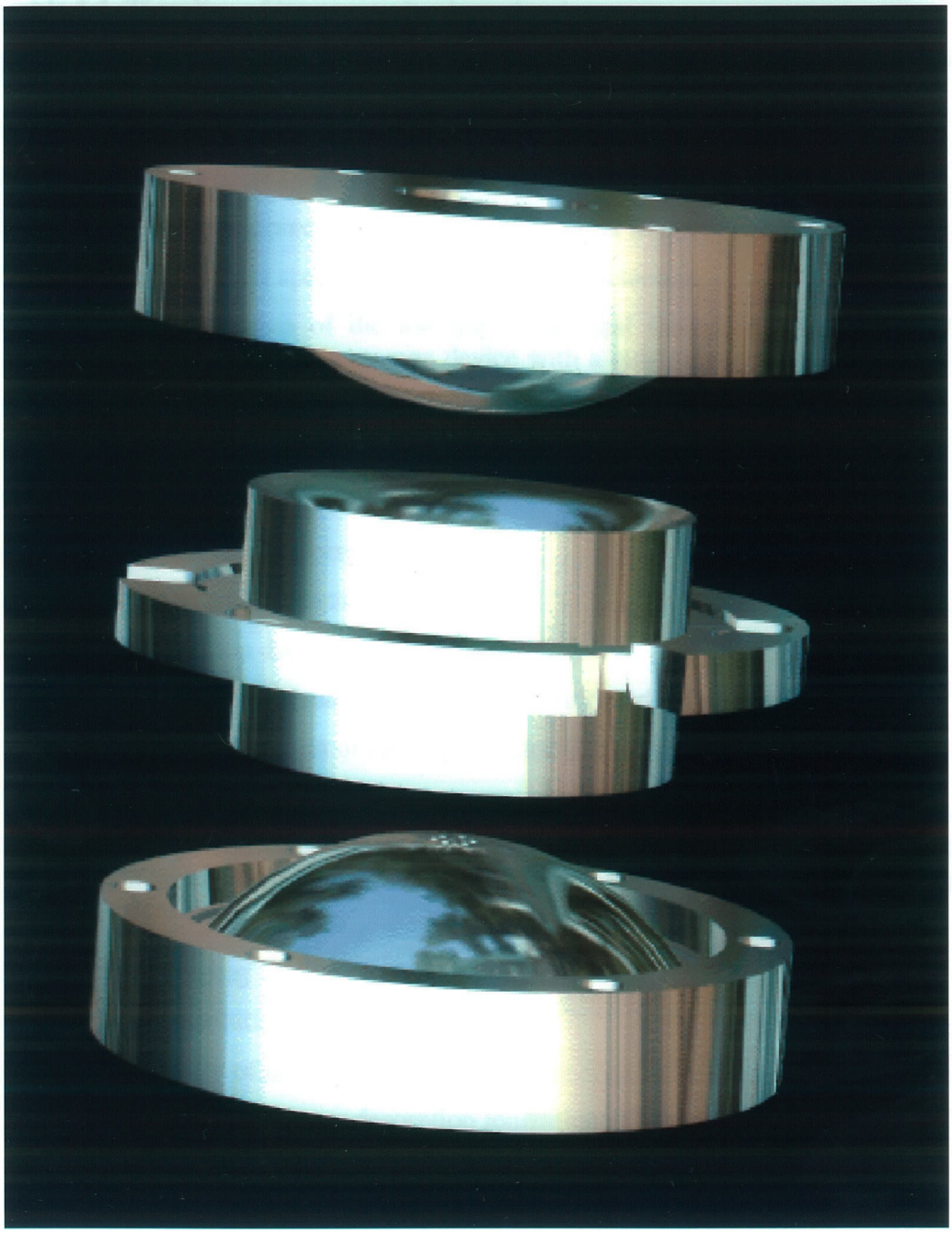

Table 1.1 Time line of ion trap technology development.

1953	Invention of quadrupole mass filter and quadrupole ion trap by Paul.
1959	Storage of single microparticles.
1959	Use as a mass spectrometer. Detection by power absorbance.
1962	Single ions stored at low temperatures to set frequency standards.
1968	Use as a mass spectrometer with external detection.
1972	Characterization of the ion trap: chemical ionization, study of ion/molecule kinetics. Used as a storage device with a quadrupole mass filter employed for mass analysis.
1976	Ions collisionally focused.
1978	Used as a selective ion reactor.
1979	Ions resonantly ejected.
1980	Used as a GC detector.
1982	Multiphoton dissociation of ions.
1983	Development of mass-selective instability mode of operation.
1984	Commercialization of ion trap detector (ITD™).
1985	Commercialization of ion trap mass spectrometer (ITMS™).
1987	High performance mass spectrometry: multiple stages of mass spectrometry, chemical ionization, photodissociation, external ion injection, mass range extension.
1990	Electrospray ionization of biopolymers.
1991	High resolution.
1991	Discovery of non-linear effects.
1992	Matrix-assisted laser desorption ionization of biopolymers.
1993	Biological problem-solving using ion trap mass spectrometry.

Washington, to investigate the properties of isolated ions (21-24). The ion trap was operated at that time in a "mass-selective stability" mode of operation. In this mode, analogous to the operation of a quadrupole mass filter, rf and dc voltages applied to the ring electrode were ramped to allow stability, hence storage, of a single (increasing) value of *m/z* in the ion trap (20). Ions were detected by resonance absorption from an external power source (25) or were ejected using a dc pulse applied to an endcap and detected using an electron multiplier (26). Due to limited mass range and resolution, these methods of mass measurement were not practical for many analytical purposes.

The chemistry community's interest in the trap was confined to several research groups until 1983 when George Stafford and co-workers at Finnigan MAT made two major advances. First, they developed the mass-selective instability mode of operation (27). The fundamental difference between this mode of operation and previous methods is that all ions created over a given time period were trapped and then sequentially ejected from the ion trap into a conventional electron multiplier detector. Thus, all ions were stored while mass analysis was performed, unlike the mass-selective stability mode of operation that had been previously employed. This new method for operating the ion trap simplified the use of the instrument. Stafford's group next discovered that a helium damping gas of ~ 1 mtorr within the trapping volume greatly improved the mass resolution of the instrument (28). Both of these discoveries led to the successful development of a commercial ion trap mass spectrometer. In later work, the addition of helium was observed to significantly improve trapping efficiencies, especially for externally injected ions (29). Subsequent innovations have been rapid. Cooks and co-workers at Purdue University have pioneered high performance techniques such as external injection of ions (29), mass range extension

(13), MS^n (14), and high resolution (15) that improved the performance of the ion trap and created interest in its application to biological molecules.

1.4 Strategies for Protein Sequencing by Tandem Mass Spectrometry

Proteins form a class of molecule that function in a key role in nearly all biological processes. The broad range of protein interactions is due to their enormous structural variability. Proteins are heteropolymers composed of at least 20 amino acids. The sequential arrangement of the amino acids determines the protein structure and function; consequently, knowledge of the amino acid sequence is the first step toward an understanding of protein function at the molecular level.

1.4.1 Classical Microsequencing Techniques

Historically, protein sequencing has been accomplished by chemical or enzymatic cleavage of a protein followed by separation and purification of the resulting peptides. Amino-terminal sequencing of the purified peptides is performed using variations of the method described by Edman and Begg (30) in which a series of chemical reactions are used to cleave the N-terminal amino acid from the peptide and identify it by retention time on a reverse phase HPLC column. The process is sequentially repeated on the shortened peptide. Background levels and repetitive yields limit the sensitivity of this technique to the high fmol to low pmol regime (31). The throughput of the technique is also rather slow, with cycle times of ~ 15 min. The most significant limitation of the Edman technique, however, is the inability to identify or sequence through post-translational modifications.

For instance, modifications such as phosphorylation are crucial regulators of signal transduction pathways (32) and it is of great interest to identify these sites of modification.

1.4.2 Protein Sequencing By Tandem Mass Spectrometry

Since proteins are heteropolymers of distinct masses (Table 1.2), mass spectrometry is a logical tool for primary structure analysis. Molecules of biological origin are typically highly polar and thermally labile, thus were not compatible with conventional ionization techniques such as electron impact (EI) and chemical ionization (CI). Three new ionization techniques developed in the 1980's were employed to effectively ionize biological molecules and, when interfaced with mass spectrometry, revolutionized the analysis of biomolecules.

1.4.3 Ionization Techniques for Biomolecules

1.4.3.1 Ionization By Atom/Ion Bombardment

In fast atom or ion bombardment (33), termed liquid secondary ion mass spectrometry (LSIMS), the sample is dissolved in a viscous liquid matrix such as monothioglycerol then bombarded with a 6-8 keV beam of atoms or ions. Peptide ions residing on the surface of the matrix are sputtered into the gas phase. Diffusion of molecules from the bulk solution serves to replenish the surface and ensure a steady current of sample ions. LSIMS mass spectra are characterized by the presence of an abundant $(M+H)^+$ ion and a low abundance of fragment ions. The spectra also contain a

Table 1.2 Abbreviations and incremental masses for the 20 commonly occurring amino acids. Mass is included for phosphorylation of serine.

Amino Acid and Abbreviation	One Letter Code	Incremental Mass[a]
Glycine - Gly	G	57.05
Alanine - Ala	A	71.08
Serine - Ser	S	87.08
Phosphoserine - Psr	S	167.06
Proline - Pro	P	97.11
Valine - Val	V	99.13
Threonine - Thr	T	101.10
Cystine - Cys	C	103.14
Leucine - Leu	L	113.16
Isoleucine - Ile	I	113.16
Asparagine - Asn	N	114.10
Aspartic Acid - Asp	D	115.09
Glutamine - Gln	Q	128.13
Lysine - Lys	K	128.17
Glutamic Acid - Glu	E	129.11
Methionine - Met	M	131.19
Histidine - His	H	137.14
Phenylalanine - Phe	F	147.18
Arginine - Arg	R	156.18
Tyrosine - Tyr	Y	163.18
Tryptophan - Trp	W	186.21

[a] corresponds to the formula -NHCHRCO- where R indicates the side chain characteristic of the particular amino acid.

relatively high background of ions derived from the matrix and sample ions that suffer radiation damage from prolonged exposure to the projectile beam (1). The technique is useful for analyzing a collection of peptides present in mixtures and has been used to characterize the molecular weights of peptides generated in tryptic mapping experiments. A limitation of the method is that signal from hydrophilic peptides is much less abundant than signal from hydrophobic peptides due to the presence of an excess of the latter on the surface of the matrix.

1.4.3.2 Matrix-Assisted Laser Desorption Ionization

In matrix-assisted laser desorption ionization (MALDI) (34, 35), the sample is dissolved in an excess (~10^6:1 of matrix:sample) of an acidic liquid matrix and air dried. The matrix and sample co-crystallize. Some common matrices used are 2,5-dihydroxybenzoic acid, α-cyano-4-hydroxycinnamic acid, or sinapinic acid (36-39). Typically, laser light from the frequency quadrupled ouput of a Nd:YAG laser at 266 nm or the output of a nitrogen laser at 337 nm is directed onto the crystals. The benzene ring of the matrix strongly absorbs the photons and desorbs into the gas phase, carrying the sample off the probe. Proton transfer is thought to occur within the ion plume, although the mechanism for this is not well understood. Ionized matrix and sample are directed into the mass spectrometer. MALDI mass spectra are characterized by the presence of an abundant $(M+H)^+$ ion and a low abundance of fragment ions depending upon the matrix used. The spectra also contain a relatively high background of ions derived from the matrix. The technique is useful for analyzing a collection of peptides present in mixtures and has been used to characterize the molecular weights of peptides generated in tryptic

mapping experiments. Signal suppression is more limited than that encountered when utilizing LSIMS techniques; thus MALDI is in more general use as a method for analyzing mixtures of peptides. In addition, MALDI is capable of ionizing very large proteins (~1 MDa) (40, 41) and has been employed for the analysis of oligonucleotides (42) and proteins (43-46) as well as for the analysis of peptide mixtures.

1.4.3.3 Electrospray Ionization

In electrospray ionization (47, 48), the sample is diluted in an acidic liquid matrix, typically 0.5% acetic acid or 0.1% trifluoroacetic acid. Methanol is added to the mixture and the resultant solution is directed into a needle. The needle is placed at a high potential (1-5 kV) and is brought close to a capillary (often heated) that is held near ground. Strong electrical fields near the tip of the needle induce droplet formation by electrohydrodynamic shearing of the charged liquid. The droplets begin to desolvate. When the force due to the surface charge density is sufficient to overcome the surface tension forces, the droplets "explode" into a number of smaller droplets. At the final stage, ions desorb from the droplets into the gas phase (49, 50). Electrospray ionization mass spectra typically contain a distribution of multiply-charged species. Often the singly-charged ion is not observed, thus MS/MS of peptides is typically accomplished on the doubly- or triply-charged ion. Signals from matrix are very low in abundance; thus the mass spectra have improved signal-to-noise ratios when compared with LSIMS and MALDI. The primary advantage of the ESI technique is that it can be easily interfaced to conventional peptide separation devices such as reverse-phase high performance liquid chromatography (HPLC) (51) or capillary electrophoresis (CE) (52, 53) that afford the separation of peptide mixtures.

Separation with subsequent analysis by mass spectrometry can be performed "on-line," reducing sample handling losses.

1.4.4 Sample Preparation

Proteins are subjected to chemical or enzymatic digestion to produce a mixture of peptides. The mixture is then fractionated by HPLC. This separation technique resolves peptides according to their hydrophobicity as well as their size. If LSIMS or MALDI are employed as the ionization technique, the presence of peptides in the eluent from the HPLC is monitored by ultraviolet (UV) absorbance and fractions corresponding to peaks in the UV chromatogram are collected for further analysis. If ESI is employed, the eluent is directed through a fused silica capillary into the electrospray needle and the separated peptide mixture is subsequently mass analyzed.

1.4.5 Fragmentation of Peptides in Low Energy CID Processes

To determine the amino acid sequence of a peptide, the molecular weight is recorded, then a fragmentation mass spectrum is collected. Peptide ions are trapped then a population of ions with a given *m/z* value is selected and resonantly excited. The ions undergo tens of thousands of collisions with neutral helium atoms within the trapping volume and become vibrationally excited. Fragmentation subsequently occurs primarily at the amide bonds, producing a ladder of sequence ions (1). The resulting charged fragments are mass analyzed to produce a mass spectrum characteristic of the original peptide structure. Knowledge of the fragmentation patterns of peptides under low energy

collision conditions allows the amino acid sequence to be reconstructed from the fragmentation mass spectrum (1).

Four major types of fragment ions are produced in the collision process. A summary of these pathways is shown in Scheme I (1). If the amount of kinetic energy converted to vibrational energy is high, cleavage of a single bond typically results and acylium ions of type "b" are produced (Pathway (**1**)). If the energy transferred is low, simultaneous bond formation and bond cleavage is favored and ions of type "y" result (Pathway (**2**)). Cleavage of at least two bonds internal to the peptide chain can also occur giving rise to ions with the general formula $NH_2{=}CHR^+$ or NH_2CHRCO^+ and are designated as type "a" (Pathway (**3**)). Ions of this type often dominate the low mass end of the spectrum. Not all amino acid residues in a peptide afford this type of fragment ion. Finally, multipoint cleavage of the peptide can produce ions with the same formula as type b ions, shown in Pathway (**4**). These ions are designated as "$b_n y_m$" where b_n and y_m indicate the points of cleavage to produce the carboxyl and amino termini of the fragment. Proline-containing peptides generate ions of this type with a higher frequency than other amino acid residues (1). Internal cleavage products can also be generated by arginine and histidine containing peptides. The major fragment ions likely to be produced in the collision activation process can be predicted for a known amino acid sequence.

1.4.6 Data Interpretation

Interpretation of peptide collision activated dissociation mass spectra is based on the above mechanistic considerations and is outlined in detail in a review by Yates *et al.* (54). When electrospray ionization is employed, peptides are generally created by trypsin

Scheme 1: Dominant collision-induced fragmentation pathways for peptides.

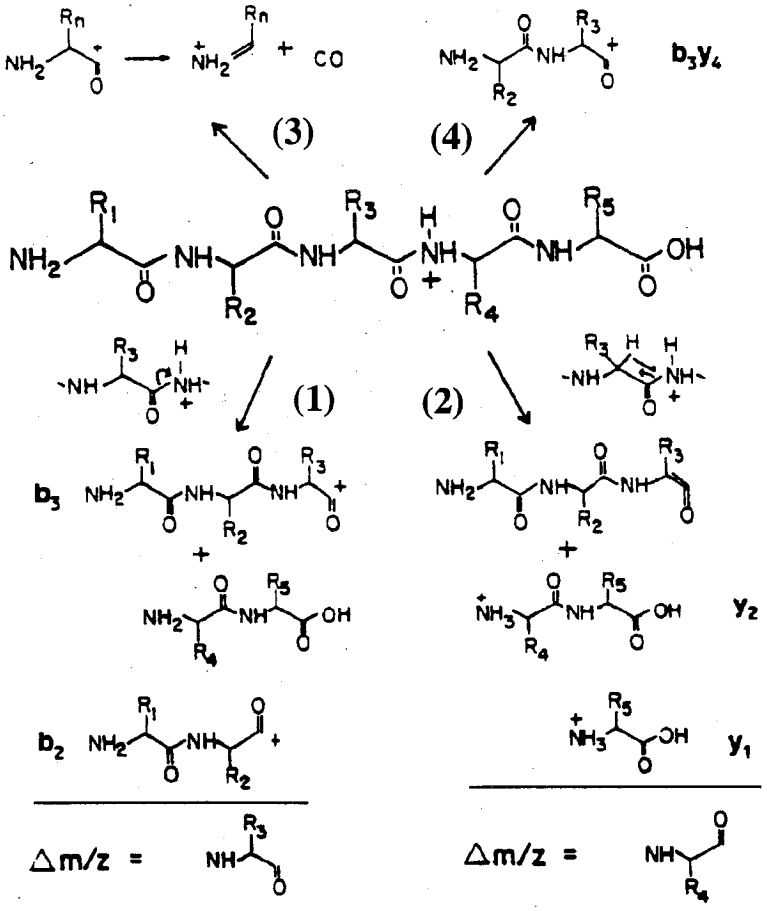

Scheme I

proteolysis and form doubly-charged ions. This stems from the presence of basic sites at both the N- and C-terminus in the form of the α-amino group and the basic amino acids Lys or Arg. Most of the CID-generated fragment ions are singly-charged. In general, a ladder of sequence ions is produced and the mass of an amino acid present at a given position in the sequence can be deduced from subtracting the masses of consecutive ion signals. Successful interpretation involves determining which ions are of type y and which are of type b so that mass differences between consecutive ions of the same type can be calculated. The masses of the largest amino acid, Trp (186 u), and the smallest amino acid, Gly (57 u), are used to create a mass window with which to interrogate the mass spectrum. Given a doubly-charged precursor ion, the mass of the singly-charged analog can be calculated. The largest ion of type y is found within the mass window below the precursor. The largest ion of type b is found within the mass window beginning at 18 u below the m/z of the precursor. If a signal corresponding to an ion of type b is generated, the spectrum is searched for the presence of the smallest ion of type y in the low mass region of the spectrum. If the peptide results from trypsin digestion, this ion will be Lys or Arg with m/z 147 or 175. These low mass ions are typically not observed in an ion trap mass spectrometer for reasons discussed in Chapter Two. The process is continued. The mass window is employed to interrogate the spectrum in the region below the identified peak, a new peak is identified, and confirmation is sought in the form of the presence of the complementary ion. Often a number of possibilities exist and must be continued until no candidate sequence ions can be determined.

Several methods can be used to verify the deduced sequence (54). Derivitizing the peptide by creating the methyl ester will add methyl groups to all of the acidic residues, as

well as the C-terminus, thus the mass of the peptide should shift and the masses of all of the ions assigned as type y should shift by 14 u. Additional 14 u shifts in mass indicate the presence of Glu, Asp, or S-carboxymethyl Cys. Acetylation of an unblocked N-terminus shifts the mass of the peptide and that of the b-type ions by 42 u. Any additional 42 u increments indicate the presence of Lys in the peptide. Losses of CO from b ions and losses of water from peptides containing Ser or Thr may also add confidence to sequence assignments.

1.4.7 Analysis of MS Data Using Known Sequences

Information generated by mass spectrometry can be correlated to sequences in genome databases to aid in protein identification or mass spectral interpretation as discussed in a recent review (54). This information may be useful for screening new data to determine if it is already contained in the sequence database and for investigation of known proteins utilizing different experimental contexts.

1.4.7.1 Peptide Mass Mapping

By digesting a protein with site-specific enzymes, the calculated masses of the predicted peptide products from the gene sequence can be compared with those observed experimentally (54). This method is useful for identifying the presence of post-translational modifications and sequence or translation errors. If the protein being studied is not known, the molecular weights of the enzymatically-generated fragments can be compared with calculated fragments from other protein sequences in the database under the

same digestion conditions. The unknown protein can be identified with high probability if the peptide maps match. A number of computer programs can be employed to perform mass map database searches (2, 54). Mass tolerances as large as 5 u and as small as 7% of the total protein mass have been used to identify proteins (54). The sensitivity of the technique is such that proteins may be correctly identified from highly similar protein families. Proteins with highly similar sequences may produce very diverse peptide maps (54). Post-translational modifications will only change the mass of the modified peptide and will not affect the rest of the mass map. The technique has proven useful for identifying proteins isolated from two-dimensional gel electrophoresis (55).

1.4.7.2 Computer-Aided Interpretation of Fragmentation Mass Spectra

A peptide mass map produces a fingerprint by which proteins can be identified. Similarly, a fragmentation mass spectrum produces a fingerprint by which a peptide sequence can be identified (54). Manual interpretation of CID mass spectra is tedious and provides a bottleneck in the ultimate throughput of the mass spectrometric analytical technique. Fortunately, a number of algorithms have been developed to afford computer-aided interpretation of CID mass spectra (2, 54). SEQUEST, an algorithm developed by Yates and Eng (56), is used in portions of this dissertation for peptide identification. The program takes the molecular weight of the peptide and searches a database for all character-based sequences of amino acids whose molecular weights add up to that of the observed peptide, within a small error tolerance. Expected b- and y-type ions are calculated for each sequence and compared with the dominant peaks in the experimental mass spectrum, generating a preliminary score. For the top 500 candidates, a theoretical mass spectrum is

generated then cross-correlated with the experimental mass spectrum and ranked. The answers generated are compared manually with the experimental mass spectrum, and the validity of the sequence assignment is determined. A search can be carried out on all sequences or just those defined by the proteolytic specificity of an enzyme or a partial amino acid sequence. Data analysis is rapid and completely automated using this software and is fast. Searching a database containing 100,000 sequences takes 2-3 min on a DecStation 3000/9000 computer. The algorithm also includes the capability for searching for sequences with user-defined post-translational modifications (57, 58).

1.4.7.3 *de novo* Computer Interpretation

Tandem mass spectrometers, especially when coupled to LC, have an enormous throughput and generate huge amounts of data. If a given fragmentation spectrum does not appear to correlate well with a peptide sequence in the database, the spectrum can be interpreted manually or by a *de novo* computer interpretation algorithm. A combinatorial approach is usually used (54). Starting at the C-terminus, amino acid masses are subtracted from the $(M+H)^+$ ion to calculate the y- and b-type ions that would be present for each amino acid at that position in the sequence. A score is calculated based on the abundance of ion signal for each possibility, and the 20 amino acids are ranked. The second iteration creates a list of 400 possibilities by extending each amino acid by an additional one. This list is ranked and only sequences with a non-zero score will be retained in the next iteration. The process is continued until the calculated sequence mass matches the m/z for the observed $(M+H)^+$ ion. This approach has been used to interpret high quality data (54).

1.5 Conclusion

Mass spectrometry can be used to obtain information about biological molecules, hence biological processes, with a faster throughput and at higher sensitivities than can be accomplished using conventional methods such as Edman degradation. The work presented in this dissertation involves the development of methodologies to extend the capabilities of the versatile ion trap mass spectrometer for the analysis of peptide mixtures and post-translational modifications.

1.6 References

1. Yates, J. R., III (1987), Ph.D. Dissertation, University of Virginia, and the references therein.

2. Burlingame, A. L., Boyd, R. K., and Gaskell, S. J. (1996) *Anal. Chem.* **68,** 12, 599R-651R, and the references therein.

3. Smith, R. D., and Light-Wahl, K. J. (1993) *Biol. Mass Spec.* **22** 493-501.

4. Smith, D. L., and Zhang, Z. Q. (1994) *Mass Spec. Rev.* **13,** 5-6, 411-429.

5. Smith, R. D., Cheng, X. S., Chen, R., and Hofstadler, S. A. (1996) *ACS Symp. Ser.* **619** 294-314.

6. Przybylski, M., and Glocker, M. O. (1996) *Angew. Chem. Int. Ed. Engl.* **35** 806-826.

7. Henderson, R. A., Michel, H., Sakaguchi, K., Shabanowitz, J., Appella, E., Hunt, D. F., and Engelhard, V. H. (1992) *Science* **255** 1264-1266.

8. Cox, A. L., Skipper, J., Chen, Y., Henerson, R. A., Darrow, T. L., Shabanowitz, J., Engelhard, V. H., Hunt, D. F., and Slingluff, C. L., Jr. (1994) *Science* **264** 716-719.

9. Slingluff, C. L., Jr., Hunt, D. F., and Engelhard, V. H. (1994) *Curr. Op. Immun.* **6** 733-740.

10. Watts, J. D., Affolter, M., Krebs, D. L., Wang, R. L., Samelson, L. E., and Aebersold, R. (1994) *J. Biol. Chem.* **269,** 47, 29520-29529.

11. Watts, J. D., Affolter, M., Krebs, D. L., Wange, R. L., Samelson, L. E., and Aebersold, R. (1996) *ACS Symp. Ser.* **619** 381-407.

12. Affolter, R., Watts, J. D., Krebs, D. L., and Aebersold, R. (1994) *Anal. Biochem.* **223** 74-81.

13. Kaiser, R. E., Jr., Cooks, R. G., Stafford, G. C., Jr., Syka, J. E. P., and Hemberger, P. H. (1991) *Int. J. Mass Spectrom. Ion Proc.* **106** 79-115.

14. Louris, J. N., Brodbelt-Lustig, J. S., Cooks, R. G., Glish, G. L., Van Berkel, G. J., and McLuckey, S. A. (1990) *Int. J. Mass Spectrom. Ion Proc.* **96** 117-137.

15. Cooks, R. G., Hoke, S. H., II, Morand, K. L., and Lammert, S. A. (1992) *Int. J. Mass Spectrom. Ion Proc.* **118/119** 1-36.

16. Kaiser, R. E., Jr., Cooks, R. G., Syka, J. E. P., and Stafford, G. C., Jr. (1990) *Rapid Commun. Mass Spectrom.* **4,** 1, 30-33.

17. Paul, W., and Steinwedel, H. (1956) , German Patent 944,900.

18. Paul, W. (1990) *Angew. Chem. Int. Ed. Engl.* **29** 739-748.

19. Cooks, R. G., McLuckey, S. A., and Kaiser, R. E. (1991) *Chem. Eng. News* **69,** 12, 26-41.

20. March, R. E., and Hughes, R. J. (Eds.) (1989) *Quadrupole Storage Mass Spectrometry*, (Winefordner, J.D. and Kolthoff, I.M., Eds.) *in* Chemical Analysis: A Series of Monographs on Analytical Chemistry and its Applications, **V102**, Wiley & Sons, New York.

21. Dehmelt, H. G. (1967) *Adv. At. Mol. Phys.* **3** 53-72.

22. Dehmelt, H. G. (1969) *Adv. At. Mol. Phys.* **5** 109.

23. Dehmelt, H. (1991) *in* Santa Fe Workshop. Foundations of Quantum Mechanics (Black, T. D., Nieto, M. M., Pilloff, H. S., Scully, M. O., and Sinclair, R. M., Eds.), May 27-31, 1991, World Scientific, Singapore, Santa Fe, NM, USA, pp. 16-22.

24. Dehmelt, H. (1995) *Phys. Scripta Vol. T* **T59** 87-92.

25. Rettinghaus, V. von G. (1967) *Z. Angew. Phys.* **22,** 4, 321-326.

26. Dawson, P. H., and Whetten, N. R. (1968) *J. Vac. Sci. Technol.* **5,** 1, 11-8.

27. Stafford, G. C., Jr., Kelley, P. E., Syka, J. E. P., Reynolds, W. E., and Todd, J. F. J. (1984) *Int. J. Mass Spectrom. Ion Proc.* **60** 85-98.

28. Louris, J. N., Cooks, R. G., Syka, J. E. P., Kelley, P. E., Stafford, G. C., Jr., and Todd, J. F. J. (1987) *Anal. Chem.* **59** 1677-1685.

29. Louris, J. N., Amy, J. W., Ridley, T. Y., and Cooks, R. G. (1989) *Int. J. Mass Spectrom. Ion Proc.* **88** 97-111.

30. Edman, P., and Begg, G. (1967) *Eur. J. Biochem.* **1** 80-91.

31. Hewick, R. M., Hunkapiller, M. W., Hood, L. E., and Dreyer, W. J. (1981) *J. Biol. Chem.* **256** 7990-7997.

32. Hunter, T. (1995) *Cell* **80** 225-236.

33. Barber, M., Bordoli, R. S., Sedgwick, R. D., and Tyler, A. N. (1981) *J. Chem. Soc. Chem. Commun.* 325-327.

34. Karas, M., Bachmann, D., Bahr, U., and Hillenkamp, F. (1987) *Int. J. Mass Spectrom. Ion Proc.* **78** 53-68.

35. Tanaka, K., Waki, H., Ido, Y., Akita, S., and Yoshida, Y. (1988) *Rapid Commun. Mass Spectrom.* **2** 151-153.

36. Schar, M., Bornsen, K. O., and Gassman, E. (1991) *Rapid Commun. Mass Spectrom.* **5** 319-326.

37. Beavis, R. C., and Chait, B. T. (1990) *Proc. Natl. Acad. Sci. USA* **87** 6873-6877.

38. Cohen, S. L., and Chait, B. T. (1996) *Anal. Chem.* **68** 31-37.

39. Strupat, K., Karas, M., and Hillenkamp, F. (1991) *Int. J. Mass Spectrom. Ion Proc.* **111** 89-102.

40. Nelson, R. W., Dogruel, D., and Williams, P. (1994) *Rapid Commun. Mass Spectrom.* **8** 627-631.

41. Nelson, R. W., Dogruel, D., and Williams, P. (1995) *Rapid Commun. Mass Spectrom.* **9** 625.

42. Limbach, P. A., Crain, P. F., and McCloskey, J. A. (1995) *Curr. Opin. Biotechnol.,* **6** 96-102.

43. Colby, S. M., King, T. B., and Reilly, J. P. (1994) *Rapid Commun. Mass Spectrom.* **8** 865-868.

44. Whittal, R. M., and Li, L. (1995) *Anal. Chem.* **67** 1950-1954.

45. Brown, R. S., and Lennon, J. J. (1995) *Anal. Chem.* **67** 1998-2003.

46. Vestal, M. L., Juhasz, P., and Martin, S. A. (1995) *Rapid Commun. Mass Spectrom.* **9** 4144-1050.

47. Fenn, J. B., Mann, M., Meng, C. K., Wong, S. F., and Whitehouse, C. M. (1989) *Science* **246** 64-71.

48. Fenn, J. B., Mann, M., Meng, C. K., and Wong, S. F. (1990) *Mass Spec. Rev.* **9** 37-70.

49. Iribarne, J. V., and Thomson, B. A. (1976) *J. Chem. Phys.* **64** 2287-2294.

50. Fenn, J. B. (1993) *J. Am. Soc. Mass Spectrom.* **4** 524-535.

51. Whitehouse, C. M., Dreyer, R. N., Yamashita, M., and Fenn, J. B. (1985) *Anal. Chem.* **57** 675-679.

52. Lee, E. D., Mueck, W., Henion, J. D., and Covey, T. R. (1988) *J. Chromatogr.* **458** 313-321.

53. Smith, R. D., Loo, J. A., Barinaga, C. J., Edmonds, C. G., and Udseth, H. R. (1989) *J. Chromatogr.* **480** 211-232.

54. Yates, J. R., III, McCormack, A. L., Link, A. J., Schieltz, D., Eng, J., and Hays, L. (1996) *Analyst* **121,** 7, R65-R76, and the references therein.

55. Henzel, W., Billeci, T., Stults, J., Wond, S., Grimley, C., and Watanabe, C. (1993) *Proc. Natl. Acad. Sci. USA* **90** 5011-5015.

56. Eng, J., McCormack, A. L., and Yates, J. R., III (1994) *J. Am. Soc. Mass Spectrom.* **5** 976-989.

57. Griffin, P. R., MacCoss, M. J., Eng, J. K., Blevins, R. A., Aaronson, J. S., and Yates, J. R., III (1995) *Rapid Commun. Mass Spectrom.* **9** 1546-1551.

58. Yates, J. R., III, Eng, J., McCormack, A. L., and Schieltz, D. (1995) *Anal. Chem.* **67** 1426-1436.

Chapter 2

Practical Aspects of Ion Trap Theory

2.1 Theoretical Overview

Quadrupole ion traps are dynamic mass analyzers that use an oscillating electric potential applied to the ring electrode, called the "fundamental rf," to focus ions toward the center of the trap. This is accomplished by creating a parabolic potential, shaped like a saddle (1), inside the trapping volume. The strength of the restoring force linearly increases as the ion trajectory deviates from the central axis, focusing the ion back to the center of the trapping volume. This is demonstrated in Figure 2.1, a simulation of ion trajectories created using SIMION 3D Version 6.0 (2). A population of trapped ions is observed to occupy only the space near the center of the trap due to the focusing effect of the oscillating electric fields. Assuming a cylindrically symmetric system, the potential an ion experiences at any point in the ion trap is given by

$$\Phi(r,z) = \frac{(U - V\cos\omega t)}{2}\left[\frac{r^2 - 2z^2}{r_o^2}\right] + \frac{(U - V\cos\omega t)}{2} \qquad \text{(Eq. 2.1)}$$

where U is the amplitude of a dc potential applied to the endcap electrodes with reference to the ring electrode, V is the amplitude of the "fundamental rf" applied to the ring electrode, ω is the angular frequency of the rf potential and r_o is the closest distance between the

Figure 2.1: Simulation of ion trajectories in the ion trap using SIMION 3D. The ion trajectories quickly collapse toward the center of the trap.

center of the trap and the ring electrode (3). The closest distance between the center of the trap and the endcap electrode is given by z_o. To obtain an ideal quadrupolar field, r_o is equal to the square root of $2z_o$. The actual geometry of the commercial ITMS is "stretched" and r_o is equal to $0.781z_o$, leading to the presence of higher-order fields within the trapping volume. The effects of non-linear resonances produced in the stretched trap have been actively studied for the last few years and have led to many new insights regarding the fundamental performance characteristics of the ion trap mass spectrometer (4-10).

The force on an ion, given by the electric field, is obtained by

$$\vec{F}(r,z) = \vec{E}(r,z) = -e\vec{\nabla}\Phi(r,z) = m\vec{a}(r,z) \qquad \text{(Eq. 2.2)}$$

and, using Newton's law, is proportional to the acceleration an ion of charge e experiences due to that force. Equation 2 may be placed in the form of the Mathieu equation (11) in the radial and axial directions when the substitutions

$$a_z = \frac{-8eU}{mr_o^2\omega^2},\quad q_z = \frac{4eV}{mr_o^2\omega^2},\quad a_r = -a_z/2,\quad q_r = -q_z/2, \text{ and } \xi = \frac{\omega t}{2} \qquad \text{(Eq. 2.3)}$$

are made. Ion trajectories are determined by solutions to the Mathieu equation and are oscillating functions with regions of stability described by the parameters a_z and q_z. Thus the stability of ion motion depends upon the mass and charge of the ion (m), the size of

the ion trap (r_o), the oscillating frequency of the fundamental rf (ω), and the amplitudes of the applied dc (U) and rf (V) voltages. One region of stability in which radial and axial stability overlap is shown in Figure 2.2. An ion of a given mass-to-charge ratio will be stably trapped anywhere within that region. The position of the ion within the stability region can be moved by changing the amplitude of the applied dc and rf voltages to change the values of a_z and q_z, termed the "working points" of the ion. Values of the working points are chosen to ensure stability or instability of an ion trajectory of interest. For the case of the commercial Finnigan ion traps, r_o = 1 cm, $\omega/2\pi$ = 1.1 MHz, with V ranging from 0 - 7500 $V_{0\text{-}p}$.

As an example, consider three working points for an ion of *m/z* 1500, shown in Figure 2.3. Values of the amplitudes for the applied dc and rf potentials are shown in parentheses. The corresponding a_z and q_z values are delineated in the figure caption. It is clear that a judicious choice for the amplitude of the applied potentials is required to ensure stability for all ions within a mass range of interest. The mass-selective instability mode of operation utilizes no dc voltage, thus the mass spectrometer is operated on the line $a_z = 0$. This corresponds to the case of maximizing the range of *m/z* values that may be stably trapped. Ion trajectories become unstable in the axial direction (between the endcap electrodes) but remain stable in the radial direction when $q_z = 0.908$. Ions are ejected through holes in the endcap electrode and are typically detected using an electron multiplier.

Trapped ions of a given *m/z* oscillate at a frequency known as the "secular frequency" that is proportional to the angular frequency of the applied signal, ω. The

Figure 2.2: Diagram showing the regions of stability in the quadrupole ion trap parameterized in terms of the operating voltages and frequencies.

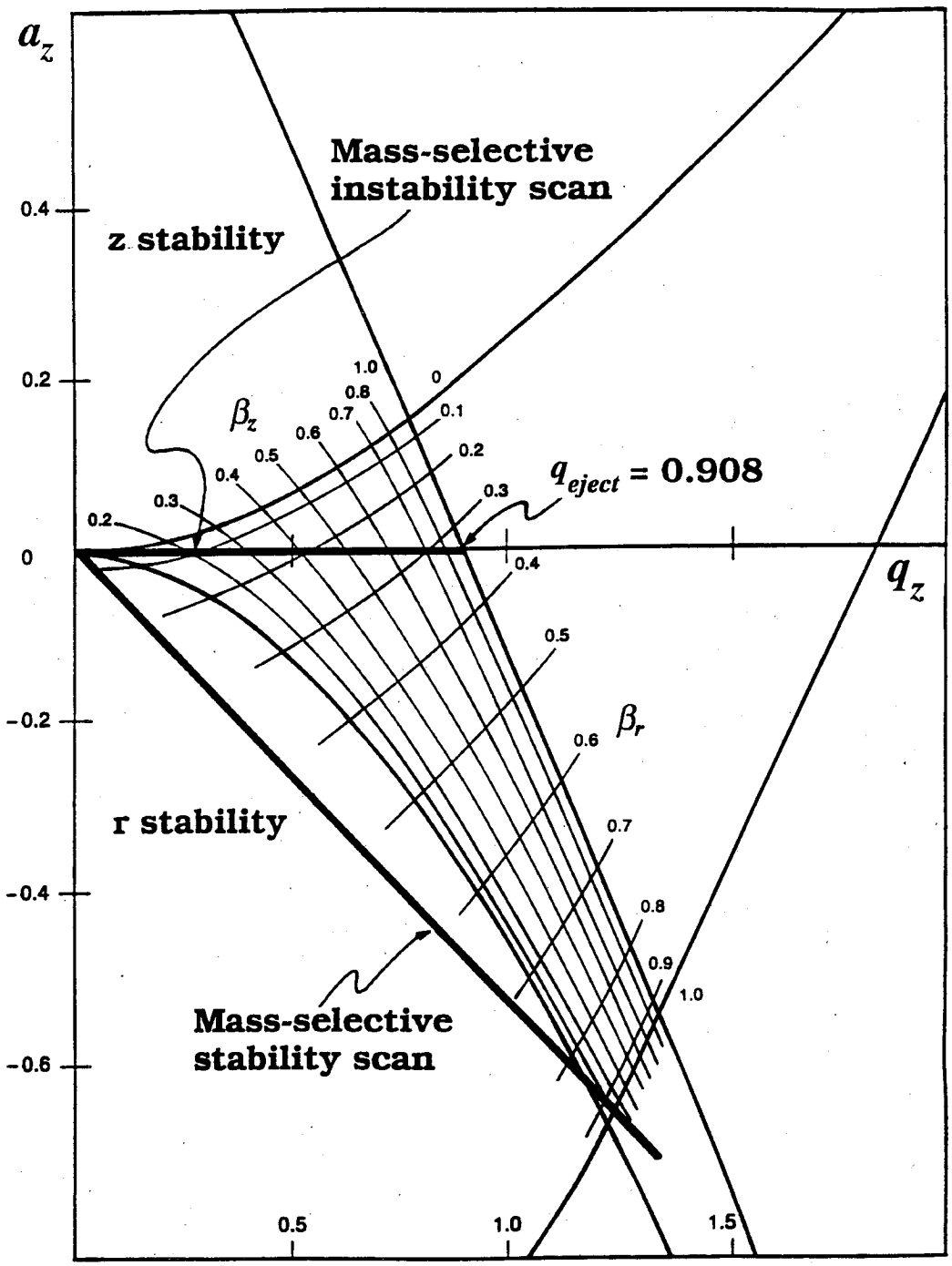
a_z
Mass-selective
instability scan
z stability
0.4
0.2
0
-0.2
-0.4
-0.6
β_z
1.0
0.8
0.7
0.6
0.5
0.4
0.3
0.2
0
0.1
0.2
0.3
q_{eject} = 0.908
0.4
0.5
β_r
0.6
0.7
0.8
0.9
1.0
q_z
r stability
Mass-selective
stability scan
0.5
1.0
1.5

Figure 2.3: Selected "working points" for an ion of *m/z* 1500. The applied dc and rf potentials are shown in parentheses, (*U, V*). The corresponding (a_z, q_z) values are as follows: (-100 V, 1000 V) $\Rightarrow$ (0.0108, 0.0539), similarly (-1000 V, 3000 V) $\Rightarrow$ (0.108, 0.162) and (-100 V, 6000 V) $\Rightarrow$ (0.0108, 0.323). A judicious choice of conditions is required to ensure trajectory stability for a wide range of *m/z* values.

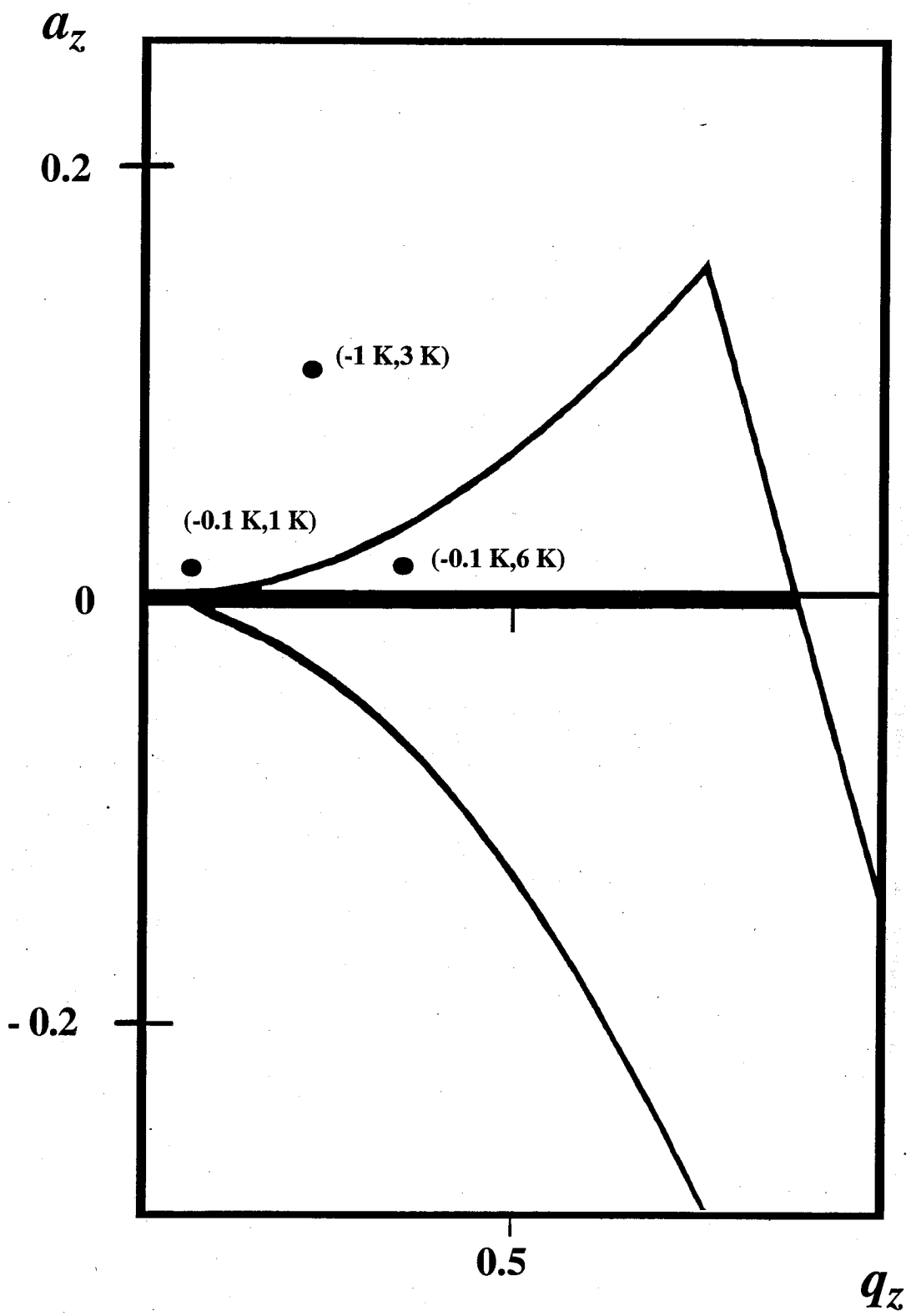
a_z
0.2
0
- 0.2
(-1 K,3 K)
(-0.1 K,1 K)
(-0.1 K,6 K)
0.5
q_z

constant of proportionality is given by $\beta_{z,r}$. For values of q_z < 0.4, β_z may be approximated by (12),

$$\beta_z^2 = a_z + q_z^2/2 \qquad \text{(Eq. 2.4)}$$

which reduces to $\beta_z = q_z/\sqrt{2}$ for the mass-selective instability mode of operation. "Resonance" conditions are induced by matching the frequency of a supplementary potential applied to the endcap electrodes to the secular frequency of the ion. The ion will absorb energy from the applied field and the trajectory will linearly increase towards the endcap electrodes until the ion becomes unstable and is ejected (3).

2.2 Practical Aspects of Ion Trap Theory

In order to measure the *m/z* value of a molecule in an ion trap, the molecule must be ionized, focused into the ion trap, trapped, ejected, and detected. Structural information is obtained by collision-induced dissociation with a helium damping gas, and a mass spectrum is generated by sequentially ejecting fragment ions from low *m/z* to high *m/z*. The mass-selective instability mode is utilized for ion ejection. The mass-selective instability line is the locus of q_z values where a_z is set to zero and maximizes the mass range that may be stably trapped. Operation of the ion trap consists of the construction of a scan function used to manipulate the working points of ions of interest. The scan function sets the amplitude of the fundamental and supplementary potentials and sets the time taken for each step. Typical scan functions for molecular weight analyses and MS/MS experiments are shown in Figure 2.4.

Figure 2.4: (**a**) Molecular weight and (**b**) MS/MS scan functions for the quadrupole ion trap mass spectrometer.

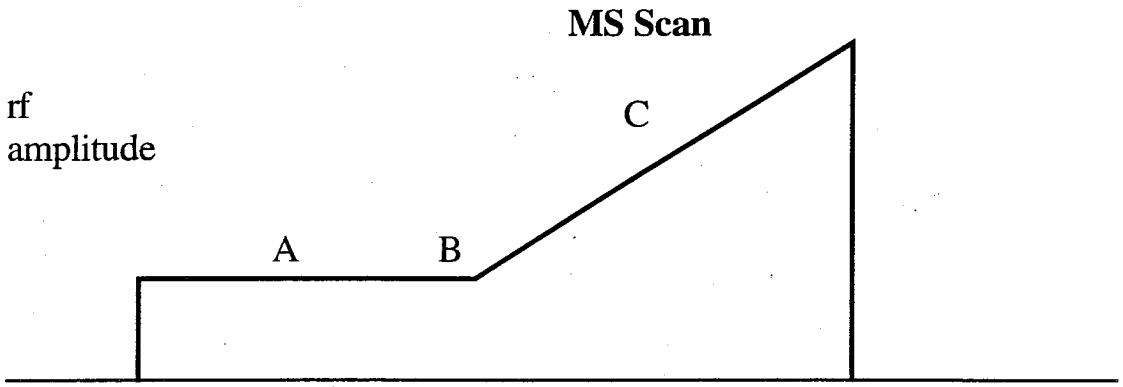

A - Ionization Period
B - Cooling Time
C - Resonance Ejection Ramp

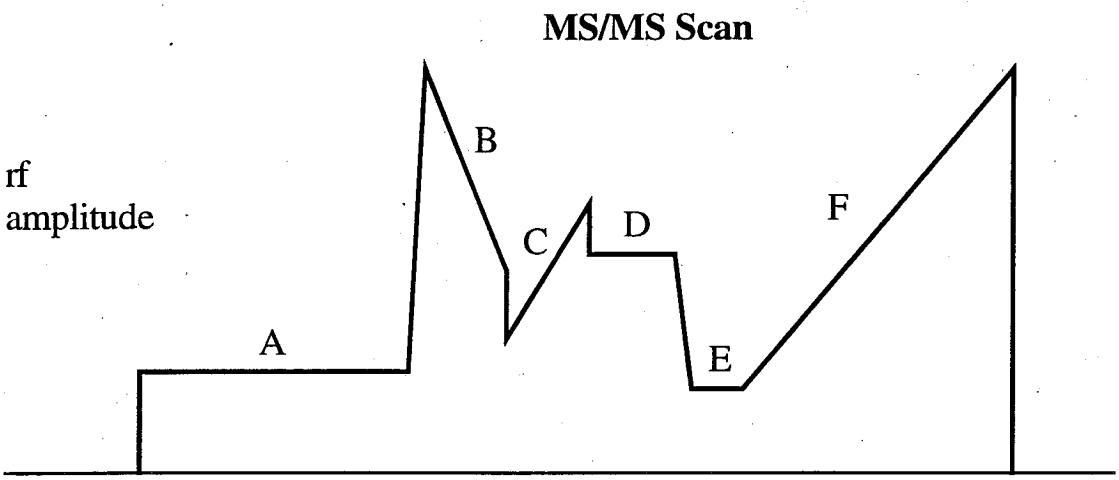

A - Ionization Period
B - Reverse Scan to eject high mass ions
C - Forward Scan to eject low mass ions
D - Resonance Excitation (Tickle) Period
E - Cooling Time
F - Resonance Ejection Ramp

2.2.1 Ion Injection

Ion traps were initially utilized to analyze volatile samples by electron impact or chemical ionization. In this case, ions were created inside the trapping volume. An interest in the analysis of biological molecules led to the need to interface suitable ionization techniques, *i.e.*, electrospray ionization and matrix-assisted laser desorption ionization, to the ion trap. These externally created ions need to be injected into the ion trap and efficiently trapped. Ions are focused by an einzel lens system and allowed into the ion trap during the ionization period. A gating lens pulses from positive to negative voltages to repel or attract ions toward the entrance endcap aperture. The time during which ions are allowed into the trap is set to maximize signal while minimizing "space-charge" effects, resulting from too many ions in the trap, that lead to an overall reduction in performance. The ion trap is typically filled with helium to a pressure of ~ 1 mtorr. Collisions with helium reduce the kinetic energy of the ions and serve to quickly contract trajectories toward the center of the ion trap, enabling trapping of injected ions. This cooling effect is demonstrated in Figure 2.5 where the ion population forms a "packet" near the center of the trap.

2.2.2 Ion Trapping

Ions of different *m/z* values may have stable orbits at the same time, as shown in Figure 2.6. From the expression for q_z in Equation 2.3, we see that

$$\frac{m}{z} \propto \frac{V}{q_z}. \qquad \text{(Eq. 2.5)}$$

Figure 2.5: Simulations show that collisions with the helium damping gas lead to the creation of an ion packet near the center of the trap.

Larger values of *m/z* will have smaller values of q_z and smaller values of *m/z* will have larger q_z values. Since ion trajectories become unstable when q_z = 0.908, a well-defined low-mass cutoff is created for a given value of the amplitude of the applied rf voltage, *V*. No ions below that mass will be trapped, but ions above that mass will be trapped with trapping efficiency decreasing for larger *m/z* values (1). Low-mass cutoffs for various amplitudes of the applied fundamental rf potential are listed in Figure 2.6. The trapping efficiency for an ion of interest depends, in part, upon the value of the low-mass cutoff, or the so-called exclusion limit (6). This can be a problem when using ionization methods that generate many low-mass matrix ions since the ion trap can accommodate on the order of 10^5 ions before space-charge seriously impairs the performance of the instrument. For example, the model peptide human angiotensin I (MW 1296) may be most efficiently trapped at a low-mass cutoff of 85 u. Matrix-assisted laser desorption ionization (MALDI) generates matrix ions above this cutoff in a ratio of ~1:10^6. In this situation, the high sensitivity of the ion trap can be most effectively utilized if the ion of interest is selectively injected into the ion trap. Current efforts revolve around selective injection utilizing shaped excitation waveforms (13) or filtered noise fields (14) to cause all ions but the ion of interest to have unstable trajectories. Other approaches include ramping the amplitude of the fundamental rf during injection to increase trapping efficiency, even at low pressures of the helium damping gas (15), as well as the addition of a quadrupole mass filter to afford selective injection of ions of interest into the ion trap (16).

2.2.3 Ion Ejection

Shown in Figure 2.6 is an example of the relative positions of three ions of differing *m/z* ratios on the mass-selective instability line, $a_z = 0$. Three different values for the amplitude of the fundamental rf signal are given. As the voltage is increased, the q_z value for the ion also increases. Figure 2.6(c) shows that at 6000 V, the ion of *m/z* 500 has been ejected from the ion trap. At the maximum amplitude of 7500 V, at *m/z* 1500 the q_z value has only reached 0.404; thus that ion cannot be ejected from the ion trap and detected. As noted above, a resonance condition may be induced by matching the frequency of an applied oscillating signal to the secular frequency of an ion in the trap (17). This will cause an ion to gain energy and the amplitude of the trajectory to linearly approach the endcap electrodes until the ion is ejected from the trap. Ejection can therefore be made to occur at voltages lower than those required for ejection at q_z of 0.908, extending the nominal mass range of the ion trap. Conceptually, this may be viewed as creating a "hole" in the stability diagram. The position of the hole is dependent upon the frequency of the supplementary potential while the size of the hole depends upon the amplitude of the signal. This effect is illustrated in Figure 2.7 where an ellipse represents a resonance point that extends the mass range by a factor of 4. At 1000 V none of the ions have q_z values approaching that of the resonance point; thus none will be detected. At 3000 V, *m/z* 500 has been ejected and *m/z* 1000 is in the process of being ejected. The q_z value for *m/z* 1500 is smaller than 0.227; thus that ion will not be ejected. At 6000 V, the q_z values for all of the ions are greater than 0.227, the q_z value of the resonance point. This example shows that when resonance

Figure 2.6: Relative positions of ions with three different mass-to-charge ratios along the mass-selective instability line, $a_z = 0$. The effect of increasing the amplitude of the fundamental rf voltage is shown in panels (**a**) through (**c**).

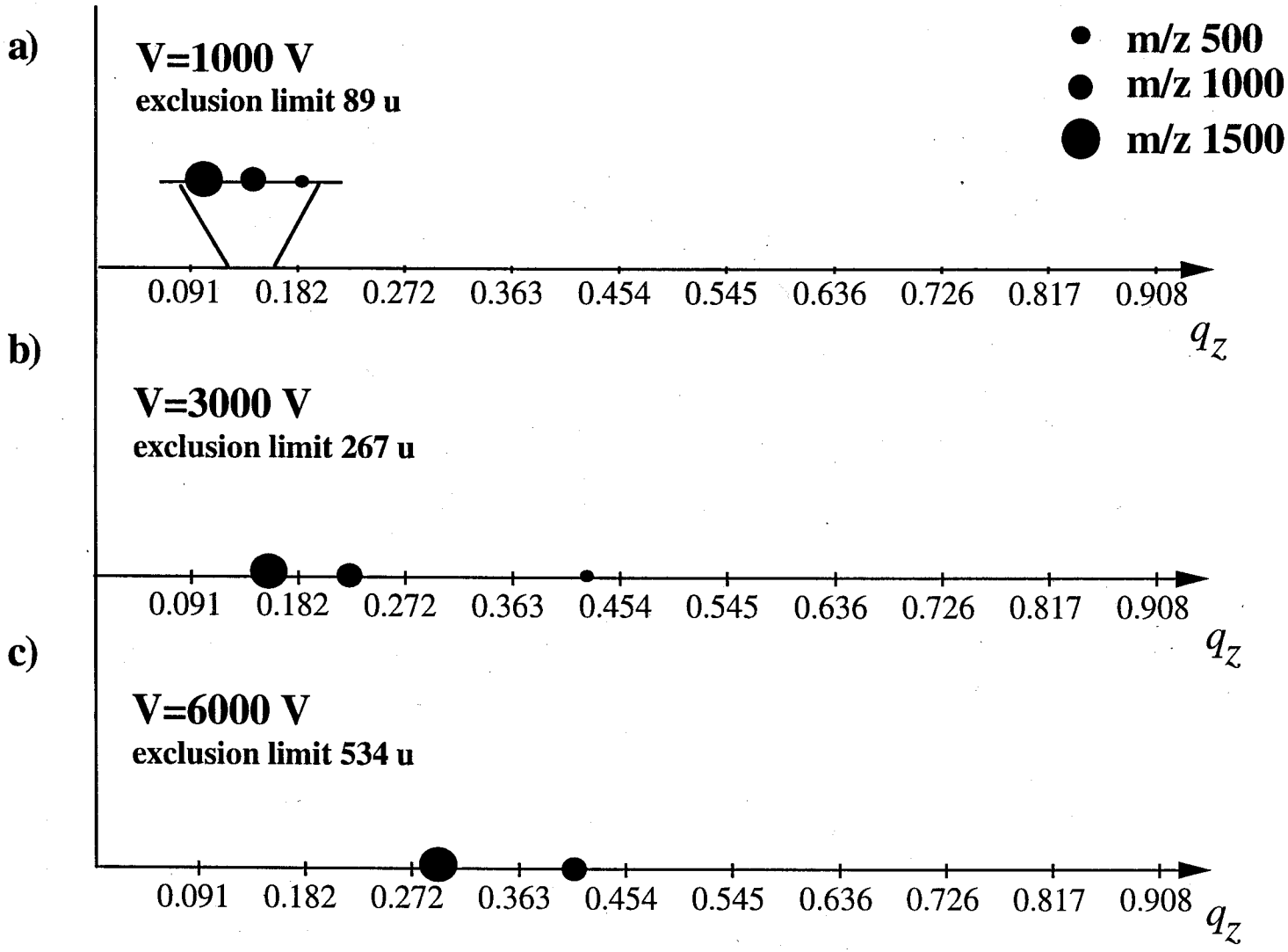
a)
V=1000 V
exclusion limit 89 u
m/z 500
m/z 1000
m/z 1500
0.091 0.182 0.272 0.363 0.454 0.545 0.636 0.726 0.817 0.908
q_z
b)
V=3000 V
exclusion limit 267 u
0.091 0.182 0.272 0.363 0.454 0.545 0.636 0.726 0.817 0.908
q_z
c)
V=6000 V
exclusion limit 534 u
0.091 0.182 0.272 0.363 0.454 0.545 0.636 0.726 0.817 0.908
q_z

Figure 2.7: The same conditions as in Figure 2.6 except a resonance point at q_z = 0.227 has been imposed to increase the effective mass range by a factor of 4. A region of instability is created that affords the ejection of ions at lower voltages than would normally be required; therefore, ions of large *m/z* can be ejected from the ion trap and detected.

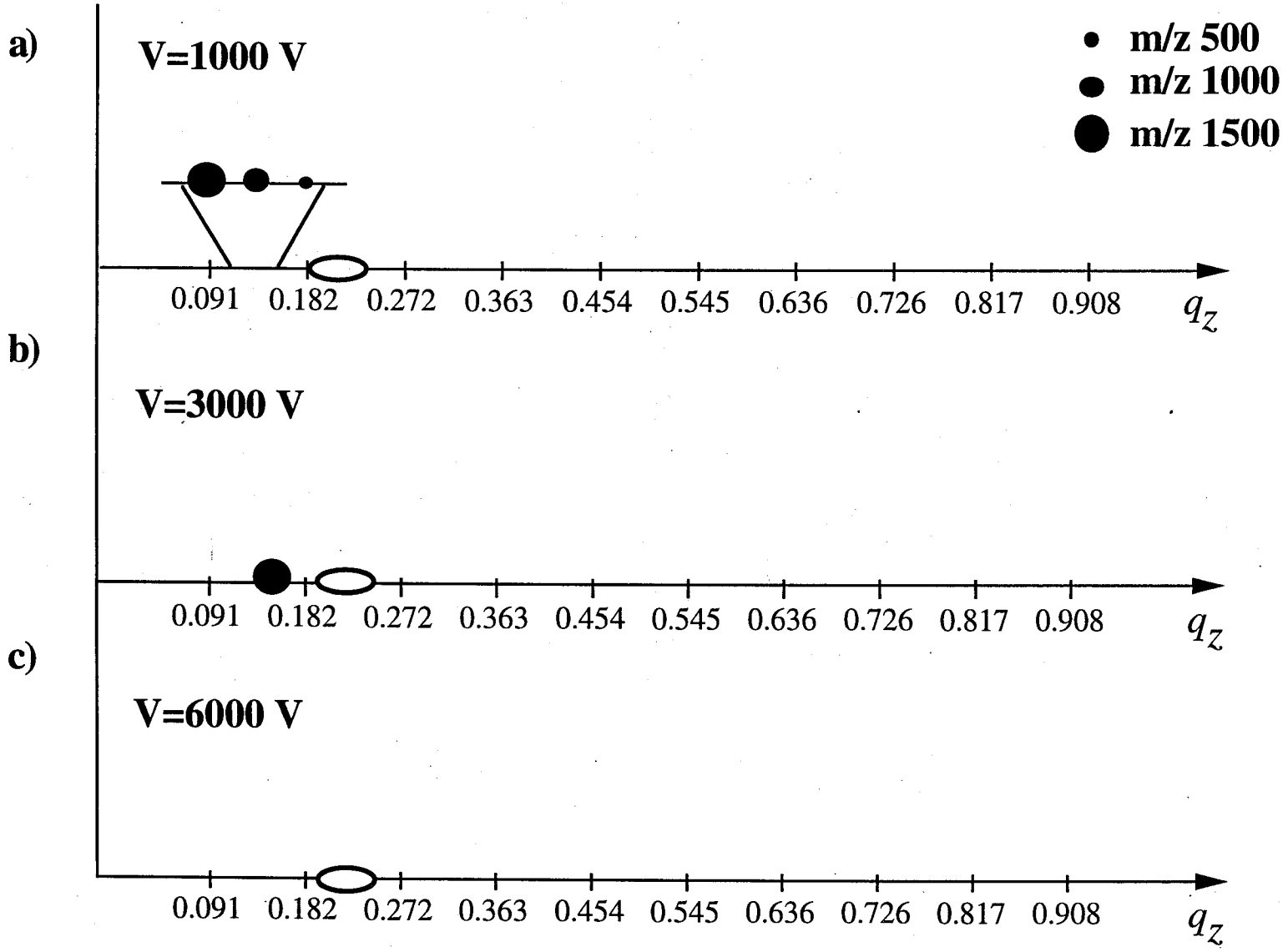
a)
V=1000 V
m/z 500
m/z 1000
m/z 1500
0.091 0.182 0.272 0.363 0.454 0.545 0.636 0.726 0.817 0.908
q_z
b)
V=3000 V
0.091 0.182 0.272 0.363 0.454 0.545 0.636 0.726 0.817 0.908
q_z
c)
V=6000 V
0.091 0.182 0.272 0.363 0.454 0.545 0.636 0.726 0.817 0.908
q_z

ejection is used and the amplitude of the voltage is ramped from low to high amplitudes, all of the ions "fall through the hole" and are ejected from the trap and detected.

2.2.4 Ion Isolation

In a typical multiple-stage mass spectrometry experiment, the ion of interest is isolated before undergoing resonance excitation or charge state determination using high resolution. Isolation in the Finnigan ITMS may be accomplished in two ways, depicted in Figure 2.8. One method, illustrated in Fig. 2.8(a), includes the combined use of dc and rf potentials to bring the q_z and a_z values of the ion to an apex of the stability diagram; all other ions will be unstable (18, 19). The other method is shown in Fig. 2.8(b) and consists of scanning the amplitude of the fundamental rf voltage in a reverse-then-forward manner while applying a resonance signal (20, 21). This allows ejection of ions with *m/z* greater than the ion of interest followed by ejection of ions having *m/z* smaller than the ion of interest. Both isolation methods are used; however, the effects of space-charge and field non-linearities on the shape of the stability diagram may degrade performance when the dc/rf isolation method is employed. A recent refinement includes the use of the stored waveform inverse Fourier transform (SWIFT) technique (13, 22) and filtered noise fields (14) to isolate ions using notched waveforms.

2.2.5 Ion Dissociation

As discussed above, when an ion approaches a region of instability in the axial direction, the deviation of its trajectory from the center of the trap will increase. When

Figure 2.8: Methods of isolating a single *m/z* in an ion trap. (**a**) A combination of dc and rf potentials are applied to bring the a_z and q_z values of the ion of interest to the apex of the stability diagram. Neighboring ions have working points that fall outside of the region of stability. (**b**) Reverse-then-forward scanning of the amplitude of the fundamental rf voltage in conjunction with the application of an auxiliary signal to create a resonance point affords ion isolation. (**i**) Reverse scanning resonantly ejects ions from high to low *m/z*. (**ii**) Forward scanning resonantly ejects ions from low to high *m/z*. (**iii**) Resultant isolation of one value of *m/z*.

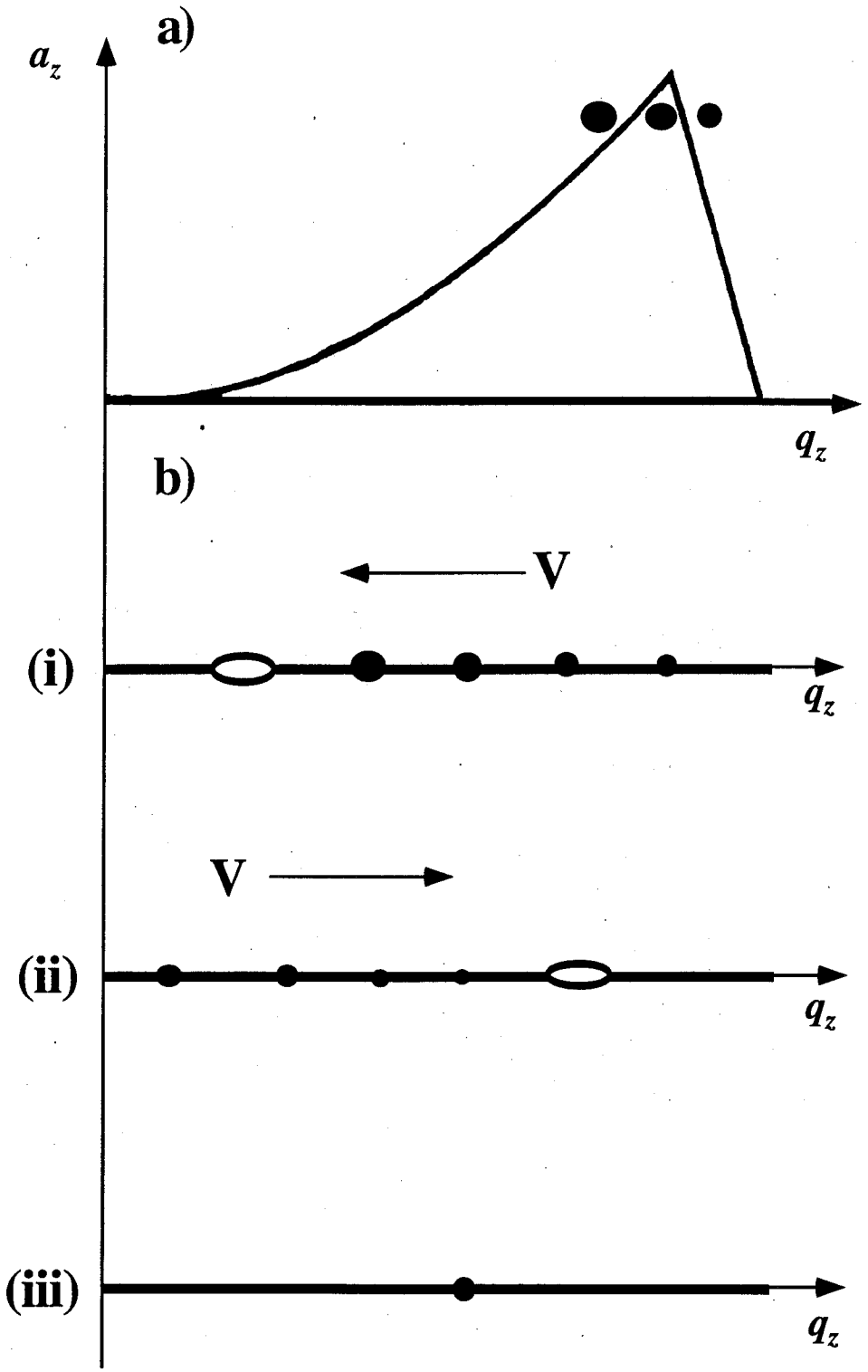
a)
a_z
q_z
b)
V
(i)
q_z
V
(ii)
q_z
(iii)
q_z

instability is induced by a resonance signal, the amplitude of the resonance signal can be adjusted to cause collisionally-induced dissociation (CID) of the ion with the helium damping gas rather than ejection from the ion trap (20). An estimated 10,000 low-energy collisions (23) transfer enough energy into peptide ions to cause random fragmentation along the peptide backbone in a manner analogous to that obtained using a triple quadrupole mass spectrometer. CID efficiency typically ranges from 40%-80%, although it approaches 100% for some favorable cases (24). The amplitude of the rf signal that sets the q_z value of the isolated ion during resonance excitation, termed the "tickle mass," must be judiciously set as it will serve to eject all ions with *m/z* value*s* below the tickle mass. This limits the amount of low *m/z* fragmentation information obtained. A complete set of complementary b- and y-type ions (25) is typically not obtained unless multiple stages of mass spectrometry are performed. The q_z value of the ion and the frequency and amplitude of the tickle voltage must be carefully tuned to optimize fragmentation. The auxiliary frequency generator outputs a single-frequency sinusoidal signal that is not sufficient to excite the envelope of ion signals resulting from isotopic abundances for ions with large *m/z* values. Stored waveform inverse Fourier transform techniques (22) and the application of random noise (26) have been successfully used to excite a broad range of ion secular frequencies. In addition, shifting the q_z value of the ion and increasing the amplitude of the tickle pulse have substantially increased the amount of fragmentation observed for large peptides (27).

2.2.6 High Resolution

The mass resolution of the ion trap mass spectrometer is a function of the number of rf cycles that the ion spends interacting with the trapping field (28). Resolution is increased by reducing the amplitude of the resonance ejection signal and reducing the ejection scan speed, nominally 5555 u/sec for the Finnigan ITMS. The scan speed is attenuated utilizing a network of resistors placed in series with the digital-to-analog converter (DAC) that controls the amplitude of the rf voltage applied to the ring electrode (17). The fixed scanning rate of the DAC is applied to smaller "windows" of rf voltages with a concomitant gain in the number of data points taken per unit mass. A dc potential is used as an offset to position the rf voltage, or mass window. This is schematically illustrated in Figure 2.9. Figure 2.9 (a) shows the unattenuated mass window resulting from scanning the amplitude of the rf voltage from 346 V to 7500 V while applying a supplementary frequency at 120 kHz to extend the mass range by a factor of 3. This increases the mass scan speed to 16665 u/s. Attenuation of the scan speed by a factor of 10 reduces the size of the mass window by the same factor, thus Figures 2.9 (b) - (d) represent a 186 u mass window created by the attenuation. The different dc offset voltages serve to position the mass window in different regions within the mass window. In (b), the mass window is positioned at 267 u, in (c) it is 800 u, and it is 1600 u in (d); therefore, different regions of the mass window are accessed. Attenuation by a factor of 100 - 300 is typically required to resolve the isotopes for singly to triply charged peptide ions to achieve resolutions of 10,000 - 30,000 at *m/z* values ranging between 500 and 2000.

Figure 2.9: Extending the resolution on the quadrupole ion trap mass spectrometer. (**a**) A normal resonance ejection scan from 90 u to 1950 u. (**b**) The scan speed is attenuated by a factor of 10 resulting in a tenfold decrease in the width of the scanning mass window. The dc offset is utilized to position the scanning window throughout the mass range. An offset of 100 V positions the window at 267 u, (**c**) 300 V positions the window at 800 u, and (**d**) 600 V positions the window at 1600 u.

a) Scan Speed = 16,665 u/s

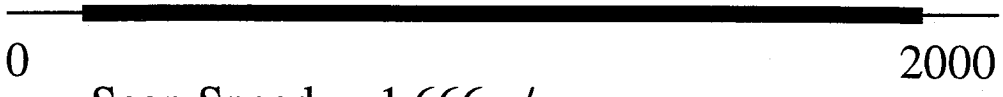

b) Scan Speed = 1,666 u/s
DC offset = 100 V

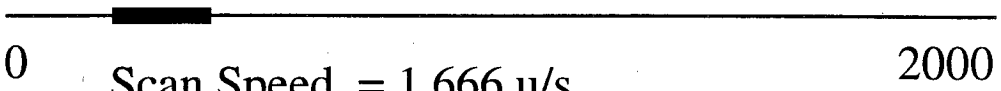

c) Scan Speed = 1,666 u/s
DC offset = 300 V

d) Scan Speed = 1,666 u/s
DC offset = 600 V

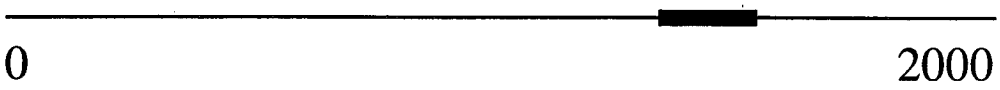

2.3 Comparison with Other Methods

As an ion storage device, an ion trap has the capability for high mass resolution, mass range, sensitivity, and MS^n that translates into versatile performance as a mass spectrometer. In comparison to triple quadrupole and TOF mass spectrometers, the ion trap is unique in its ability to perform MS^n. All three techniques are about equal in terms of mass accuracy and sensitivity. When utilizing electrospray ionization or MALDI, mid-fmol to low pmol levels of sample are typically used to obtain both MS and MS/MS spectra (29, 30), similar to results obtained by triple quadrupole and TOF mass spectrometry. Lower levels are possible, but are not routine at the present. Sensitivity is improved by varying the ion collection time and selectively injecting the ion of interest. The ion trap, with MALDI, has shown equivalent performance to TOF mass spectrometers at low mass range with the added advantage of exact precursor ion selection and MS^n. It is unlikely the ion trap will be as suitable for ultra-high mass analysis as TOF mass spectrometers due to hardware limitations of the auxiliary frequency generator used to extend the mass range. High molecular weight spectra obtained for singly-charged proteins (30 - 50 kDa range) have shown results comparable to those obtained using a linear time-of-flight (TOF) mass spectrometer without the implementation of delayed extraction techniques.

There are several limitations of the performance of quadrupole ion trap mass spectrometers. The alternate scan modes of triple quadrupole mass spectrometers such as precursor ion and neutral loss scans are currently not possible. Furthermore, the number

of ions injected into the ion trap must be carefully controlled since space-charging can degrade the performance of the instrument. This problem is solved through a rapid pre-scan that assesses the ion current injected into the trap for ~50 μs, then sets the ionization time to maximize the signal while minimizing space charge. Finally, when MS/MS is performed, all ions with q_z values below that of the resonance point will be ejected from the ion trap; therefore, a complete sequence of complementary b- and y-type ions typically cannot be obtained. Cotter *et al.* have recently shown that using low q_z values in conjunction with a heavier target gas affords full tandem mass spectra; consequently, the ejection of low *m/z* fragment ions during CID is not a fundamental limitation of the ion trap (31). Perhaps one major advantage of the ion trap not easily overlooked is the size of the instrument. As lab space becomes tighter, the size of the ion trap and ease of maintenance becomes a considerable advantage.

2.4 The New Generation of Ion Traps

In the past, the ITMS has not been an instrument well-suited for the robust and routine analyses required by biochemists and biologists. High performance innovations to the ITMS developed over the last several years have been used to build a new generation of ion trap mass spectrometer, the Finnigan MAT LCQ. This instrument has been carefully designed to interface with atmospheric pressure ionization techniques that are optimal for the analysis of biomolecules. The operating characteristics of the instrument have been changed by using a fundamental rf of 760 kHz instead of 1.1 MHz, an electrode spacing of 0.707 cm instead of 1.0 cm, and a q_z value of 0.83 instead of 0.908 for resonance ejection

of ions (32). Ion injection into the ion trap has been optimized using a lensing system that consists of two rf-only octopoles, resulting in a narrow spatial and energy distribution of the injected ions (16, 33). Selective injection, trapping, and excitation of ions is performed using tailored waveforms, analogous to the SWIFT technique (34). Unit mass resolution, or the ability to separate an *m/z* value of 1500 from 1501, is maintained over the 2000 dalton mass range with a mass accuracy of 0.015% (35). These figures of merit are comparable with the performance of current triple quadrupoles. It is expected that the mass range of the LCQ will increase to 5000 daltons in the next year.

The most striking feature of the new ion trap is the software control of instrument operation. Ion traps are operated through the use of a scan function that sets the ion injection time, trapping voltages, cooling time, tickle voltages, and voltage ramping for acquisition of the mass spectrum. Once a scan function is established for a given experiment, it can be used again but some parameters may need to be changed based on the *m/z* value of the ion of interest. For example, MS, MS/MS, MS^n and high resolution experiments all require the construction of unique scan functions. Significant interaction and expertise with the software was required with the older ion traps. The LCQ was developed with Ion Trap instrument Control Language (ITCL), a computer language that controls all of the elements of the scan function. For example, the hypothetical ITCL command "*hires 1200*" would set up the scan function to isolate the ion at *m/z* 1200 then slow the scan rate to achieve high mass resolution. All parameters required are automatically set with the one ITCL command, compared with the necessity to manually set a number of parameters using the ITMS software.

The ITCL language also enables the user to perform data-dependent experiments. A mass scan can return to the computer program all the information it acquires during the

scan. For example, a command such as "*hires mass(1)*" would perform a high resolution mass scan on the most intense ion returned from the previous mass scan. Very complicated data-dependent routines such as "on-the-fly" tandem mass spectrometry can be performed by stringing together commands in the form of a computer program. A graphical user interface is employed to simplify the use of the ITCL language and to edit the type of experiment desired during the course of an analysis. An *m/z* measurement, followed by a high resolution scan to separate the isotopes of the desired ion for charge state determination, followed by tandem mass spectrometry, is achieved by selecting the experiment through the user interface. The software can automatically select precursor ions based on some predefined criteria such as abundance, presence, or absence of an ion in a predefined list. No user intervention in the process is required except for the initial setup of the analysis. This level of control is unprecedented in mass spectrometry. In fact, the reliance on embedded software control is so great that instrument upgrades will essentially require downloading software from a CD-ROM to change operational parameters, obviating the need for expensive additions of hardware. A number of different automated, data-dependent experiments are possible including full range MS at unit resolution, MS^n with n=1 to 10, single ion monitoring (SIM) and single reaction monitoring (SRM), charge state determination (utilizing the "ZoomScan") of up to +4 ions, and unit resolution isolation up to *m/z* 1200.

2.5 Conclusion

The quadrupole ion trap is an extremely versatile instrument capable of performing multiple stages of mass spectrometry with one mass analyzer. High resolution techniques

afford easy charge-state determination, facilitating the interpretation of data generated by electrospray ionization. The sensitivity and performance characteristics of the instrument, especially the automated experiments developed for the newly commercialized ion traps, make quadrupole ion trap mass spectrometry an attractive technique to apply to the analysis of biological and biochemical problems as is demonstrated in the following chapters.

2.6 References

1. McLuckey, S. A., Van Berkel, G. J., Goeringer, D. E., and Glish, G. L. (1994) *Anal. Chem.* **66,** 13, 689A-696A.

2. Dahl, D. A. (1995) , Lockheed Martin Idaho Technologies, Idaho Falls, ID.

3. March, R. E., and Hughes, R. J. (1989) *Quadrupole Storage Mass Spectrometry,* (Winefordner, J.D. and Kolthoff, I.M., Eds.) *in* Chemical Analysis: A Series of Monographs on Analytical Chemistry and its Applications, **V102**, Wiley & Sons, New York.

4. Paradisi, C., Todd, J. F. J., Traldi, P., and Vettori, U. (1992) *Org. Mass Spectrom.* **27** 251-254.

5. Paradisi, C., Todd, J. F. J., Traldi, P., and Vettori, U. (1992) *Rapid Commun. Mass Spectrom.* **6** 641-646.

6. Williams, J. D., Reiser, H.-P., Kaiser, R. E., Jr., and Cooks, R. G. (1991) *Int. J. Mass Spectrom. Ion Proc.* **108** 199-219.

7. Williams, J. D., Cox, K. A., Cooks, R. G., McLuckey, S. A., Hart, K. J., and Goeringer, D. E. (1994) *Anal. Chem.* **66** 725-729.

8. Guidugli, F., and Traldi, P. (1991) *Rapid Commun. Mass Spectrom.* **5** 343-348.

9. Eades, D. M., Johnson, J. V., and Yost, R. A. (1993) *J. Am. Soc. Mass Spectrom.* **4** 917-929.

10. Cox, K. A., Williams, J. D., Cooks, R. G., and Kaiser, R. E., Jr. (1992) *Biol. Mass Spectrom.* **21** 226-241.

11. McLachlan, N. W. (1947) *in* Theory and Applications of Mathieu Functions, Clarendon, Oxford.

12. Wuerker, R. F., Shelton, H., and Langmuir, R. V. (1959) *J. Appl. Phys.* **30** 342-349.

13. Soni, M. H., and Cooks, R. G. (1994) *Anal. Chem.* **66** 2488-2496.

14. McLuckey, S. A., Goeringer, D. E., and Glish, G. L. (1991) *J. Am. Soc. Mass Spectrom.* **2** 11-21.

15. Doroshenko, V. M., and Cotter, R. J. (1993) *Rapid. Commun. Mass Spectrom.* **7** 822-827.

16. Jonscher, K. R., and Yates, J. R., III (1996) *Anal. Chem.* **68** 659-667.

17. Kaiser, R. E., Jr., Cooks, R. G., Stafford, G. C., Jr., Syka, J. E. P., and Hemberger, P. H. (1991) *Int. J. Mass Spectrom. Ion Proc.* **106** 79-115.

18. Dawson, P. H., Hedman, J., and Whetten, N. R. (1969) *Rev. Sci. Instrum.* **40** 1444-1450.

19. Mather, R. E., Waldren, R. M., and Todd, J. F. J. (1978) *Dyn. Mass Spectrom.* **5** 71-85.

20. Louris, J. N., Cooks, R. G., Syka, J. E. P., Kelley, P. E., Stafford, G. C., Jr., and Todd, J. F. J. (1987) *Anal. Chem.* **59** 1677-1685.

21. Kaiser, R. E., Jr., Louris, J. N., Amy, J. W., and Cooks, R. G. (1989) *Rapid Commun. Mass Spectrom.* **3** 225-229.

22. Julian, R. K. (1993) *Anal. Chem.* **65** 1827-1833.

23. Cooks, R. G., McLuckey, S. A., and Kaiser, R. E., Jr. (1991) *Chem. Eng. News* **69** 26-41.

24. Cooks, R. G., and Kaiser, R. E., Jr. (1990) *Acc. Chem. Res.* **23** 213-219.

25. Roepstorff, P., and Fohlman, J. (1984) *Biomed. Mass Spectrom.* **11** 601.

26. McLuckey, S. A., Goehringer, D. E., and Glish, G. L. (1992) *Anal. Chem.* **64** 1455-1460.

27. Qin, J., and Chait, B. T. (1995) *Proc. of the 43rd ASMS Conf. on Mass Spectrom. and Allied Topics* May 21-26, Atlanta, GA, American Society for Mass Spectrometry, p. 1100.

28. Fischer, E. (1959) *Z. Phys.* **156** 1-5.

29. Yates, N. A., Shabanowitz, J., and Hunt, D. F. (1994) *Abs. Paps. Am. Chem. Soc.* **208** 132-ANYL.

30. Qin, J., and Chait, B. T. (1995) *Proc. of the 43rd ASMS Conf. on Mass Spectrom. and Allied Topics*, May 21-26, Atlanta, GA, American Society for Mass Spectrometry, p. 989.

31. Cotter, R. (1996) Photonics West Conference, Jan. 27-Feb. 3.

32. Schwartz, J. C., Bier, M. E., Taylor, D. M., Zhou, J., Syka, J. E. P., James, M. S., and Stafford, G. C. (1995) *Proc. of the 43rd ASMS Conf. on Mass Spectrom. and Allied Topics*, May 21-26, Atlanta, GA, American Society for Mass Spectrometry, p. 1114.

33. Bier, M. E., Schwartz, J. C., Zhou, J., Taylor, D., Syka, J., James, M., Fies, B., and Stafford, G. (1995) *Proc. of the 43rd ASMS Conf. on Mass Spectrom. and Allied Topics*, May 21-26, Atlanta, GA, American Society for Mass Spectrometry, p. 1117.

34. Taylor, D., Schwartz, J., Zhou, J., James, M., Bier, M., Korsak, A., and Stafford, G. (1995) *Proc. of the 43rd ASMS Conf. on Mass Spectrom. and Allied Topics*, May 21-26, Atlanta, GA, American Society for Mass Spectrometry, p. 1103.

35. Land, A. P., Wheeler, K., Mylchreest, I. C., Sanders, M., and Jardine, I. (1995) *Proc. of the 43rd ASMS Conf. on Mass Spectrom. and Allied Topics*, May 21-26, Atlanta, GA, American Society for Mass Spectrometry, p. 653.

Chapter 3

Matrix-Assisted Laser Desorption of Peptides and Proteins on a Quadrupole Ion Trap Mass Spectrometer

3.1 Overview

The use of ultraviolet matrix-assisted laser desorption ionization (MALDI) to ionize peptides and proteins for analysis in a quadrupole ion trap is described. An ion source was modified to accommodate a fiber optic to transmit laser radiation from a nitrogen laser (337 nm) to the tip of the sample probe containing peptide or protein samples in a matrix of 2, 5-dihydroxy benzoic acid (DHB) or sinapinic acid. Detection limits are demonstrated with 10 fmol of sperm-whale myoglobin. The dimer of sperm-whale myoglobin was also observed at *m/z* 34,430. A comparison is made between the tandem mass spectrum (MS/MS) of human angiotensin I desorbed by MALDI and the mass spectrum for the peptide desorbed by liquid secondary ion mass spectrometry. Both spectra were found to contain abundant structural information.

In a practical application of the technique, the dominant phosphorylation site of the P protein from Sendai virus is localized by MALDI/quadrupole ion trap mass spectrometry. The P protein from Sendai virus, a murine *paramyxovirus*, is reported in the literature to be a highly phosphorylated protein. *In vitro* studies have detected phosphorylation in different regions of the protein while a single phosphopeptide was

observed using *in vivo* techniques. Analysis by mass spectrometry revealed two phosphopeptides proximal in the P protein sequence.

3.2 Instrument Development

3.2.1 Introduction

Ultraviolet matrix-assisted laser desorption ionization (MALDI) has been an effective means of creating ions for the molecular weight analysis of large biomolecules (1-4) and complex mixtures of peptides and proteins (5). The pulsed nature of the ionization event and the high velocities of the resulting ions has limited its use mainly to time-of-flight mass spectrometers, although this technique has been applied more recently to magnetic sector instruments with integrating array detectors (6, 7) and ion trap mass spectrometers (8-13). Instruments such as the Fourier-transform mass spectrometer (FTMS, FT-ICR) and the quadrupole ion trap mass spectrometer (ITMS) function as ion storage devices and hence are well-suited for use with pulsed ionization techniques. Additionally, these instruments are capable of analyzing small quantities of sample and performing multi-stage tandem mass spectrometry (MS^n) experiments (14-16). These features, in conjunction with the utility of MALDI for the ionization of peptides and proteins present in complex mixtures, create a powerful approach for structural characterization of peptides and proteins.

Interfacing MALDI to ion trap mass spectrometers presents a unique challenge. Ions are created with high velocities and wide angular distributions which may be difficult to trap in the mass analyzer (17). Two approaches have been used in FTMS instruments to

trap these ions. The first approach takes advantage of collisional damping to trap the desorbed ions. Buchanan and co-workers pulsed argon into the ion cyclotron resonance (ICR) cell concurrent with the laser pulse to damp the velocity of the ions to a level where they could be trapped in the magnetic field (8, 9). Mass analysis was delayed until the argon was pumped from the ICR cell to improve mass resolution. Russell and co-workers employed a laser desorption ion source recessed slightly from the entrance of the ICR cell which was designed to allow a small volume of helium to be pulsed into the source concurrent with the laser radiation (12). The velocity of the desorbed ions was damped as they collided with helium in the source and then drifted from the source into the ICR cell. A second approach utilized by Wilkins and co-workers created a potential well between the trapping plates to constrain the desorbed ions once they entered the ICR cell (10). Proteins as large as 34,000 Da have been ionized, trapped, and analyzed by this method.

The trapping of ions in quadrupole ion traps is less problematic since the ion trap is operated with ~1 mtorr of helium in the trap volume. Ions injected into or created in the trap lose kinetic energy as they undergo collisions with the helium (18). Two approaches utilizing laser desorption have been used to introduce ions into the ion trap. In the first, employed by Louris and co-workers, ions were generated near the endcap aperture then extracted and focussed axially into the ion trap (19). Rather than transmit the laser radiation through the cavity of the trap, the sample probe was recessed from the entrance aperture and the probe tip irradiated by a fiber optic at an angle of ~90° relative to the ion-optical path. Ions were extracted and focused into the entrance endcap aperture using an einzel lens. A second approach involved radial desorption of ions into the cavity of the ion trap through a hole in the ring electrode (20-22). In this case two holes were drilled on opposite sides of the electrode, one for insertion of the sample probe into the wall of the ring

electrode and the other for transmitting the laser radiation to the sample probe. Ions were then desorbed directly into the cavity of the ion trap. The above two methods were pioneered with non-matrix assisted laser desorption techniques.

Cox and co-workers demonstrated MALDI using an arrangement similar to that of Louris and co-workers and successfully observed bovine insulin B-chain (11). Chambers and co-workers obtained a mass spectrum of horse cytochrome c using a MALDI arrangement as described in Ref. 21 (13). Both of these examples illustrate that MALDI experiments can be conducted on ITMS instruments.

The objectives of this study were to extend the earlier work of Cox and co-workers, to determine if an external ionization source on a quadrupole ion trap can be used to focus protein ions created by MALDI into the ion trap, and to obtain an estimate of the detection limits of the technique. In addition, we examined the feasibility of performing MS/MS experiments on peptide ions generated from MALDI to determine the potential for extending protein sequence analysis to MALDI-ITMS. A preliminary account of this work has been presented (23). At the same conference, Bier and co-workers also presented a preliminary account of peptide and protein analysis using MALDI-ITMS with mass range extension by reducing the fundamental rf frequency to extend the nominal mass range of the ion trap (24).

3.2.2 Experimental

3.2.2.1 Ionization Source

The external MALDI source was constructed of modified components from a Finnigan MAT continuous-flow fast atom bombardment ion source (Bioprobe source

block, Finnigan MAT, San Jose, CA, USA) to improve positioning of the fiber optic. The sample probe was electrically isolated from the ion source block with a Vespel sleeve to allow the application of an independent potential to the probe. In general the probe was kept near ground potential. Lenses 1 and 2 were modified by drilling the aperture to a diameter of 0.150" to afford a wider angle of ion acceptance into the optical path. The diameter of lens 3 was 0.125". The sample probe was approximately 0.100" from the first lens. Typical voltages for the lenses were as follow: lens 1 -2 V, lens 2 -196 V, lens 3 -24 V, and the ion trap was floated at -9 V. An ion gating lens was positioned prior to the entrance aperture of the endcap electrode and its potential was varied between +36 V (gate closed) and -186 V (gate open). The helium pressure in the mass analyzer region was nominally 1 mTorr.

The 200 μm fiber optic (Radiant Communications Corporation, South Plainfield, NJ, USA) was passed into the vaccum manifold through a 1/8" diameter inlet on a custom vaccum flange (MDC, Hayward, CA, USA). A hole was drilled through lens 1 to position the optical fiber so that the transmitted radiation impinged upon the probe tip at an angle of approximately 45°. The fiber optic was coupled to a VSL-337 nitrogen laser (Laser Science, Inc., Newton, MA, USA) using a single-mode adapter. The laser was rated at 3 mW maximum average power and 175 μJ/pulse maximum energy (at 10 Hz). A 200 μm or 400 μm optical fiber was employed to transmit the beam. The laser power exiting the fiber optic was estimated to be 3.7×10^7 W/cm^2 for the 200 μm fiber and 1.45×10^7 W/cm^2 for the 400 μm fiber. These estimates are based on coupling efficiencies of 20% (200 μm) and 40% (400 μm fiber). Laser repetition rates were typically ~4.5 Hz (220 ms/cycle) for single-stage mass spectrum scans and ~3.7 Hz (270 ms/cycle) for MS/MS scans and were adjusted by entering a delay in the ITMS scan function. A laser pulse was

initiated from the TTL signal used to trigger the ion gate on the ITMS electronics. A diode and emitter-follower were used to protect the gate signal, while an RC delay was placed between two non-inverting CMOS hex buffers to obtain a TTL signal to trigger the laser ~500 μs after the rise of the gate.

3.2.2.2 Mass Spectrometry

A quadrupole ion trap using components of an ITMS (Finnigan MAT) and a triple quadrupole mass spectrometer, TSQ 70 (Finnigan MAT), was constructed at Finnigan MAT. The ITMS was housed in the differentially pumped region of the TSQ 70 vacuum manifold facilitating the coupling of commercially available TSQ 70 ion sources to the ion trap. A 3 kV lens was placed near the exit endcap electrode to focus ions to the 20 kV conversion dynode/electron multiplier assembly. The rf signal from the ITMS electronics was directed onto the ring electrode *via* a ceramic feedthrough in a central flange in the vacuum manifold. The signal from the electron multiplier was transferred to the ITMS electronics and the resulting mass spectrum displayed on a Compaq 386 computer. The auxiliary frequency generator in the ITMS electronics was used to place a supplementary rf signal on the endcap electrodes. Typically, 6 microscans were summed in the memory of the Compaq 386 computer and transferred to a DECStation 2100 workstation where each set of scans were further averaged using modified ICIS software. A 2-6 point mass calibration curve was generated with the software (created by Joe Zhou at Finnigan MAT) to display calibrated spectra. Calibration curves were stable for several days if conditions were not altered (*e.g.*, mass range and helium pressure).

An example of a single-stage mass spectrum ion trap scan function is shown in Figure 3.1(a) and typically included a 100 ms delay to adjust the laser cycle, followed by a 5 ms ionization period during which ions were injected into the ion trap. During ion injection the amplitude (700-3500 $V_{0\text{-}p}$) of the fundamental rf was chosen to optimize signal intensity for the ion of interest. Typically, the rf amplitude was increased to a constant value for 6 ms to eject low mass matrix ions and to reduce space charge effects. The conversion dynode and electron multiplier were set at -15 kV and 1.7 kV, respectively for data acquistion.

The ITMS scan function used to record an MS/MS spectrum is shown in Figure 3.1(b) and typically included a 50 ms cycle time delay, 5 ms ionization period, and 6 ms ejection pulse. A precursor ion was isolated with a 30 ms reverse scan with resonance ejection applied to remove ions with mass-to-charge ratios higher than that of the ion of interest and a 30 ms forward scan to eject ions of mass-to-charge ratios lower than that of the ion of interest (25, 26). The ion was then brought into resonance at a q_z value of 0.2-0.3 with a small supplementary rf voltage (0.5-2.5 V) which was applied for 30 ms to promote fragmentation via collisions with the helium bath gas. The mass spectrum resulting from the fragmentation products was then acquired using the appropriate mass range.

3.2.2.3 Sample Preparation

Porcine renin substrate tetradecapeptide (1759 Da), human angiotensin I (1296 Da), bovine insulin (5734 Da), sperm-whale myoglobin (17,199 Da), and porcine elastase (25,898 Da) were purchased from Sigma Chemical Company (Saint Louis, MO, USA)

Figure 3.1: (**a**) ITMS scan function for a molecular weight scan. (**b**) ITMS scan function for an MS/MS scan. MS/MS is accomplished by isolating the ion of interest with a combination of forward and reverse scans, then inducing collision-induced dissociation *via* resonance excitation.

a) MS Scan Function

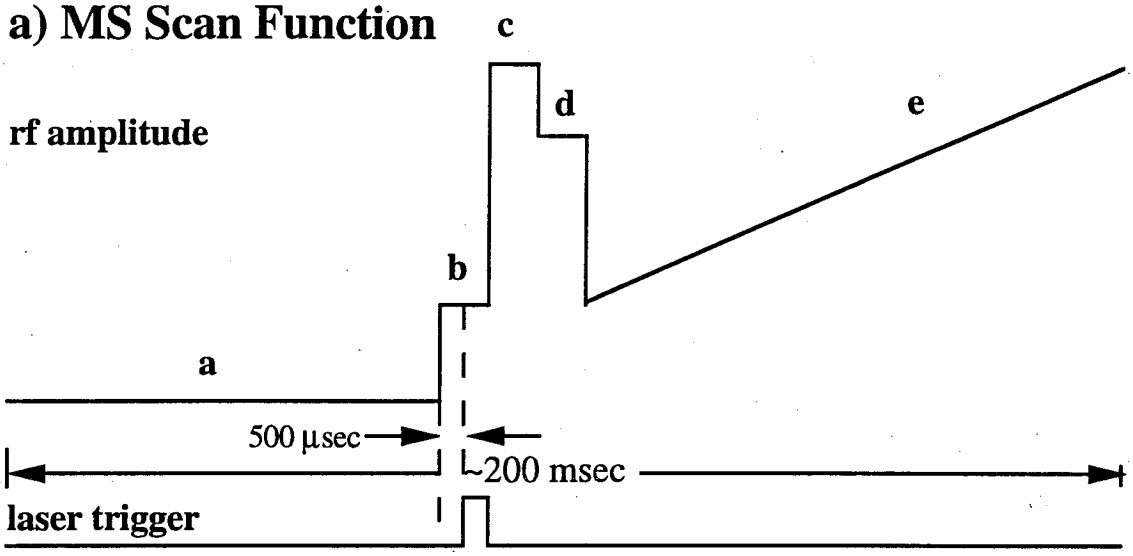

a - delay to adjust laser cycle
b - ionization period
c - pulse to eject low mass ions
d - turn on multiplier
e - acquisition

b) MS/MS Scan Function

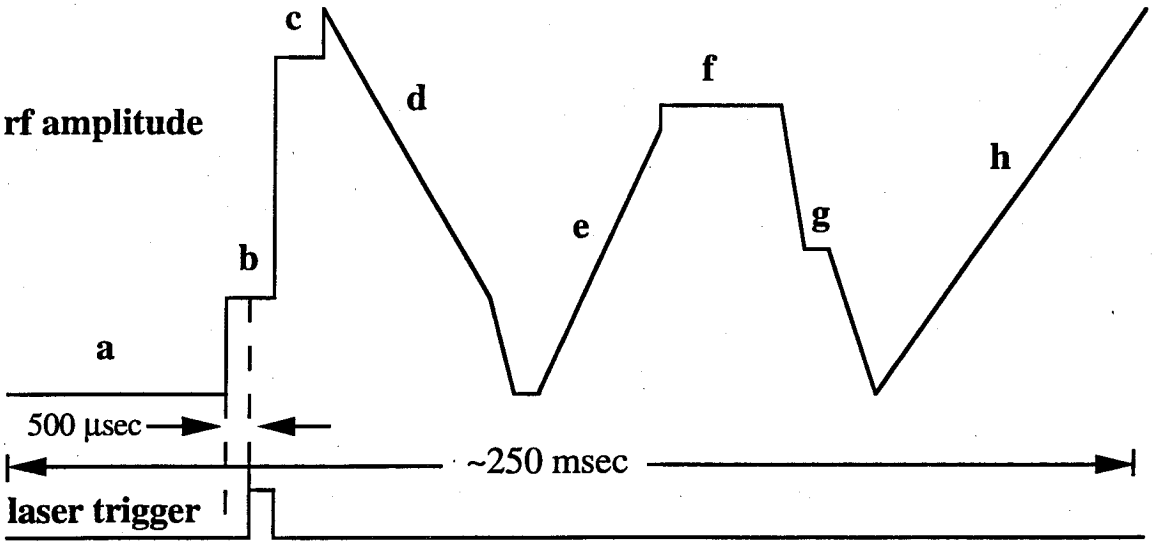

a - delay to adjust laser cycles
b - ionization period
c - pulse to eject low mass matrix ions
d - reverse scan to eject ions above *m/z* of interest
e - forward scan to eject ions below *m/z* of interest
f - "tickle"
g - turn on multiplier
h - acquisition

and used without further purification. 2,5-Dihydroxybenzoic acid (DHB) and sinapinic acid were purchased from Aldrich Chemical Company (Milwaukee, WI, USA). Sample and matrix were dissolved in a 1:1 mixture of ultrapure water and high-performance liquid chromatography (HPLC) grade acetonitrile (EM Science, Gibbstown, NJ, USA). Sample stock solutions were at a concentration of ~1 nmol/μL with matrix solutions at ~1000-2000 nmol/μL. Spectra were acquired using equivolume mixtures of sample and matrix giving a 1:1,000 sample-to-matrix ratio deposited onto a 0.050" stainless steel probe tip. Sample dilutuions for detection limit experiments were carried out on a polished Teflon plate and aliquots of sample and matrix solutions were mixed to obtain the desired concentration.

3.2.3 Results and Discussion

MALDI is a versatile technique for the ionization of peptides and proteins. In light of the utility of this ionization method, it was of interest to couple a MALDI source to a quadrupole ion trap mass spectrometer for the analyses of peptides and proteins. Previous research on a MALDI-ITMS using a fiber optic to transmit laser radiation has demonstrated the ability to analyze molecules up to 3500 Da in molecular weight (27). The analysis of larger peptides or proteins by this approach has recently been reported by Chambers and co-workers; however, they were unable to observe ions with values of *m/z* greater than 13,000 Da and realized a significant drop in sensitivity above *m/z* 3000 (13). Here we report the mass analysis of proteins of molecular weight up to 26 kDa by

MALDI-ITMS using an external ion source and fiber optic transmission of radiation from a nitrogen laser.

Initial MALDI experiments utilized an ion source configuration similar to that of Wright and co-workers (28). In this experiment the laser beam was directed orthogonal to the sample probe and intercepted the probe surface at an angle of 45°. The intensity of the ion signals observed with this method were weak (signal-to-noise ratio 3:1) and sporadic. In laser desorption experiments using a UV absorbing matrix, Beavis and Chait noted that the ion plume is directed normal to the probe surface and that the ion velocity is 750 m/sec (17). This would account for the relatively weak ion signals since it is unlikely that the lensing system would be able to redirect the initial 45° trajectories of the fast moving ions into the ion optical path. The ion source was then modified to place the probe surface perpendicular to the ion optical path and to position the fiber optic at an angle of ~45° relative to the probe surface normal. This configuration is depicted in Figure 3.2.

Shown in Figure 3.3 is the mass spectrum of the tetradecapeptide, renin substrate, obtained by desorbing a 1:2000 mixture of 250 fmol of peptide and DHB applied to the sample probe. All ions below 95 u had unstable trajectories during injection and were ejected from the trap. In this manner the effects of space charge were reduced by limiting the number of low-mass matrix ions in the trap. Peptide ions were resonantly ejected with an auxiliary field frequency of 89,202 Hz having 8.8 V_{p-p} amplitude. To determine the reproducibility of mass measurements and resolution, a total of 10 mass spectra were acquired from the 250 fmol sample. Mass resolution and mass measurement accuracy averaged 300 (measured as full width at half height (FWHH)) and 0.082%, respectively.

For the analysis of proteins, the fiber optic was switched to a 400 μm diameter fiber to increase the area of irradiation. The laser power density based on estimated

Figure 3.2: Schematic diagram of the MALDI-QITMS system. The ion trap electrodes are located in the analyzer region of the differentially pumped vacuum manifold of a TSQ 700 triple quadrupole mass spectrometer.

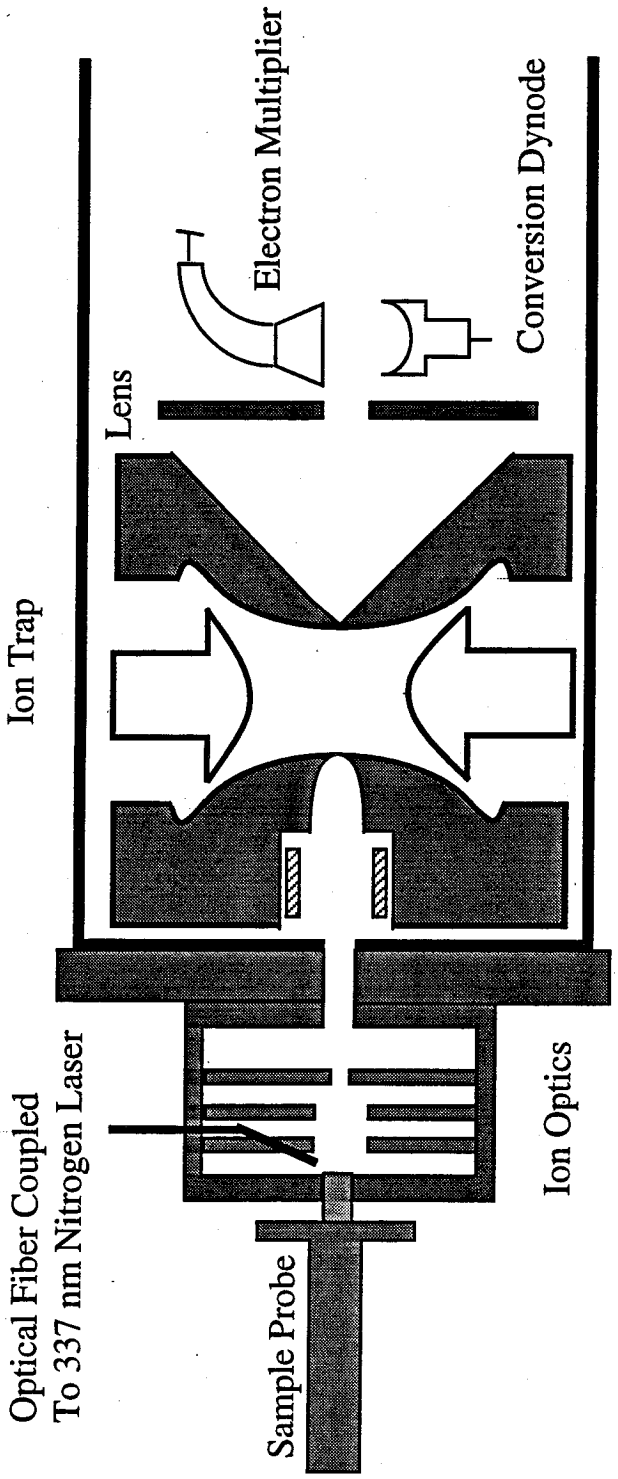
Optical Fiber Coupled
To 337 nm Nitrogen Laser
Sample Probe
Ion Optics
Ion Trap
Lens
Electron Multiplier
Conversion Dynode

Figure 3.3: Mass spectrum of 250 fmol of tetradecapeptide renin substrate in a 1:2000 ratio with 2,5-dihydroxybenzoic acid. $[M+H]^+$ = 1758.9 (average). The exclusion limit was 95 u and resonance ejection occurred at a frequency of 89,202 Hz, 8.8 V_{p-p} amplitude.

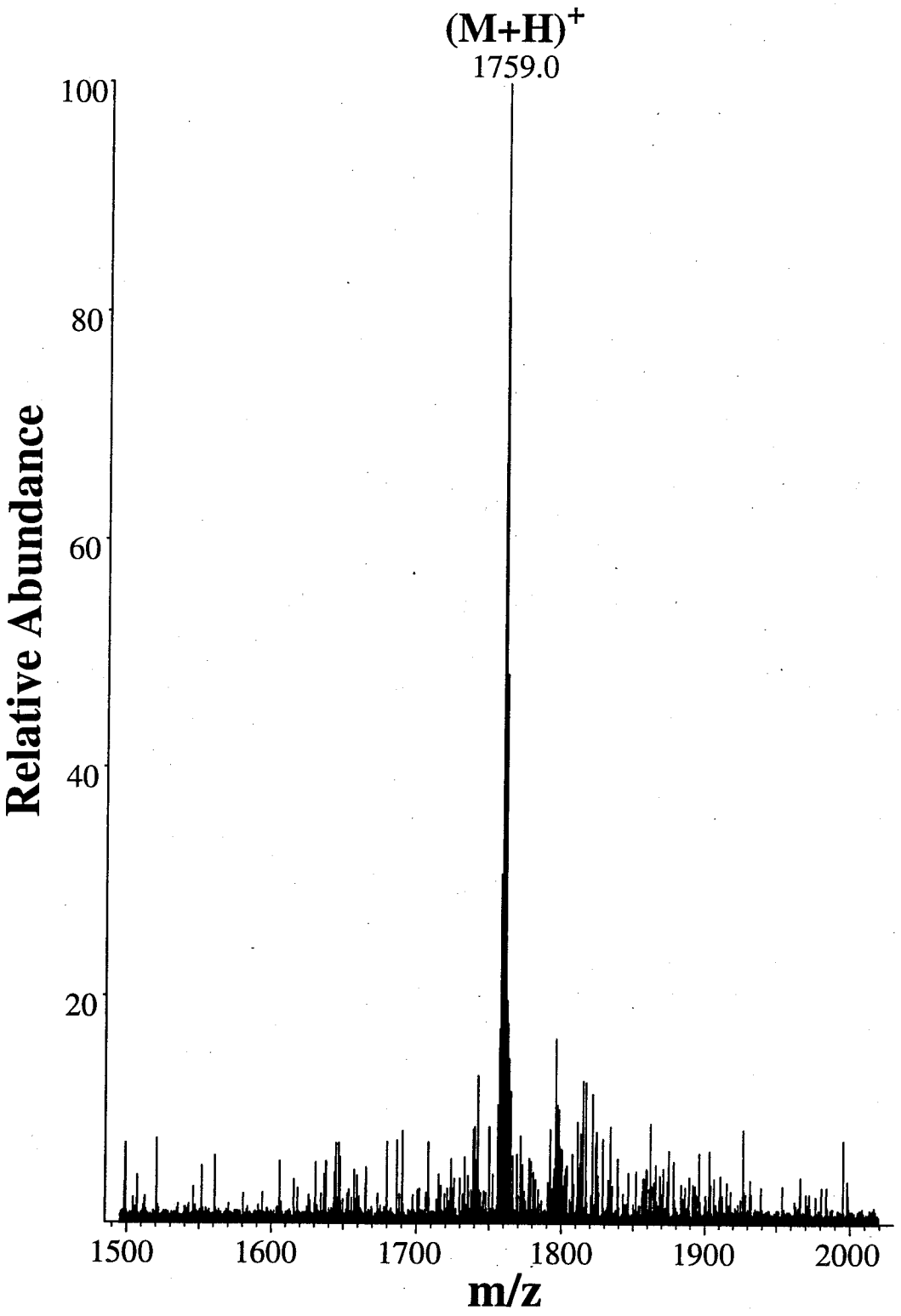
(M+H)+
1759.0
100
80
60
40
20
Relative Abundance
1500
1600
1700
1800
1900
2000
m/z

coupling efficiencies provided by the manufacturer show the laser power of the 400 μm fiber optic to be less than that of the 200 μm fiber optic (by roughly 3-fold) but still within the range necessary for matrix-assisted laser desorption (10^7 W/cm^2). Shown in Figures 3.4(a) and 3.4(b) are the mass spectra of bovine insulin and cytochrome c desorbed using a 400 μm fiber optic. The mass spectra result from 60 and 114 laser shots, respectively, with each spectrum exhibiting mass resolution of approximately 100. In both examples ions below *m/z* 300 were excluded from the trap. Some fragmentation may have occurred, indicated by the appearance of ions characteristic of insulin B chain. The mass resolutions calculated were comparable to those observed on time-of-flight instruments due, in part, to the increased scan rate associated with mass range extension using resonant ejection. Schwartz and co-workers have observed that mass resolution can be increased dramatically with a slowing of the scan speed by keeping ions near resonance for a longer period of time prior to ejection from the ion trap (29). In these experiments no attempts were made to increase the mass resolution by decreasing the scan speed.

3.2.3.1 Tandem Mass Spectrometry

Multiple-stage mass spectrometry performed on the ion trap has been demonstrated by a number of groups (14-16, 20). Ions in the trap may be resonantly excited by the application of a supplementary rf voltage on the endcap electrodes corresponding to the secular frequency of the precursor ion. The amplitude of the supplementary rf must be chosen to optimize fragmentations due to collisions with the helium bath gas without ejecting the ions corresponding to the protonated molecule. The amplitude of the rf voltage

Figure 3.4: (**a**) Bovine insulin in 2,5-dihydroxybenzoic acid at a ratio of 1:1000. Ions below 300 u were not trapped and ions were ejected at 23,351 Hz, 5.2 V_{p-p}. $[M+H]^+$ = 5707 (average). (**b**) Bovine cytochrome *c* in a 1:1000 mixture with sinapinic acid. $[M+H]^+$ = 12223 (average). The exclusion limit was 330 u and ions were resonantly ejected at 7,848 Hz, 9 V_{p-p}.

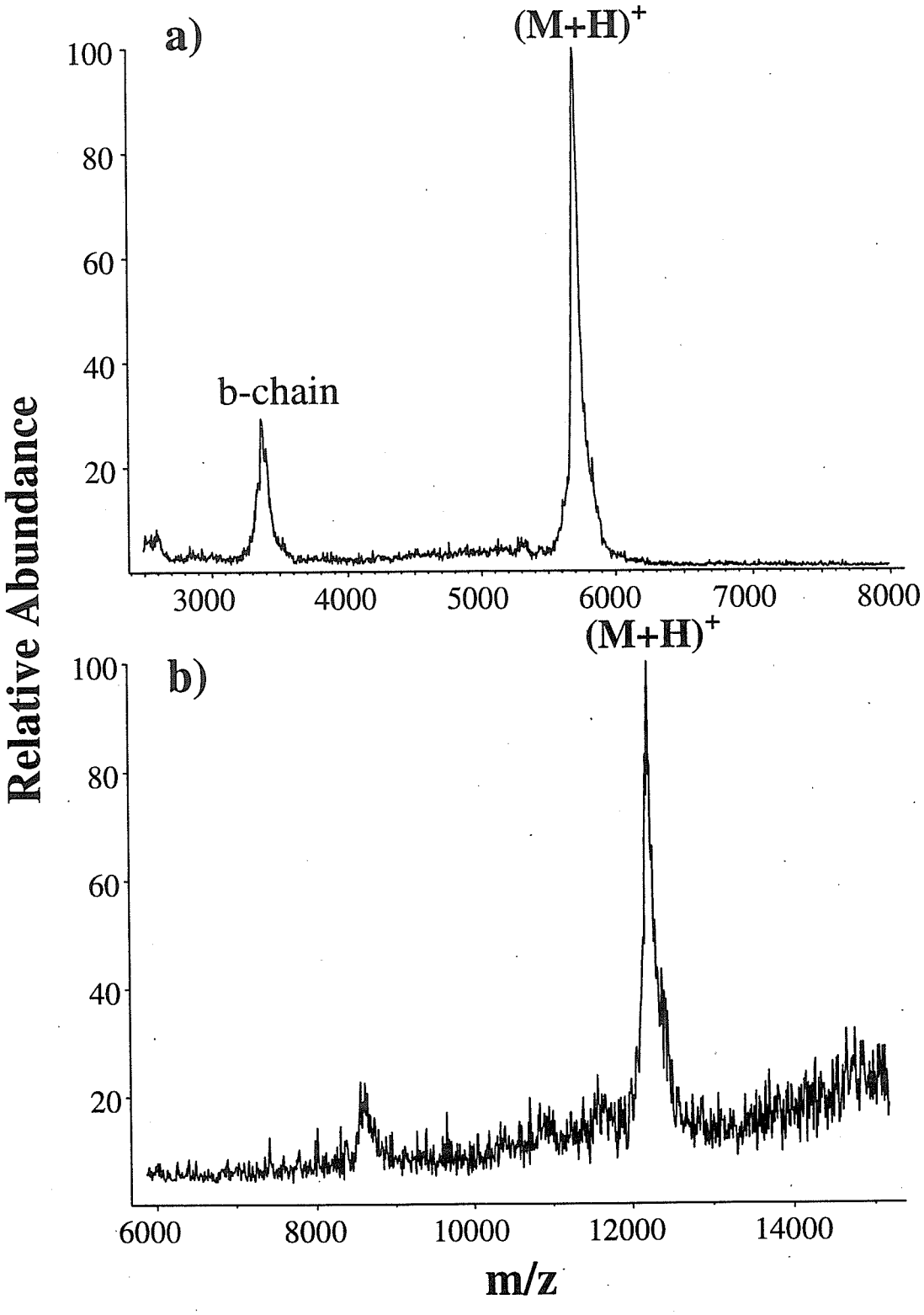
a)
(M+H)+
b-chain
100
80
60
40
20
3000
4000
5000
6000
7000
8000
b)
(M+H)+
6000
8000
10000
12000
14000
m/z
Relative Abundance

is experimentally determined. Kaiser and co-workers demonstrated MS/MS of peptide ions produced from liquid secondary ion mass spectrometry (LSIMS) (14). The mass spectrum was rich in structural information showing abundant b- and y-type ions. Shown in Figure 3.5 are the MS/MS spectra of angiotensin I produced by peptides desorbed/ionized by (a) MALDI (in a 1:1000 ratio with DHB) and (b) LSIMS (in a thioglycerol matrix) using resonance excitation at a q_z of 0.3. All ions with *m/z* values below 430 u were ejected during excitation. The excitation frequency for the MALDI spectrum was 120,632 Hz at an amplitude of 3.18 V_{p-p}, while that for the LSIMS spectrum was 121,552 Hz at an amplitude of 3.10 V_{p-p}. In both examples 100 scans were averaged representing 600 laser or Cs^+ ion pulses. The mass spectra are nearly identical. The predominant fragment ions observed in the spectra are b- and y-type ions. Signals resulting from neutral losses of water, ammonia, and carbon monoxide (a-type ions) are also present. The peak marked with an asterisk is thought to result from surface interactions. The extent of fragmentation observed in the MS/MS spectrum is encouraging since fragment ions are observed for all amide bonds in the peptide except one.

3.2.3.2 Trapping large protein ions: effect of ionization exclusion limit

At a given ion kinetic energy, the exclusion limit specifies the ion of lowest *m/z* that can maintain a stable trajectory within the ion trap. Theoretically, at a given kinetic energy, the optimal rf voltage is proportional to the square root of the mass of the injected ion (27)

$$V_{rf} = \frac{z_o \omega}{\sqrt{KE \cdot m}} \qquad \text{(Eq. 3.1)}$$

Figure 3.5: (**a**) MALDI-MS/MS spectrum of angiotensin I in 2,5-dihydroxybenzoic acid at a 1:1000 ratio. The precursor ion was resonantly excited at 120,632 Hz, 3.18 $V_{p\text{-}p}$. (**b**) LSIMS/MS spectrum of angiotensin I in a thioglycerol matrix. The precursor ion was excited at 121,552 Hz, 3.10 $V_{p\text{-}p}$. Both spectra result from 600 laser/Cs^+ shots. In both cases, fragment ions are observed for all but one amide linkage.

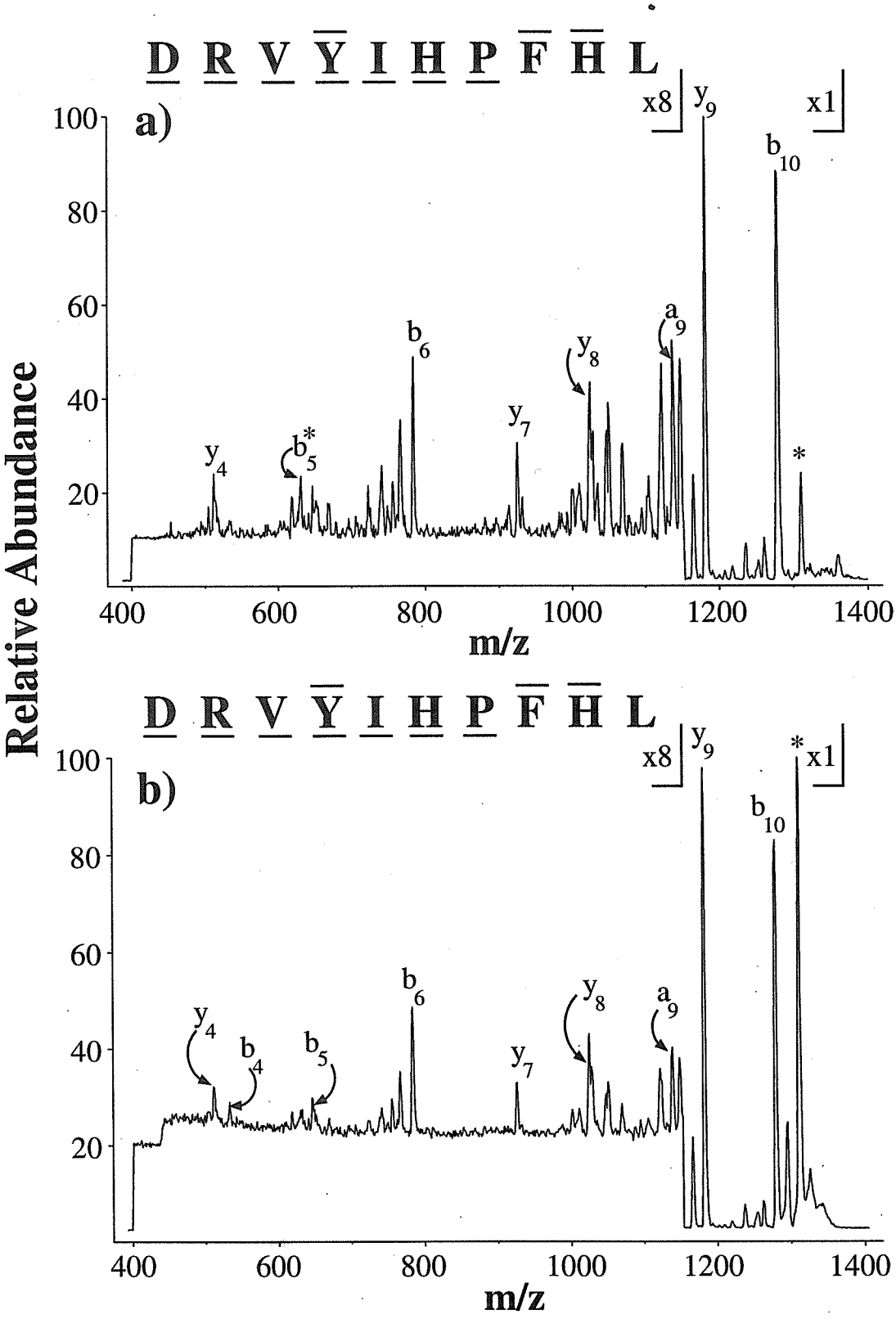
D R V Y I H P F H L
a)
x8
x1
y9
b10
a9
b6
y8
y7
y4
b*5
*
100
80
60
40
20
400
600
800
1000
1200
1400
m/z
Relative Abundance
D R V Y I H P F H L
b)
x8
y9
*
x1
b10
a9
b6
y8
y4
b4
b5
y7
100
80
60
40
20
400
600
800
1000
1200
1400
m/z

where V_{rf} = optimal rf amplitude, z_o = distance from the center of the trap to the endcap vertex, and ω = fundamental frequency (1.1 MHz). Kaiser, using CsI cluster ions generated by LSIMS, showed that the exclusion limit is linear with respect to the square root of the mass of the injected ions over a large mass range (<6000 Da) (27). The range of optimal rf voltages used to trap an ion of specific mass and energy is generally narrow and may cause significant mass discrimination. To estimate the conditions for trapping large ions generated by MALDI, optimal rf voltages were determined for a variety of peptide ions generated by LSIMS, ranging in *m/z* from 1295 (angiotensin I) to 3500 (bovine insulin B chain). The experimental optimal rf voltage expressed as an exclusion limit was found to be proportional to the square root of the mass of the injected ion as predicted by theory. In addition, these conditions were found to be suitable for trapping ions generated by MALDI. Figure 3.6 is a graph of the exclusion limits used to trap MALDI ions *vs.* the square root of the mass of the injected ion. A linear relationship is found over a large mass range and therefore this relationship can be used to predict the exclusion limit necessary to trap ions of a desired *m/z*.

Shown in Figure 3.7 is the mass spectrum of a mixture of whale myoglobin (17,199 Da) and porcine elastase (25,898 Da). The dimer of myoglobin (34,399 Da) also appears. This experiment illustrates that proteins with a molecular weight difference of at least 17 kDa may be trapped and mass analyzed under the same set of conditions. However, this does not imply that the conditions were optimal for all the ions and some mass discrimination may have occurred. The exclusion limit of 430 u was chosen to optimize trapping efficiency for the dimer of myoglobin. The mass range was extended to 40,000 u using a resonance signal at 5883 Hz, with 5 V_{p-p} amplitude. These conditions

Figure 3.6: Optimal rf voltage expressed as an exclusion limit *vs.* square root of mass. The relationship appears to be linear throughout the mass range.

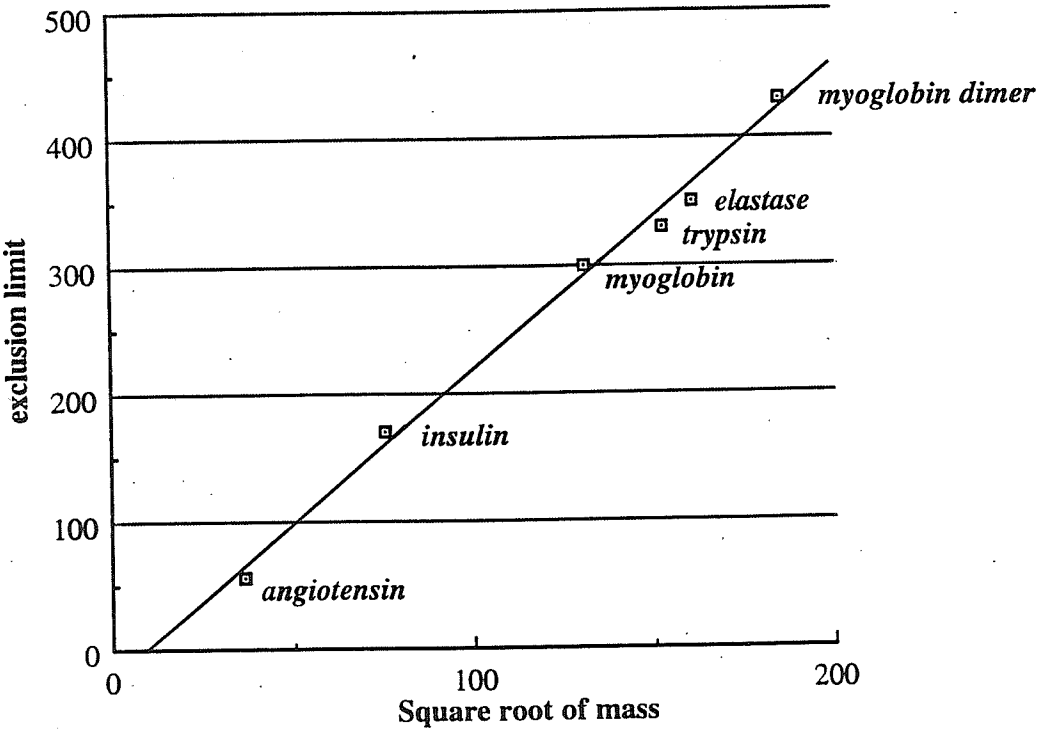
500
400
300
200
100
0
exclusion limit
0
100
200
Square root of mass
myoglobin dimer
elastase
trypsin
myoglobin
insulin
angiotensin

Figure 3.7: Mass spectrum of 50 pmol porcine elastase, $[M+H]^+$ = 25,871 (average), and 100 pmol of myoglobin, $[M+H]^+$ = 17,143 (average). The dimer of myoglobin appears at $[M+H]^+$ = 34,430 (average). The exclusion limit was 430 amu and ions were ejected using a signal at 5883 Hz, 5 V_{p-p}.

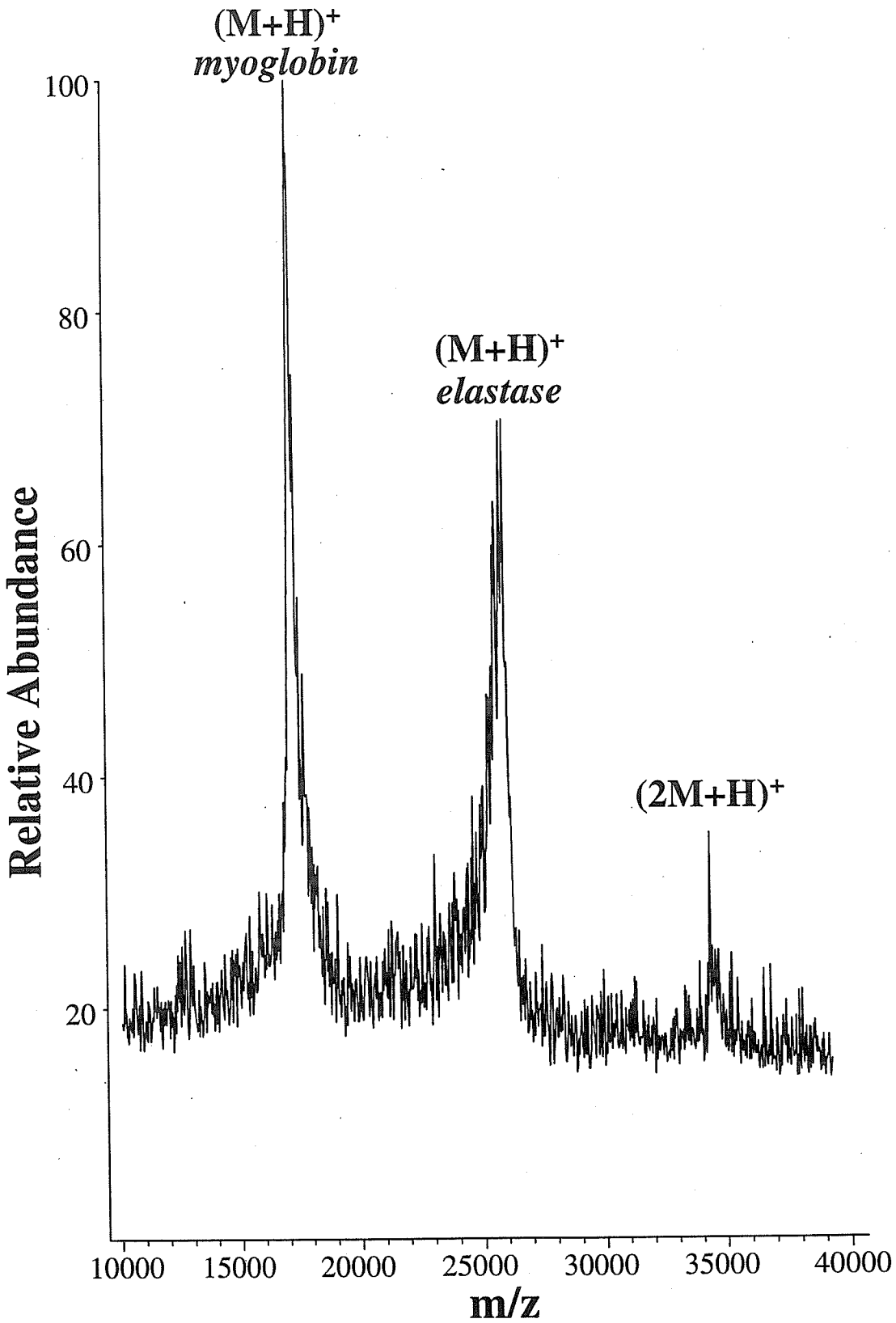
(M+H)+
myoglobin
(M+H)+
elastase
(2M+H)+
Relative Abundance
100
80
60
40
20
10000
15000
20000
25000
30000
35000
40000
m/z

resulted in a mass resolution of 31 and 85 for elastase and the dimer, respectively. Proteins of higher molecular weight should be observable by reducing the fundamental rf frequency to extend the nominal mass range of the ion trap (24).

3.2.3.3 Detection Limits

The detection limit of a mass spectrometer is a good indicator of the utility of the system for a given application. Protein ions generated by MALDI from 1 fmol of cytochrome *c* and 700 fmol of a β-galactosidase subunit (MW 116 kDa) have been observed on a time-of-flight instrument (20, 30). Additionally, 2.1 amol of a peptide, gramicidin S, has been observed on an ITMS interfaced with LSIMS (14). Thus, the potential for a high sensitivity technique based on a MALDI and ITMS combination for the analysis of peptides and proteins is clearly evident. To test the system's ability to detect low quantities of sample, successively smaller amounts of sample and matrix were applied to the sample probe and analyzed. To insure that no sample was carried over between each analysis, the probe tip was filed down, soaked in 5% acetic acid, and sonicated in methanol for 10 min. A matrix blank was used to verify that no sample remained on the probe tip. Analyses of the protein myoglobin using 500 to 0.1 fmol of the sample applied to the probe was attempted. Below 10 femtomoles ions were observed, but the signal was sporadic. Stable signal was observed at the 10 fmol level.

Shown in Figure 3.8 is the mass spectrum for 10 fmol of myoglobin. A total of 10 scans were averaged from 60 laser shots and a mass resolution of 50 with a signal-to-noise ratio of 5:1 was observed. As has been noted in the literature, the local homogeneity of the

Figure 3.8: 10 fmol of whale myoglobin in sinapinic acid at a 1:11 x 10^6 ratio. $[M+H]^+$ = 17,294 (average). The exclusion limit was 330 u and resonance ejection occurred at 7848 Hz, 9 V_{p-p}. The mass spectrum results from averaging 10 scans.

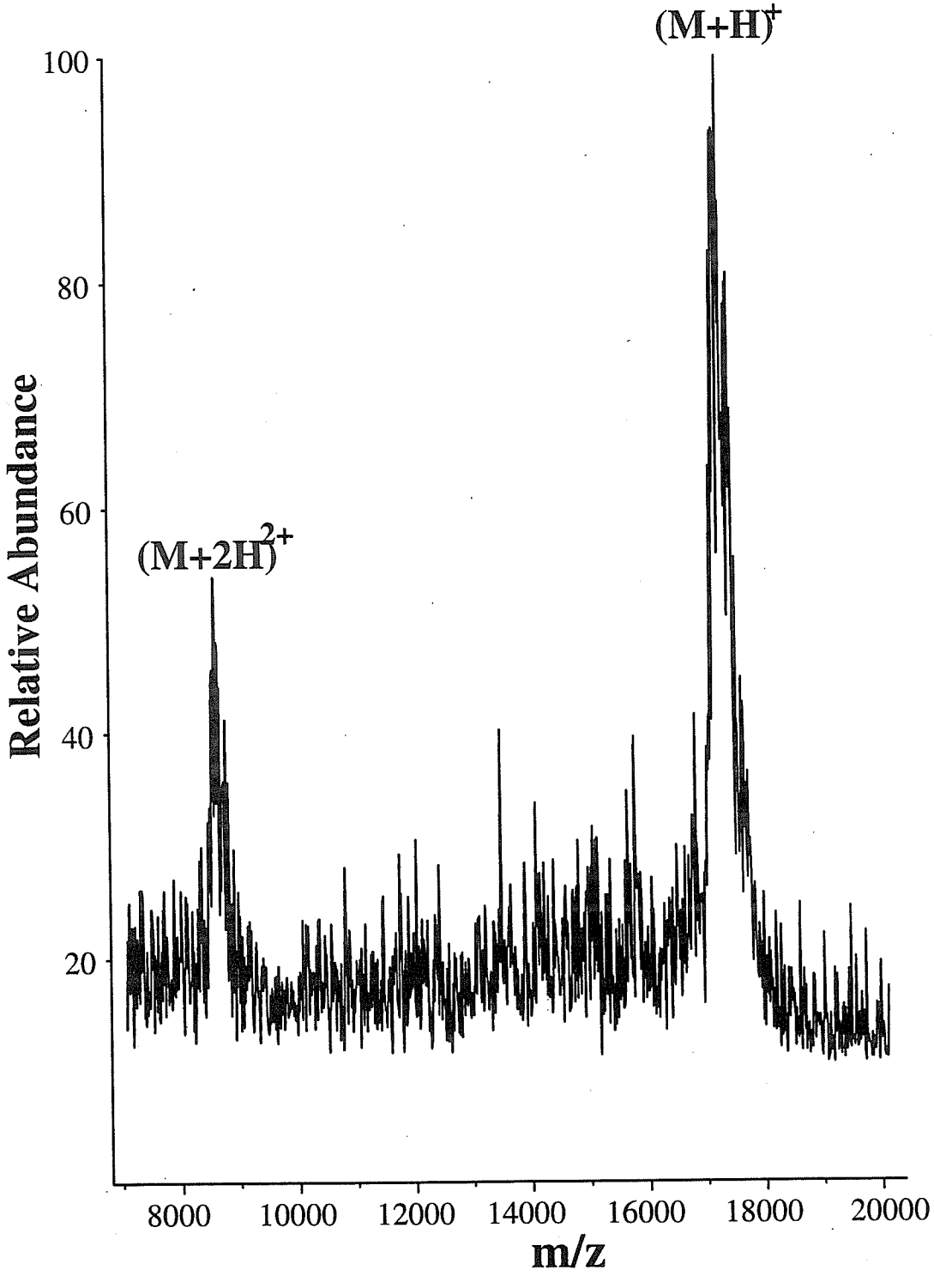
(M+H)+
100
80
60
40
20
Relative Abundance
(M+2H)2+
8000
10000
12000
14000
16000
18000
20000
m/z

matrix/analyte solution is an important parameter for successful MALDI-MS, as is the analyte:matrix ratio (31, 32). Optimization of the sample preparation and deposition may produce more consistent signal at lower sample levels.

3.3 Application of MALDI/ITMS for Analysis of Phosphopeptides

3.3.1 Overview

The P protein from Sendai virus, a murine *paramyxovirus*, is reported in the literature to be a highly phosphorylated protein. *In vitro* studies have detected phosphorylation in different regions of the protein while a single phosphopeptide, identified as the sole phosphorylation site, was observed using *in vivo* techniques. In this work, using a direct approach, two phosphorylation sites of the P protein from Sendai virus are localized by matrix-assisted laser desorption ionization (MALDI)/quadrupole ion trap mass spectrometry. A computer-aided approach is used to confirm peptide identification.

3.3.2 Introduction

Sendai virus is the murine prototype of the *paramyxovirus* family, belonging to the order of Mononegalvirales. Related human pathogens include a number of types of parainfluenza virus, mumps, measles, and respiratory syncytial virus; as well as the more distantly related *filoviruses*, Marburg and Ebola. Animal pathogens comprise Newcastle disease, cattle and bird parainfluenza viruses, canine distemper, and murine pneumonia.

An understanding of the functioning of the Sendai virus prototype would provide insights into the function and replication of these ubiquitous human and animal viruses.

The genome of the Sendai virus consists of a single-strand of RNA with negative polarity that codes for at least six structural and five non-structural proteins (33-35). The RNA core is encapsidated by a helical nucleocapsid protein (NP). Virions enter cells directly through surface membranes, and viral replication and transcription, mediated by viral polymerase, begins immediately in the cytoplasm. Polymerase activity is carried out by the polymerase-associated phosphoprotein, P protein, of MW 65,000 u and the large protein, L protein, of MW 200,000 u (36, 37). Almost all of the viral proteins are phosphorylated; however, the P protein appears to be more heavily phosphorylated on a mole-per-mole basis (38, 39). The P protein also seems to be modular in nature (40). N-terminal and C-terminal domains are conserved among *paramyxoviruses* (52% and 69% homology, respectively) while a 100 residue region in the middle is variable with ~11% homology (41, 42). The C-terminal domain has been shown to stabilize the L protein (43) and the N-terminal region interacts with the NP protein and has been shown to be essential for RNA encapsidation as well as RNA synthesis (44).

A number of studies were undertaken to locate sites of post-translational modification to understand the role phosphorylation plays in the function of the P protein. *In vitro* experiments reported conflicting results where phosphorylation sites were detected in the first N-terminal quarter of the protein (39) or in the second N-terminal quarter of the protein (45). More recent work (46) showed that cell-free phosphorylation using virion-associated protein kinase (VAPK) as a phosphorylating agent caused phosphorylation of both serine and threonine. In contrast, intracellular experiments in which the phosphorylation state of the P protein was analyzed during virus replication indicated that

phosphorylation occurred only on serine residues. The number of detected phosphorylation sites also differed between the *in vitro* and the *in vivo* techniques. Enzymatic digestion of the VAPK-phosphorylated P protein using trypsin, followed by two-dimensional thin layer electrophoresis (2D TLE), produced four major spots and nine minor spots (46). Similar experiments utilizing intracellular analysis produced one major spot with several minor spots and it was concluded that the P protein in infected cells was primarily phosphorylated at one or a set of adjacent sites (46). Site-directed mutagenesis was subsequently used to identify the primary location of phosphorylation on the P protein (47). In a parallel effort described here, direct analysis using quadrupole ion trap mass spectrometry was employed to identify P protein phosphorylation sites.

3.3.3 Experimental

3.3.3.1 Mass Spectrometry

A quadrupole ion trap mass spectrometer (ITMS) (Finnigan MAT, San Jose, CA, USA) placed in the vacuum manifold of a TSQ 70 triple quadrupole mass spectrometer (Finnigan MAT) was interfaced to an external matrix-assisted laser desorption ionization (MALDI) source as described previously (48). A 200 μm core fused silica optical fiber was used to ionize the sample by irradiation with a 337 nm beam from a nitrogen laser (Laser Science, Inc., Newton, MA, USA). The ion trap volume was filled with helium to an uncorrected pressure of 5×10^{-4} Torr, then argon was added using a separate needle valve to bring the final uncorrected pressure to 5.5×10^{-4} Torr. The addition of ~10% (pressure/pressure) argon to the trapping volume serves to improve the trapping efficiency (49), the resolution of the mass spectrum, and slightly increases the amount of

fragmentation achieved upon injection into an ion trap. The ion beam was focused into the ion trap using a three-element einzel lens. Typical lens voltages were as follows: Lens 1 -5 V, Lens 2 -190 V, Lens 3 -20 V, Ion gate -200 V (open)/+ 200 V (closed), trap float -11 V, and the probe was held at 5 V.

The ion trap scan employed to obtain a single-stage mass spectrum consisted of the following steps (48): A 100 ms delay was used to adjust the laser cycle to ~4.5 Hz. Ions were allowed into the ion trap during a 5 ms ionization period when the gating tube lens was set to "open." The TTL signal used to trigger the ion gate operation was also employed to trigger the laser to fire ~500 μs after the ion gate opened. The rf level during the ionization period was typically set to 1154 $V_{0\text{-}p}$. This enabled ions with *m/z* values above 100 u to be stably trapped. The amplitude of the rf voltage was ramped to 7500 $V_{0\text{-}p}$ in order to eject matrix ions with *m/z* values less than 650 u. The electron multiplier was then turned on. Data acquisition was accomplished by ramping the amplitude of the rf signal while applying a supplementary signal to the endcap electrodes to resonantly eject ions through the endcap electrode and into the conversion dynode/electron multiplier detection system (25, 50). Details appear in the relevant figure captions. The conversion dynode and electron multiplier were set at -15 kV and 1.2 kV, respectively, for data acquisition. Supplemental signals were also applied to the endcap electrodes to cause amplification of ion trajectories by resonance excitation (14). Subsequent ion fragmentation was induced by collisions with the helium damping gas and afforded amino acid sequence information. Mass spectra were displayed on a Compaq 386 PC then ported to a DECStation 2100 for data acquisition and analysis. Baseline subtraction at a given threshhold was performed to remove artifacts due to software normalization.

A LaserMAT (Finnigan MAT) linear time-of-flight (TOF) instrument was also used to screen fractions for the presence of phosphopeptides and to determine the number of peptides in each sample. Ions generated by the MALDI process were extracted from the source and accelerated into a field-free flight tube employing a 20 kV potential. Detection was accomplished using a 15 kV conversion dynode coupled to an electron multiplier.

3.3.3.2 Sample Preparation

Recombinant ^{32}P labeled P protein from Sendai virus was infected into CV1 cells and purified by immunoprecipitation (47) then enzymatically digested with trypsin or chymotrypsin. A portion of the protein digests were separated by 2D TLE. Spots on the gel were excised and peptides extracted (46). Aliquots of both the protein digests and the extracted peptides, estimated to contain 1-3 nmol of material, were lyophilized and reconstituted in 0.1% trifluoroacetic acid (TFA) (Aldrich Chemical Co., Milwaukee, WI, USA) to a concentration of 0.1 - 1 mM. This material served as a stock solution and was stored at -4° C.

3.3.3.2.1 Chromatography

Aliquots of the stock solutions representing an estimated 250 pmol of material were loaded onto a 20 µL Peek injection loop and concentrated by washing with 100% Solvent A (0.1% TFA) on an α-Chrom column (300 Å pore diameter packed with Reliasil C_{18}, 2 mm X 10 cm, Upchurch Scientific, WA, USA) using an ABI 140B dual pump solvent delivery system (Applied Biosystems, Foster City, CA, USA) pumping at a flowrate of 75 µL/min. Peek materials were utilized instead of stainless steel to minimize

sample losses due to interaction of phosphopeptides with iron. Peptides were separated by reverse phase high performance liquid chromatography (HPLC) and eluted utilizing a 60 min gradient of 0-80% Solvent B (70:30:0.085 acetonitrile (HPLC grade, EM Science, Gibbstown, NJ, USA):water:TFA, v:v:v). Peptides were detected by monitoring UV absorbance at a wavelength of 220 nm. Fractions were collected into polypropylene microcentrifuge tubes, lyophilized to dryness (Savant Instruments, Farmingdale, NY, USA) and stored at -4°C. Samples were subsequently reconstituted in 10 - 15 µL of 0.1% TFA prior to analysis.

3.3.3.2.2 Edman Degradation

Manual Edman degradation was performed by reconstituting lyophilized fractions in 10 µL of 5% phenylisothiocyanate in pyridine added to 10 µL of 50% aqueous pyridine followed by heating at 37°C for 30 min. The organic layer was extracted twice with 20 µL of 2:1 heptane:ethyl acetate and the aqueous material lyophilized. Cleavage of the N-terminal amino acid residue was accomplished by adding 10 µL of TFA to the sample, heating at 37°C for 15 min, then lyophilizing. A final extraction was made using 30 µL of water combined with 50 µL of *n*-butyl chloride. The sample was lyophilized then reconstituted in 0.1% TFA and applied to the probe tip as described below.

3.3.3.2.3 MALDI

Matrix consisted of a saturated solution of α-cyano-4-hydroxycinnamic acid (Aldrich Chemical Co., Milwaukee, WI, USA) in an equivolume mixture of 0.1% TFA and acetonitrile. A 1/2 µL aliquot of sample was co-deposited onto a gold-plated stainless

steel probe tip with 1 μL of matrix and allowed to air dry. The probe was then inserted into the vacuum chamber utilizing a ball valve and the laser was employed to ionize the sample.

3.3.3.3 Data Analysis

A database consisting of the transcribed genetic sequence of the P protein was constructed. The PEPM™ (Finnigan MAT) algorithm (51) was used to identify all possible sequences of amino acid residues in the database with molecular weights within +/- 5 u of the experimentally determined molecular weight for the peptide of interest. The software also listed the predicted y-, b- and a-type ions (nomenclature described in (52)) to aid in the analysis of the fragmentation mass spectra. SEQUEST, a database searching algorithm developed in our laboratory (53), was employed to confirm the identification of the amino acid sequences. A list of possible sequences in the P protein database was generated and theoretical fragmentation mass spectra constructed. The experimental fragmentation mass spectra were then compared to theoretical fragmentation mass spectra, scored, and ranked. Peaks in the mass spectra labeled with a "P" refer to fragmentation products generated from a phosphorylated peptide. The notation "γ" refers to the loss of a guanidino group from an Arg-containing ion while "*" refers to the loss of water or ammonia. Peaks labeled with $b_n y_m$ refer to internal cleavage products from fragmentation at Pro, His, or Arg residues, *e.g.*, given a peptide sequence LPQGW, b_2y_1 corresponds to PQGW, b_2y_2 corresponds to PQG, etc.

3.3.4 Results and Discussion

3.3.4.1 Peptide Mapping

Purified Sendai virus P protein was enzymatically digested using trypsin. Resultant peptides were separated by HPLC, fractions collected, and samples for mass spectrometric analysis prepared as described above. The MALDI ion trap and the MALDI TOF were used to screen the fractions for phosphopeptides and to provide a peptide map of the P protein. The ion trap was employed to obtain molecular weight information. The TOF was used to determine the number of peptides in each fraction since the ion trap mass spectra were complicated by the presence of fragmentation products. Some degree of fragmentation of peptide ions upon injection into ion trap mass spectrometers is common. The decomposition provided by metastable decay using the matrix α-cyano-4-hydroxycinnamic acid affords abundant sequence-specific fragmentation products which can be diagnostic for the structure of known biological molecules (54-58). The sequence-specific fragmentation produced upon injection into the ion trap provided verification of peptide assignment without the need to perform an additional tandem mass spectrometry experiment. Figure 3.9 shows the amino acid sequence of the P protein and the sequence coverage obtained by tryptic mapping. The tryptic map covered ~61% of the protein by mass with most of the coverage on the N-terminal half of the protein where the phosphorylation sites were expected (39, 45). Trypsin digestion produces 71 expected peptides. Thirty-four peptides were mapped, representing 48% of the expected trypsin fragments. The molecular weights for 25 of the peptides not identified were below the low-mass cutoff determined by the matrix ejection pulse and were not detected. The remaining 12 peptides accounted for 26% of the sequence and were not unambiguously

Figure 3.9: Amino acid sequence of the P protein of Sendai virus. Underlined residues are from peptides identified by tryptic mapping. The letter "c" below a residue indicates the phosphopeptide identified from the chymotrypsin digest, the letter "t" below a residue indicates the phosphopeptide identified from the trypsin digest, and the letter "o" indicates residues from a peptide overlapping that identified from the chymotrypsin digest.

```
1--------10---------20---------30---------40---------50

MDQDAFILKE DSEVEREAPG GRESLSDVIG FLDAVLSSEP TDIGGDRSWL

HNTINTPQGP GSAHRAKSEG EGEVSTPSTQ DNRSGEESRV SGRTSKPEAE

AHAGNLDKQN IHRAFGGRTG TNSVSQDLGD GGDSGILENP PNERGYPRSG

IEDENREMAA HPDKRGEDQA EGLPEEVRGS TSLPDEGEGG ASNNGRSMEP

GSSHSARVTG VLVIPSPELE EAVLRRNKRR PTNSGSKPLT PATVPGTRSP
                                                c ccccccccc
PLNRYNSTGS PPGKPPSTQD EHINSGDTPA VRVKDRKPPI GTRSVSDCPA
cc  tttttt ttttttttt ttttttttt tt
NGRSIHPGLE TDSTKKGIGE NTSSMKEMAT LLTSLGVIQS AQEFESSRDA

SYVFARRALK SANYAEMTFN VCGLILSAEK SSARKVDENK QLLKQIQESV

ESFRDTYKRF SEYQKEQNSL LMSNLSTLHI ITDRGGKTDN TDSLTRSPSV

FAKSKENKTK ATRFDPSMET LEDMKYKPDL IREDEFRDEI RNPVYQERDT

EPRASNASRL LPSKEKPTMH SLRLVIESSP LSRAEKAAYV KSLSKCKTDQ

EVKAVMELVE EDIESLTN
```

identified. The P protein was also digested with chymotrypsin to identify phosphopeptides not observed in the trypsin digest.

3.3.4.2 Trypsin Digestion

3.3.4.2.1 MALDI/Time-of-Flight Mass Spectrometry

One trypsin-generated peptide from HPLC fraction #16 with *m/z* 2911 was detected. The mass spectrum illustrated in Figure 3.10 shows detection of two major peaks with *m/z* values of 2911 and 2991. These differ in mass by 80 u, corresponding to the addition of HPO_3 to the hydroxyl group on the side chain of Ser. The mass difference suggests that the lighter peptide is the non-phosphorylated version of the heavier peptide. The mass corresponds to that of the tryptic peptide 255-282 and confirmation of the assignment using the ion trap mass spectrometer is discussed below. Four serine residues are contained within the sequence, thus the site of phosphorylation cannot be assigned based on the molecular weight data.

3.3.4.2.2 MALDI/Ion Trap Mass Spectrometry

Analysis of trypsin-generated HPLC fraction #16 afforded the mass spectrum shown in Figure 3.11. The dominant peak in the spectrum was at *m/z* 2909, correlating with the signal observed using the TOF mass spectrometer. A small peak at *m/z* 2989 was observed. The mass difference of 80 u again indicates that the heavier peptide was probably the phosphorylated analog of the lighter peptide. A strong signal is also observed at *m/z* 2890. This signal corresponds both to a loss of ~98 u (neutral loss of phosphoric acid from the phosphopeptide at *m/z* 2989) and a loss of water from the unphosphorylated

Figure 3.10: Linear time-of-flight mass spectrum for the phosphopeptide of *m/z* 2909 resulting from trypsin digestion of the P protein. Ten laser shots were summed.

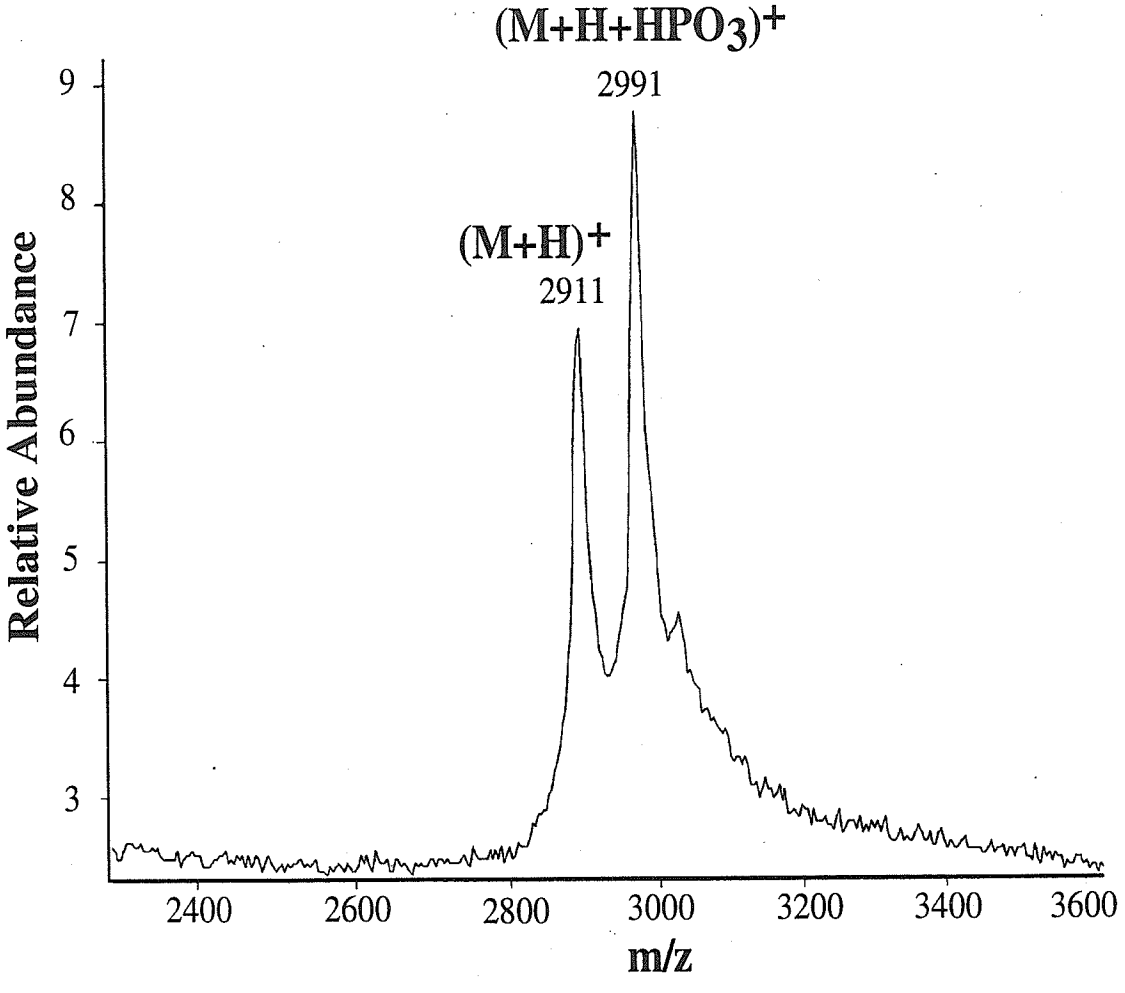
(M+H+HPO3)+
2991
(M+H)+
2911
Relative Abundance
9
8
7
6
5
4
3
2400
2600
2800
3000
3200
3400
3600
m/z

Figure 3.11: Fragmentation mass spectrum for the phosphopeptide of *m/z* 2909 resulting from trypsin digestion of the P protein. The ion trap was set to stably trap ions with *m/z* values larger than 90 u. Matrix ions were ejected by ramping the amplitude of the rf voltage from 20 u to 650 u while applying a supplementary signal at 520,300 Hz, 5.6 V (peak-to-peak, endcap-to-endcap). The mass spectrum was acquired by ramping the amplitude of the rf voltage from 35 u to 650 u while applying a supplementary signal at 59,124 Hz, 8.0 V (peak-to-peak, endcap-to-endcap). (**a**) Sequence and expected *m/z* values of fragmentation products for the unphosphorylated form of residues 255-282. Observed ions are underlined. Ions corresponding to phosphorylated fragmentation products are shown above (b-type ions) and below (y-type ions) the unphosphorylated fragmentation products. (**b**) Fragmentation mass spectrum for *m/z* 2909. (**c**) Result of SEQUEST analysis.

a)

									1069				1452	
164	278	365	466	523	610	707	804	861	989	1086	1184	1271	1372	1500
Tyr	**Asn**	**Ser**	**Thr**	**Gly**	**Psr**	**Pro**	**Pro**	**Gly**	**Lys**	**Pro**	**Pro**	**Ser**	**Thr**	**Gln**
2909	2746	2632	2545	2444	2387	2300	2203	2106	2049	1921	1824	1727	1640	1539
2989	2826	2712			2467									

1695			2074		2275	2332	2447			2716		2971	P-b
1615	1744	1881	1994	2108	2195	2252	2367	2468	2565	2636	2735	2891	b
Asp	**Glu**	**His**	**Ile**	**Asn**	**Ser**	**Gly**	**Asp**	**Thr**	**Pro**	**Ala**	**Val**	**Arg**	
1411	1296	1167	1029	916	802	715	658	543	442	345	274	175	y
													P-y

b)

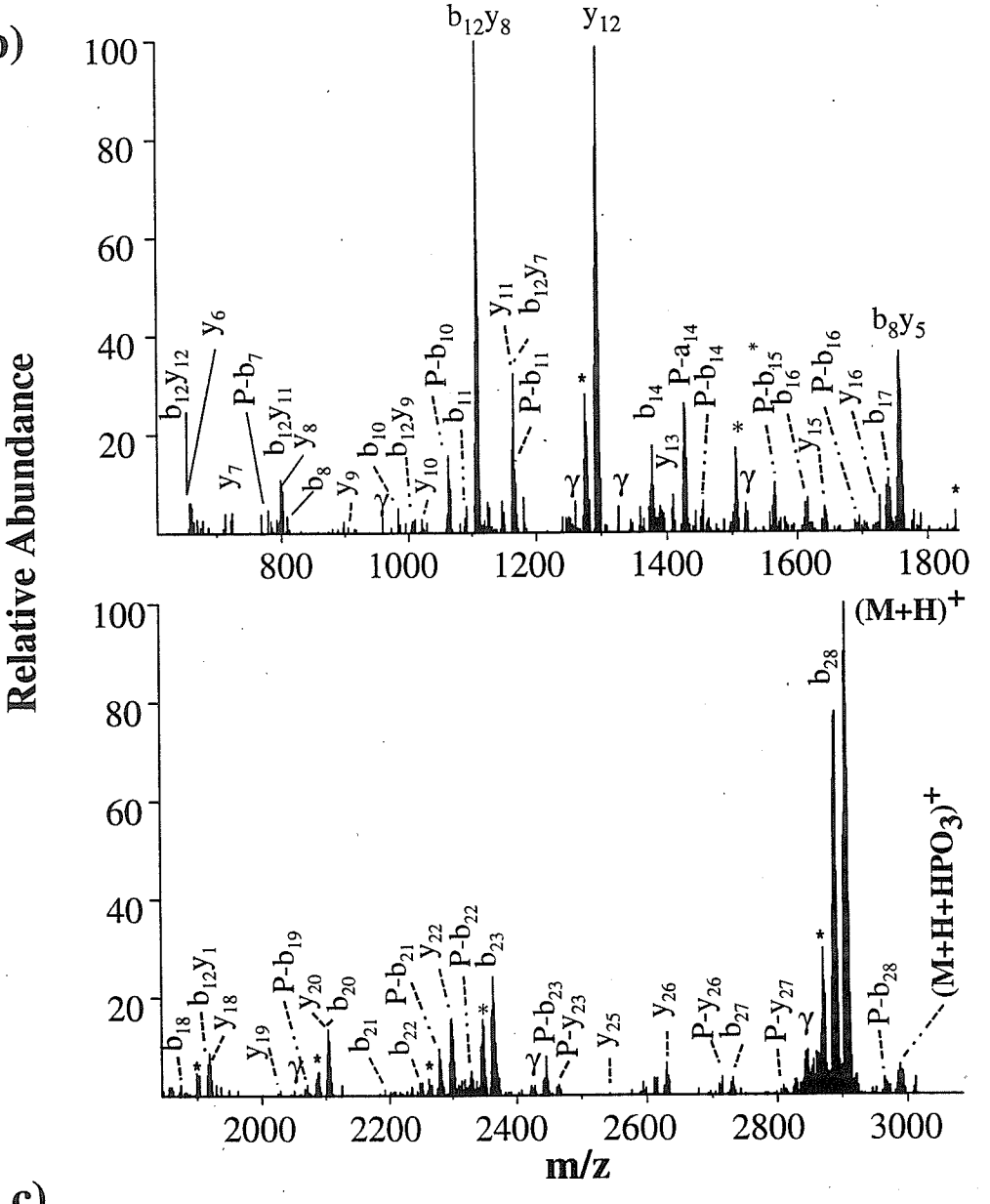

c)

#	Rank/Sp	(M+H)+	Cn	Sp	Ions	Peptide
1	1/1	2911.1	1.0000	77.4	14/81	(R)YNSTGSPPGKPPSTQDEHINSGDTPAVR
2	2/3	2910.2	0.3621	28.7	8/81	(A)TVPGTRSPPLNRYNSTGSPPGKPPSTQD
3	3/8	2908.2	0.3353	15.7	6/84	(S)GSKPLTPATVPGTRSPPLNRYNSTGSPPG
4	4/6	2910.1	0.2894	17.8	7/75	(-)MDQDAFILKEDSEVEREAPGGRESLS
5	5/4	2911.2	0.2225	22.0	7/66	(L)LKQIQESVESFRDTYKRFSEYQK

peptide. This loss of 98 has been shown to be a signature for the presence of phosphorylated serine and threonine (58-60).

A search of the P protein sequence using PEPM™ identified 37 possible peptides with *m/z* values within +/-5 u of 2909. Of these, five contained Lys or Arg at the C-terminus, corresponding to peptides produced by trypsin digestion. Only one of the five sequences corresponded to an expected tryptic fragment, residues 255-282. Theoretical values of b- and y-type ions for the sequence were calculated and compared to the fragment ions observed in the mass spectrum, shown in Figure 3.11(b). The observed fragment ions correspond to the product ions expected for the tryptic fragment 255-282, YNSTGSPPGKPPSTQDEHINSGDTPAVR, confirming the sequence assignment made using TOF analysis. The expected fragmentation products for the unphosphorylated sequence are displayed in Figure 3.11(a) and observed ions underlined. Unphosphorylated sequence ions corresponding to the major peaks in the mass spectrum were identified as were minor peaks arising from fragmentation of the phosphorylated species. The presence of a series of y- and b-type ions served to confirm the sequence assignment. Signal suppression of b-type ions is due to the large number of proline residues present. A number of signals were present corresponding to internal cleavages of the peptide modulated by proline and histidine residues. These peptides provided particularly strong signals when the C-terminal amino acid was Asp, in agreement with recent observations (58). The signal from the phosphorylated molecular ion was weak and a series of low abundance peaks afforded by fragmentation of the phosphopeptide were present. The presence of the y_{23} ion as well as its phosphorylated analog indicate that Ser-260 is the most likely site of phosphorylation. The phosphorylated analogs of $y_{26\text{-}28}$ as well as b_{10}, b_{14}, b_{16}, b_{19}, $b_{21\text{-}23}$, b_{26} and b_{28} also serve to confirm the identification. Contributions to low

abundance signals can also arise from the presence of other co-eluting peptides. Site-directed mutagenesis experiments (47) have shown that - S P - is a consensus sequence for phosphorylation of the P protein. The phosphopeptide generated using the trypsin digest contains four serine residues at Ser-257, Ser-260, Ser-267, and Ser-275. Only Ser-260 is followed by a proline; thus, the identification of Ser-260 as the phosphorylated residue would agree with the proposed mechanism of a proline-mediated kinase.

The SEQUEST database searching program was subsequently used to confirm the sequence assignment. Results in Figure 3.11(c) indicate that the expected sequence was chosen as the first-ranked choice. The final ranking is determined by the value for C_n and the answer is assumed to be reliable if the C_n value for the first choice is much greater than the C_n value for the second choice (53). This is the case for the sequence assignment in Figure 3.11(c); thus, the manually determined answer was verified by computer-aided interpretation. Additional stages of mass spectrometry were done on the most abundant fragmentation products (MS/MS and MS^3); however, no additional sequence information was obtained. Sub-digestion of the fraction on the probe tip using Asp-N was attempted, but the resulting peptides were not detected. The same phosphorylated peptide sequence was identified using sample extracted from the 2D-TLE experiment (data not shown).

The SEQUEST program is capable of searching sequences for post-translational modifications, such as phosphorylation. For the phosphopeptides identified in this work, the best results were obtained by searching using the unphosphorylated mass on a sequence database where phosphorylation was not included. We infer from this that the facile loss of phosphoric acid from the phosphopeptide tends to suppress further fragmentation; therefore, fragmentation proceeds primarily from the unphosphorylated species. Similar effects have been observed on another MALDI-ITMS (57).

3.3.4.3 Chymotrypsin Digestion

3.3.4.3.1 MALDI/Time-of-Flight Mass Spectrometry, Fraction #13

In previous work (54), digestion with chymotrypsin and subsequent 2D-TLE of the peptides produced two spots. In the present work, two candidate phosphopeptides were also observed when screening the fractions collected from the chymotrypsin digest. Two major peaks of *m/z* 1738 and *m/z* 1807 from HPLC fraction #13 were detected in the mass spectrum displayed in Figure 3.12. The 69 u difference between the peaks does not correlate well with the expected 80 u mass difference between ions resulting from the phosphorylated and unphosphorylated forms of the peptide. However, subsequent analysis of this fraction by ion trap mass spectrometry revealed the presence of a co-eluting peak at *m/z* 1728, corresponding to the non-phosphorylated version of the peptide of *m/z* 1807. The broadened peak in Figure 3.12 that was assigned to *m/z* 1738 results from the combined presence of *m/z* 1728 and *m/z* 1743, a co-eluting peptide identified as the chymotryptic fragment HIITDRGGKTDNTDSL, residues 429-444. The low resolution linear TOF mass spectrometer was not able to discriminate between the peaks at that molecular weight. The peptide of *m/z* 1728 corresponds to the chymotryptic fragment from residues 240-255. Ser-249 is the only serine residue contained in this sequence; thus the site of phosphorylation was straightforward to assign.

3.3.4.3.2 MALDI/Ion Trap Mass Spectrometry, Fraction #13

Analysis of chymotrypsin-generated HPLC fraction #13 produced the mass spectrum shown in Figure 3.13(b). The dominant peak in the mass spectrum was at *m/z* 1709. An abundant signal at *m/z* 1807 correlated with that observed on the time-of-flight

Figure 3.12: Linear time-of-flight mass spectrum for the phosphopeptide of *m/z* 1728 resulting from chymotrypsin digestion of the P protein. Ten laser shots were summed. The mass assignment for the $(M+H)^+$ peak is incorrect due to the presence of a co-eluting peptide that served to broaden the peak. The mass resolution of the instrument was too low to separate the peaks.

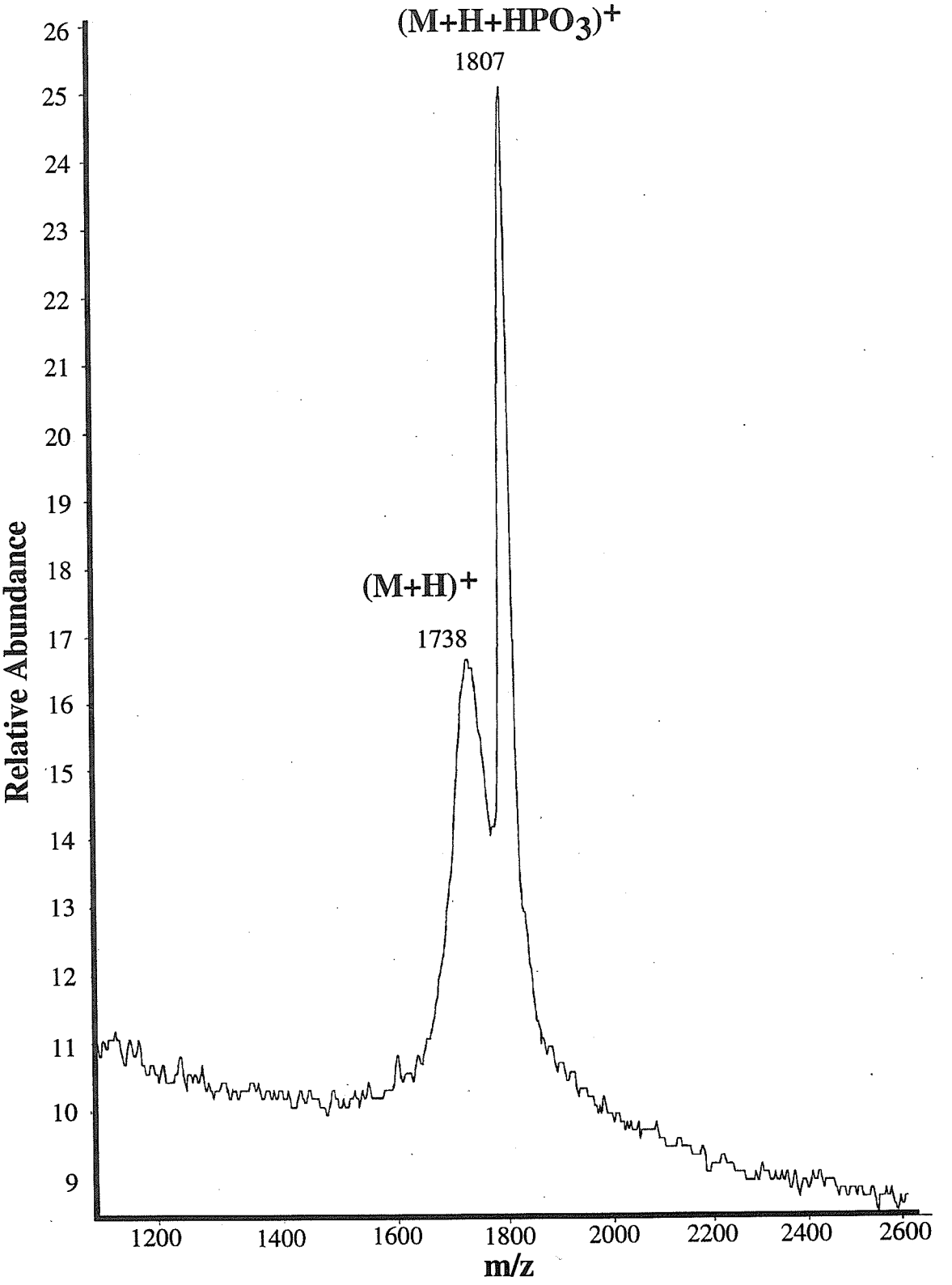
(M+H+HPO3)+
1807
(M+H)+
1738
Relative Abundance
m/z
26
25
24
23
22
21
20
19
18
17
16
15
14
13
12
11
10
9
1200
1400
1600
1800
2000
2200
2400
2600

instrument. A small peak at *m/z* 1728 was also observed. The mass difference of 79 u indicates that the peptide at *m/z* 1728 is the non-phosphorylated version of the peptide at *m/z* 1807. The mass difference of 98 u between the peaks at *m/z* 1807 and *m/z* 1709 suggests that the lighter peptide results from the facile loss of phosphoric acid from the heavier peptide as well as from the loss of water from *m/z* 1728. The presence of a low abundance signal from a co-eluting peak at *m/z* 1743 corresponding to residues 429-444 was also observed.

The PEPM™ software was used to search the P protein database for amino acid sequences with the mass 1728 Da. Of 36 possible peptides identified, 7 contained a C-terminal residue resulting from chymotrypsin cleavage on the carboxyl side of tyrosine, tryptophan, leucine, or phenylalanine. Five of these peptides corresponded to expected chymotrypsin-generated fragments. One step of manual Edman degradation was performed as described above, and the resulting mass spectrum is depicted in Figure 3.14. The mass-to-charge ratios of the ions shifted by approximately 100 u, *e.g.*, 950 u $\rightarrow$ 850 u, 1487 u $\rightarrow$ 1388 u, 1667 u $\rightarrow$ 1567 u, 1709 u $\rightarrow$ 1610 u, indicating valine or threonine as likely candidates for the N-terminal residue. Only two peptides out of the five possibilities contained Val or Thr at the N-terminus. Expected values for b- and y-type ions were calculated and compared with the experimental spectrum in Figure 3.13(b). The sequence of the chymotryptic peptide TPATVPGTRSPPLNRY, residues 240-255, fit the experimental data, strongly suggesting the phosphorylation site was at Ser-249. This peptide was also generated as the top-ranked choice by SEQUEST, shown in Figure 3.13(c). The expected fragmentation products for the peptide sequence are displayed in Figure 3.13(a) and observed ions are underlined. The presence of a series of b- and y-type ions served to confirm the sequence identification. Some signal suppression following Pro

Figure 3.13: Fragmentation mass spectrum for the phosphopeptide of *m/z* 1728 resulting from chymotrypsin digestion of the P protein. The ion trap was set to stably trap ions with *m/z* values larger than 100 u. Matrix ions were ejected by ramping the amplitude of the rf voltage from 20 u to 650 u while applying a supplementary signal at 520,300 Hz, 5.6 V (peak-to-peak, endcap-to-endcap). The mass spectrum was acquired by ramping the amplitude of the rf voltage from 30 u to 650 u while applying a supplementary signal at 89,202 Hz, 10.4 V (peak-to-peak, endcap-to-endcap). (**a**) Sequence and expected *m/z* values of fragmentation products for the unphosphorylated form of residues 240-255. Observed ions are underlined. Ions corresponding to phosphorylated fragmentation products are shown above (b-type ions) and below (y-type ions) the unphosphorylated fragmentation products. (**b**) Fragmentation mass spectrum for *m/z* 1728. (**c**) Result of SEQUEST analysis.

a)

									1048		1243		1470		1789	P-b
102	199	270	371	470	567	624	725	881	968	1066	1163	1276	1390	1546	1709	b
Thr	**Pro**	**Ala**	**Thr**	**Val**	**Pro**	**Gly**	**Thr**	**Arg**	**Psr**	**Pro**	**Pro**	**Leu**	**Asn**	**Arg**	**Tyr**	
1727	1626	1529	1458	1357	1258	1161	1104	1002	846	759	662	565	452	338	182	y
1807		1609				1241		1182	926							P-y

b)

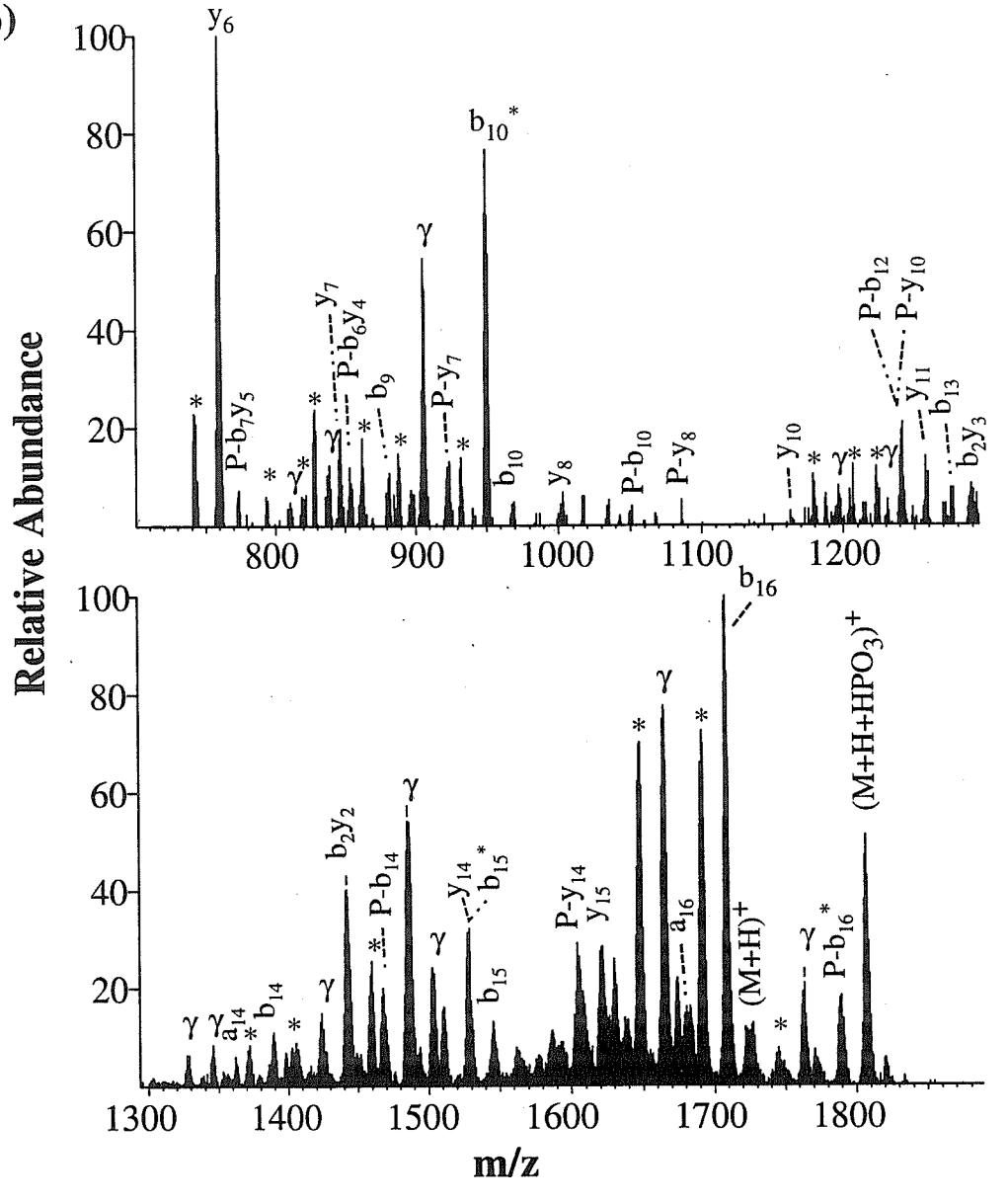

c)

#	Rank/Sp	(M+H)+	Cn	Sp	Ions	Peptide
1	1/1	1728.0	1.0000	53.2	9/45	(L)TPATVPGTRSPPLNRY
2	2/12	1725.9	0.5704	9.1	4/45	(G)GKTDNTDSLTRSPSVF
3	3/3	1728.0	0.4490	24.8	7/45	(L)RLVIESSPLSRAEKAA
4	4/6	1728.0	0.3178	15.3	6/42	(E)SSRDASYVFARRALK
5	5/26	1727.8	0.7774	2.1	2/45	(P)STQDEHINSGDTPAVR

or Gly was observed. A loss of 43 u, corresponding to the loss of the guanidino group from b-type ions containing arginine, was observed for most of the b-ions. Similar losses have been observed for the Arg-containing model peptide angiotensin using this instrument. The presence of phosphorylated analogs of b_{10} and y_7, as well as y_8, y_{10}, b_{12}, b_{14}, and b_{16} afforded positive identification of Ser-249 as the site of phosphorylation. The Edman degradation results (Figure 3.14) confirm the identification as well with the presence of the phosphorylated analogs of b_9 and y_7, as well as b_{11}, b_{14}, and y_{13}. An internal cleavage product RSPPLN, as well as its phosphorylated analog, were also observed. Further confirmation for the sequence identification was provided by analysis using electrospray ionization on a TSQ700 triple quadrupole mass spectrometer (data not shown) and by site-directed mutagenesis. The identification of the site of phosphorylation agrees with the proline-mediated kinase mechanism discussed above (47). The same results were obtained by analysis of peptides extracted from one of the spots on the 2D-TLE gel (data not shown).

3.3.4.3.3 MALDI/Time-of-Flight Mass Spectrometry, Fraction #25

The mass spectrum depicted in Figure 3.15 results from analysis of HPLC fraction #25 and shows the presence of two major peaks. The signals at *m/z* 2732 and *m/z* 2811 differ by 79 u; thus the lighter peptide appears to be the non-phosphorylated version of the heavier peptide. The mass of this peptide did not correspond to an expected chymotryptic fragment. Further analysis by ion trap mass spectrometry (see below) was used to assign the peptide to residues 228-253, a peptide overlapping that identified from HPLC fraction #13.

Figure 3.14: Fragmentation mass spectrum resulting from one stage of manual Edman degradation of *m/z* 1728. Operating conditions were as described for the analysis of *m/z* 1728.

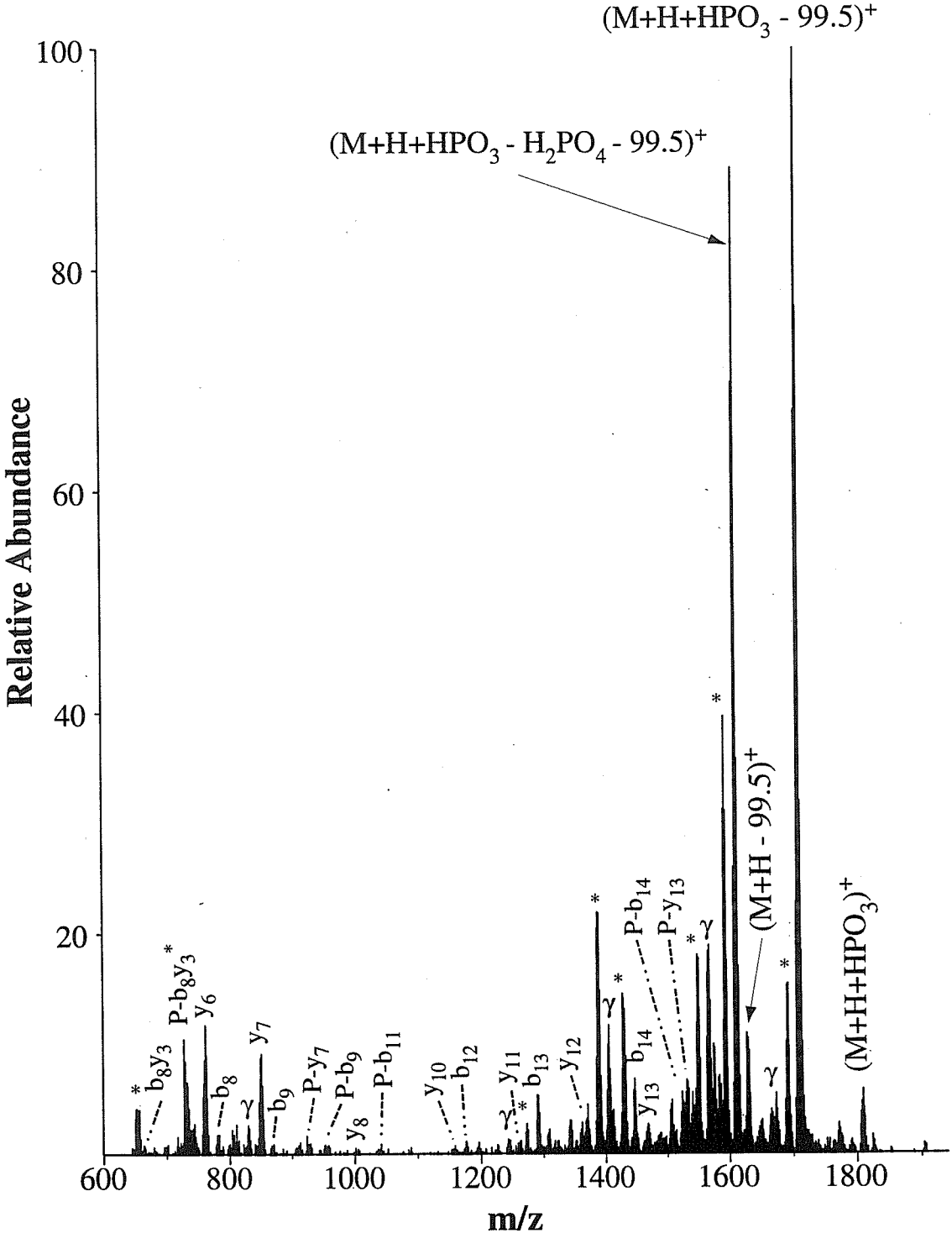
(M+H+HPO3 - 99.5)+
(M+H+HPO3 - H2PO4 - 99.5)+
(M+H - 99.5)+
(M+H+HPO3)+
Relative Abundance
m/z
100
80
60
40
20
600
800
1000
1200
1400
1600
1800
b8y3
P-b8y3
y6
b8
y7
b9
P-y7
P-b9
y8
P-b11
y10
b12
y11
b13
y12
b14
y13
P-b14
P-y13

3.3.4.3.4 MALDI/Ion Trap Mass Spectrometry, Fraction #25

Mass spectrometric analysis of chymotrypsin-generated HPLC fraction #25 afforded the mass spectrum depicted in Figure 3.16 (b). The dominant peak in the spectrum was at *m/z* 2710 and an abundant signal was also observed at *m/z* 2728, correlating with data obtained by TOF methods. The phosphorylated analog appeared with low abundance at *m/z* 2809, an 80 u mass difference from the peak at *m/z* 2728 and a 98 u mass difference from the peak at *m/z* 2710. Again, a facile loss of phosphoric acid was observed.

PEPM™ was used to search the database for all peptides with *m/z* values of 2730 u +/- 5 u. The search produced 35 possible peptides. Of these, four sequences theoretically resulted from cleavage with chymotrypsin. Signals at 2616 u and 2599 u were used to generate possibilities for the largest b- and y-type ions. The largest y-type ion could correspond to a loss of 112 u or 129 u, indicating L, I, N, K, Q, and E as possibilities. The largest b-type ion could correspond to a loss of 95 u or 112 u, indicating L, I, N, and P as possibilities. Sequences for all peptides with these possible terminating ions were investigated. Mass assignment errors in the ion trap can arise from the use of a two-point calibration rather than a five-point calibration for the extended mass range, as well as shifting caused by space-charge effects; thus the mass windows considered were rather large. An MS/MS experiment (data not shown) indicated that the peaks at *m/z* 2175 and 1294 were from the precursor ion at *m/z* 2730. Expected sequence ions for 20 possible sequences were compared with the experimental mass spectrum. The sequence with the best fit corresponded to residues 228-253,

Figure 3.15: Linear time-of-flight mass spectrum for the phosphopeptide of *m/z* 2730 resulting from chymotrypsin digestion of the P protein. Ten laser shots were summed.

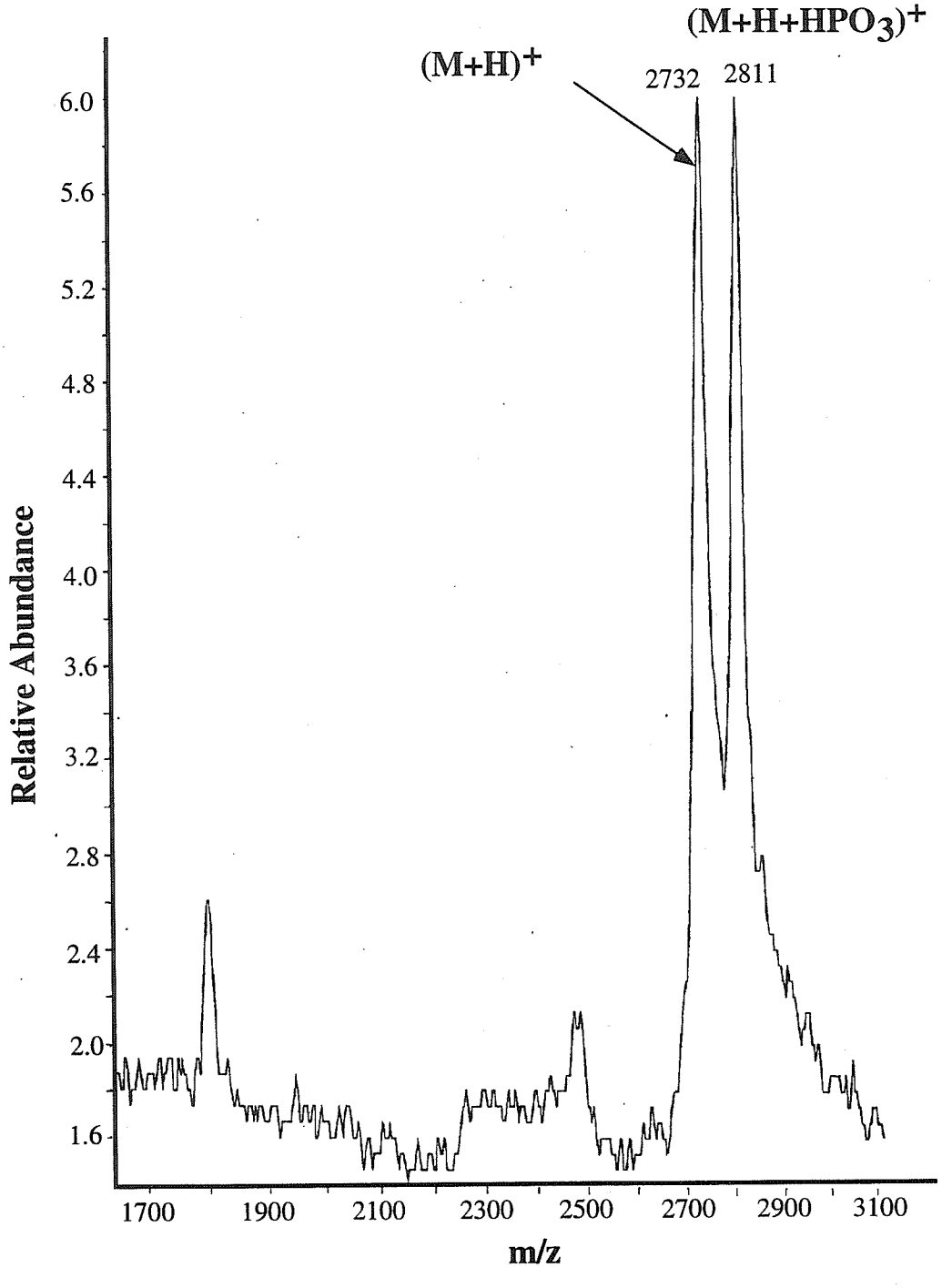
(M+H+HPO3)+
(M+H)+
2732
2811
6.0
5.6
5.2
4.8
4.4
4.0
3.6
3.2
2.8
2.4
2.0
1.6
Relative Abundance
1700
1900
2100
2300
2500
2700
2900
3100
m/z

Figure 3.16: (**a**) Sequence and expected m/z values of fragmentation products for the unphosphorylated form of residues 228-253. Observed ions are underlined. Ions corresponding to phosphorylated fragmentation products are shown above (b-type ions) and below (y-type ions) the unphosphorylated fragmentation products. (**b**) Fragmentation mass spectrum for phosphopeptide of *m/z* 2730 resulting from chymotrypsin digestion of the P protein. The ion trap was set to stably trap ions with *m/z* values larger than 120 u. Matrix ions were ejected by ramping the amplitude of the rf voltage from 20 u to 500 u while applying a supplementary signal at 242,300 Hz, 9.6 V (peak-to-peak, endcap-to-endcap). The mass spectrum was acquired by ramping the amplitude of the rf voltage from 50 u to 650 u while applying a supplementary signal at 35,371 Hz, 5.6 V (peak-to-peak, endcap-to-endcap).

a)

129	285	441	538	639	753	840	897	984	1113	1210	1323	1424	1521	1592
Lys	**Arg**	**Arg**	**Pro**	**Thr**	**Asn**	**Ser**	**Gly**	**Ser**	**Lys**	**Pro**	**Leu**	**Thr**	**Pro**	**Ala**
2729	2601	2445	2289	2192	2091	1977	1890	1833	1746	1618	1521	1408	1307	1210
	2681			2272	2171	2057		1913		1698	1601		1387	1290

									2677		P-b
1693	1792	1889	1946	2047	2203	2290	2387	2484	2597	2711	b
Thr	**Val**	**Pro**	**Gly**	**Thr**	**Arg**	**Psr**	**Pro**	**Pro**	**Leu**	**Asn**	
1139	1038	938	841	784	683	527	440	343	246	133	y
	1118			864							P-y

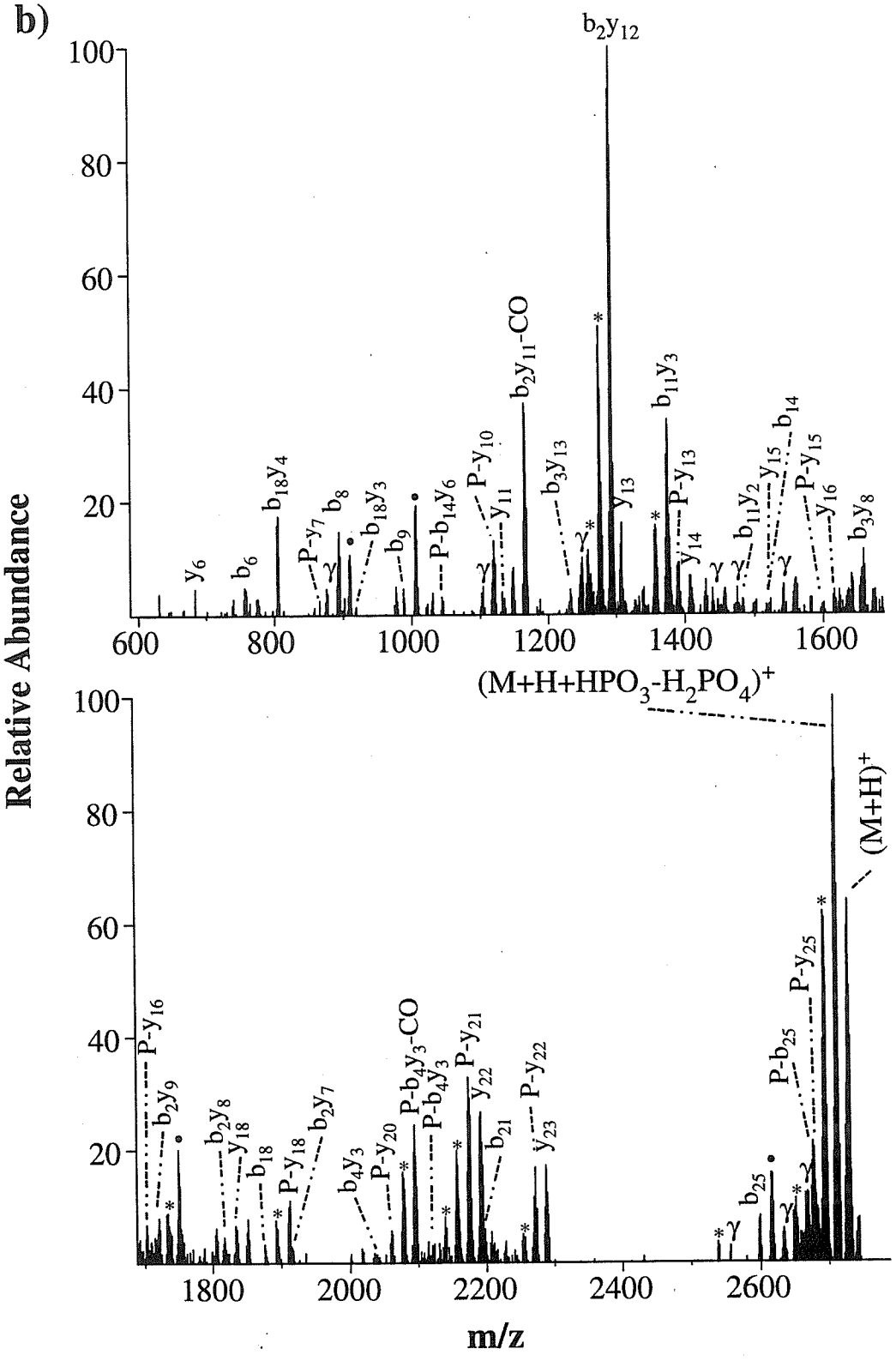
b)
Relative Abundance
100
80
60
40
20
600
800
1000
1200
1400
1600
b_2y_{12}
b_2y_{11}-CO
$b_{11}y_3$
$b_{18}y_4$
b_{14}
b_3y_8
$(M+H+HPO_3-H_2PO_4)^+$
$(M+H)^+$
1800
2000
2200
2400
2600
m/z

KRRPTNSGSKPLTPATVPGTRSPPLN. This peptide overlaps the phosphopeptide with *m/z* 1728 from residues 240-255. The expected fragmentation products appear in Figure 3.16(a) and observed signals are underlined. The presence of a series of b- and y-type ions were sufficient to verify the sequence assignment. As expected, fragmentation was suppressed in the vicinity of proline residues and signal from a number of internal cleavage products was observed. There are 3 serine residues found in this peptide. Since only peak differences of 80 u were observed using the TOF, we assume that the overlap peptide was phosphorylated at only one site. The observation of phosphorylated analogs of b_{25}, y_{25}, y_{22-20}, y_{18}, y_{16-15}, y_{13-12}, y_{10}, and y_8 serve to confirm the site of phosphorylation on Ser-249 rather than on Ser-234 or Ser-236. In addition, only Ser-249 is followed by a proline residue, agreeing with the proposed kinase mechanism (47). The same results were obtained by analysis of peptides extracted from one of the spots on the 2D-TLE gel (data not shown).

3.3.5 Conclusion

Three phosphopeptides were observed using MALDI/quadrupole ion trap mass spectrometry. Digestion with trypsin produced one phosphopeptide corresponding to residues 255-282, while digestion with chymotrypsin produced two phosphopeptides that overlapped in sequence. The smaller peptide corresponding to residues 240-255 contained one serine residue at Ser-249. The larger overlap peptide corresponded to residues 228-253 with Ser-249 again identified as the site of phosphorylation.

In parallel work using site-directed mutagenesis (47), deletion mutants were screened to locate a putative region of phosphorylation. The dominant phosphorylation region corresponded to residues 238-254 containing one serine at Ser-249. Deletion of Ser-249 or mutagenesis in that region of the peptide resulted in more extensive phosphorylation of the minor phosphopeptides, particularly a minor phosphopeptide located between residues 253 and 316. Experiments to investigate the effect of deleting residues 253 - 316 on the overall state of phosphorylation were not carried out. Concurring with these results, we believe Ser-249 is indeed a dominant phosphorylated residue in the P protein. The question remains as to why the phosphorylated peptide fragment containing Ser-260 was observed using mass spectrometry and not detected, except as a minor species, by classical genetics experiments. One possibility is that the fragment ionized particularly well by MALDI and that the other minor phosphopeptides were not observed because of low stoichiometries. Another possibility is that the structure of the region of the protein surrounding Ser-260 precluded efficient incorporation of labeling agents, reducing its detectability by autoradiography. More work is required to determine the exact location of the phosphorylation site of the peptide fragment.

The functional significance of P protein phosphorylation is unclear. Phosphorylation has been proposed to aid in multimerization of the P protein and the maintainance of its structural integrity (47), enabling viral replication and transcription. With the determination of the phosphorylation sites on the P protein, classical genetics can be employed to elucidate the precise role of phosphorylation in Sendai virus functioning.

3.4 References

1. Karas, M., Bachmann, D., Bahr, U., and Hillenkamp, F. (1987) *Int. J. Mass Spectrom. Ion Proc.* **78** 53-68.

2. Tanaka, K., Waki, H., Ido, Y., Akita, S., and Yoshida, Y. (1988) *Rapid Commun. Mass Spectrom.* **2** 151-153.

3. Karas, M., Bahr, U., Ingendoh, A., Nordhoff, E., Stahl, B., Strupat, K., and Hillenkamp, F. (1990) *Anal. Chim. Acta* **241** 175-185.

4. Hillenkamp, F., Karas, M., Beavis, R. C., and Chait, B. T. (1991) *Anal. Chem.* **63** 1193A-1202A.

5. Beavis, R. C., and Chait, B. T. (1990) *Proc. Natl. Acad. Sci. USA* **87** 6873-6877.

6. Hill, J. A., Annan, R. S., and Biemann, K. (1991) *Rapid Commun. Mass Spectrom.* **5** 395-399.

7. Annan, R. S., Kochling, H. J., Hill, J. A., and Biemann, K. (1992) *Rapid Commun. Mass Spectrom.* **6** 298-302.

8. Hettich, R. L., and Buchanan, M. V. (1991) *J. Am. Soc. Mass Spectrom.* **2** 22-28.

9. Hettich, R. L., and Buchanan, M. V. (1991) *J. Am. Soc. Mass Spectrom.* **2** 402-412.

10. Castro, J. A., Koster, C., and Wilkins, C. (1992) *Rapid Commun. Mass Spectrom.* **6** 239-241.

11. Cox, K. A., Williams, J. D., Cooks, R. G., and Kaiser, R. E. (1992) *Biol. Mass Spectrom.* **21** 226-241.

12. Russell, D. H., and Solouki, T. (1992) *Proc. Natl. Acad. Sci. USA* **89** 5701-5704.

13. Chambers, D., Goeringer, D. E., McLuckey, S. A., and Glish, G. (1993) *Anal. Chem.* **65** 14-20.

14. Kaiser, R. E., Jr., Cooks, R. G., Syka, J. E. P., and Stafford, G. C., Jr. (1990) *Rapid Commun. Mass Spectrom.* **4** 30-33.

15. Hunt, D. F., Shabanowitz, J., Yates, J. R., III, Zhu, N.-Z., Russell, D. H., and Castro, M. (1987) *Proc. Natl. Acad. Sci. USA* **84** 620-623.

16. Cody, R. B., Jr., Amster, I. J., and McLafferty, F. W. (1985) *Proc. Natl. Acad. Sci. USA* **82** 6367-6370.

17. Beavis, R. C., and Chait, B. T. (1991) *Chem. Phys. Lett.* **181** 479-484.

18. Louris, J. N., Amy, J. W., Ridley, T. Y., and Cooks, R. G. (1989) *Int. J. Mass Spectrom. Ion Proc.* **88** 97-111.

19. Louris, J. N., Brodbelt-Lustig, J. S., Kaiser, R. E., Jr., and Cooks, R. G. (1988) *Proc. of the 36th ASMS Conf. Mass Spectrom. and Allied Topics*, June 5-10, San Francisco, CA, American Society for Mass Spectrometry, p. 968.

20. Heller, D. N., Lys, I., Cotter, R. J., and Uy, O. M. (1989) *Anal. Chem.* **61** 1083-1086.

21. Glish, G. L., Goeringer, D. E., Asano, K. G., and McLuckey, S. A. (1989) *Int. J. Mass Spectrom. Ion Proc.* **94** 15-24.

22. Goeringer, D. E., Glish, G. L., and McLuckey, S. A. (1991) *Anal. Chem.* **63** 1186-1192.

23. Jonscher, K., Currie, G., McCormack, A. L., and Yates, J. R., III (1992) *Proc. of the 40th ASMS Conf. on Mass Spectrom. and Allied Topics*, May 31-June 5, Washington, DC, American Society for Mass Spectrometry, p. 701.

24. Bier, M. E., Schwartz, J., Jardine, I., and Stafford, G. C. (1992) *Proc. of the 40th ASMS Conf. on Mass Spectrom. and Allied Topics*, May 31-June 5, Washington, DC, American Society for Mass Spectrometry, p. 1017.

25. Kaiser, R. E., Jr., Louris, J. N., Amy, J. W., and Cooks, R. G. (1989) *Rapid Commun. Mass Spectrom.* **3** 225-229.

26. Louris, J. N., Cooks, R. G., Syka, J. E. P., Kelley, P. E., Stafford, G. C., Jr., and Todd, J. F. J. (1987) *Anal. Chem.* **59** 1677-1685.

27. Kaiser, R. E. (1990), Ph.D. Dissertation, Purdue University.

28. Wright, L. G., Cooks, R. G., and Wood, K. V. (1985) *Biomed. Mass Spec.* **12** 159-162.

29. Schwartz, J. C., Syka, J. E. P., and Jardine, I. (1991) *J. Am. Soc. Mass Spectrom.* **2** 198-204.

30. Beavis, R. C., and Chait, B. T. (1989) *Rapid Commun. Mass Spectrom.* **3** 233-237.

31. Beavis, R. C., and Chait, B. T. (1989) *Rapid Commun. Mass Spectrom.* **3** 432-435.

32. Doktycz, S. J., Savickas, P. J., and Kreuger, D. A. (1991) *Rapid Commun. Mass Spectrom.* **5** 145-148.

33. Kingsbury, D. W. (1991) *in* Fundamentals of Virology (Fields, B. N., and Knipe, D. M., Eds.), Raven Press, New York, pp. 507-524.

34. Dillon, P. J., and Gupta, K. C. (1989) *J. Virology* **63** 974-977.

35. Vidal, S., Curran, J., and Kolakofsky, D. (1990) *J. Virology* **64** 239-246.

36. Hamaguchi, M., Yoshida, T., Nishikawa, K., Naruse, H., and Nagai, Y. (1983) *Virology* **128** 105-117.

37. Horikami, S. M., Curran, J., Kolakofsky, D., and Moyer, S. A. (1992) *J. Virology* **66** 4901-4908.

38. Lamb, R. A., Mahy, B. W. J., and Choppin, P. W. (1976) *Virology* **69** 116-131.

39. Hsu, C., and Kingsbury, D. W. (1982) *Virology* **120** 225-234.

40. Curran, J., and Kolakofsky, D. (1990) *Enzyme* **44** 244-249.

41. Curran, J., Boeck, R., and Kolakofsky, D. (1991) *EMBO J.* **10** 3079-3085.

42. Matsuoka, Y., Curran, J., Pelet, T., Kolakofsky, D., Ray, R., and Compans, R. W. (1991) *J. Virology* **65** 3406-3410.

43. Smallwood, S., Ryan, K. W., and Moyer, S. A. (1994) *Virology* **202** 154-163.

44. Curran, J., Pelet, T., and Kolakofsky, D. (1994) *Virology* **202** 875-884.

45. Vidal, S., Curran, J., Orvell, C., and Kolakofsky, D. (1988) *J. Virology* **62** 2200-2203.

46. Byrappa, S., Hendricks, D. D., Pan, Y.-B., Seyer, J. M., and Gupta, K. C. (1995) *Virology* **208** 408-413.

47. Byrappa, S., Pan, Y.-B., and Gupta, K. C. (1996) *Virology* **216** 228-234.

48. Jonscher, K. R., Currie, G., McCormack, A. L., and Yates, J. R., III (1993) *Rapid Commun. Mass Spectrom.* **7** 20-26.

49. Morand, K. L., Cox, K. A., and Cooks, R. G. (1992) *Rapid Commun. Mass Spectrom.* **6** 520-523.

50. Kaiser, R. E., Jr., Cooks, R. G., Stafford, G. C., Jr., Syka, J. E. P., and Hemberger, P. H. (1991) *Int. J. Mass Spectrom. Ion Proc.* **106** 79-115.

51. Watkins, P. J. F., Jardine, I., and Zhou, J. X. G. (1991) *Bioch. Soc. Trans.* **19** 957-962.

52. Roepstorff, P., and Fohlman, J. (1984) *Biomed. Mass Spectrom.* **11** 601.

53. Eng, J. K., McCormack, A. L., and Yates, J. R., III (1994) *J. Am. Soc. Mass Spectrom.* **5** 976-989.

54. Jonscher, K. R., and Yates, J. R., III (1994) *Proc. of the 42nd ASMS Conf. on Mass Spectrom. and Allied Topics,* May 29-June 3, Chicago, IL, American Society for Mass Spectrometry, pp. 216-217.

55. Qin, J., and Chait, B. T. (1995) *Proc. of the 43rd ASMS Conf. on Mass Spectrom. and Allied Topics*, May 21-26, Atlanta, GA, American Society for Mass Spectrometry, p. 1100.

56. Qin, J., and Chait, B. T. (1995) *J. Am. Chem. Soc.* **117** 5411-5412.

57. Qin, J., and Chait, B. T. (1995) *Proc. of the 43rd ASMS Conf. on Mass Spectrom. and Allied Topics*, May 21-26, Atlanta, GA, American Society for Mass Spectrometry, p. 989.

58. Qin, J., Steenvoorden, R. J. J. M., and Chait, B. T. (1996) *Anal. Chem.* **68** 1784-1791.

59. Gibson, B. W., and Cohen, P. (1990) *Meth. Enzym.* **193** 480-501.

60. Jonscher, K. R., and Yates, J. R., III (1993) *Proc. of the 41st ASMS Conf. on Mass Spectrom. and Allied Topics*, May 31-June 4, San Francisco, CA, American Society for Mass Spectrometry, 695a.

Chapter 4

Mixture Analysis Using a Quadrupole Mass Filter/Quadrupole Ion Trap Mass Spectrometer

4.1 Overview

A hybrid tandem mass spectrometer is constructed by interfacing a quadrupole mass filter (Q) to a quadrupole ion trap mass spectrometer (QITMS) and is evaluated for the analysis of mixtures. The mass filter is set to selectively inject ions of a particular *m/z* or, in scanning mode, to sequentially inject ions into the QITMS for subsequent manipulation and detection. Performance of the instrument is demonstrated using a mixture of ions created by electron impact ionization of perfluorotributylamine (FC-43) and peptide ions generated by pulsed Cs^+ bombardment. Resulting data is compared to those obtained utilizing only the ion trap. Molecular weight, fragmentation, and high resolution analyses for the sequentially injected mass-filtered peptides show improved performance over similar measurements employing only the ion trap mass spectrometer. Performance is optimized when ions are not rf-isolated in the QITMS. Using the hybrid, a resolution of 33,200 is achieved for angiotensin I. Dramatic reduction of space charge-induced signal suppression is demonstrated for LSIMS of Glu-fibrinopeptide B. "On-the-

fly" collision-induced dissociation is performed for *m/z* 502 from FC-43, where fragmentation is induced by increasing the ion injection energy. Collision-induced dissociation efficiencies for fragmentation of angiotensin I by resonance excitation are investigated as a function of cooling time for different modes of operation of the hybrid. A current limitation of the instrument is the time required to port the data for acquisition.

4.2 Introduction

The ability to structurally characterize molecules contained in mixtures has been greatly simplified by combining two or more mass analyzers. The first mass analyzer (MS-1) functions as a device to separate ions of interest from the mixture and to pass the ions into a reaction or activation region. Fragmentation may be induced by depositing sufficient vibrational or electronic energy into the ion using collisional activation (1), surface activation (2), or photoactivation (3) methods. The resultant dissociation products may be analyzed in the second mass analyzer (MS-2) to reveal structurally important features. Although most common instruments utilized for mixture analysis consist of two mass analyzers separated in space, multiple stages of mass spectrometry are feasible by separating ion selection, activation, and product analysis in time employing ion trap mass spectrometers (4). Most commercially available instruments capable of performing mixture analysis are based on mass analyzers of the same type (5-7), but numerous examples of hybrid instruments have appeared in the literature (8-13). Hybrid instruments may afford extension of mixture analysis capabilities by combining the strengths of two different types of mass analyzers.

Due to their versatility and ion storage capabilities, quadrupole ion trap mass spectrometers (QITMS) have been used in a number of different hybrid configurations. Magnetic sector instruments have been employed as MS-1 with ion trap mass spectrometers utilized as MS-2 (14-17). A disadvantage of the sector hybrids is that the second stage of the mass spectrometer must be floated to high voltages; thus quadrupole mass filters (Q) were investigated as MS-1 candidates for various tandem combinations, notably triple quadrupole configurations (18, 19). Quadrupole mass filters have been interfaced to quadrupole ion traps to select and transmit a single *m/z* value to the ion trap in a Q/ion trap/Q configuration (20, 21). A Q/Q/ion trap configuration, where the first quadrupole was utilized as a selective mass filter and the second quadrupole operated in rf-only mode as a beam transmitter, was employed to obtain structural information for filtered molecules. The voltage at which the ion trap electrode assembly was floated relative to ground was raised to increase the kinetic energy of the ions and to enhance ion dissociation upon injection into the ion trap (22, 23). Fragmentation may also be induced in a quadrupole ion trap when resonance excitation (24) is utilized; thus the ion trap may function as both collision cell and MS-2.

Although multiple stages of mass spectrometry may be performed within the same collision cell of a quadrupole ion trap, a limitation of utilizing the quadrupole ion trap as the only mass analyzer is its dynamic range. Typically, no more than ~10^5 ions may be trapped before space charge distorts the electric fields, causing reduced sensitivity, mass accuracy, and resolution (25). Shaped excitation pulses (26) and filtered noise field techniques (27) have been used for notch injection of molecules of interest. Subsequent reduction in space charge effects has been demonstrated (28). These techniques, typically utilizing stored waveforms from a function generator applied to the endcap electrodes of

the ion trap, have been used for broadband ejection of low mass matrix ions and for the selected injection of one or more species in a mixture. Notch injection requires *a priori* knowledge of the *m/z* value for the ion of interest or the use of a "pre-scan" to measure the *m/z* values of injected ions in order to calculate the resonance frequency of the notch. An alternative approach is to employ a quadrupole mass filter to pre-process the ion population by "step scanning" the quadrupole over narrow mass windows in order to sequentially transmit components of a mixture into an ion trap for further manipulation.

This chapter describes the assembly of a quadrupole mass filter/quadrupole ion trap mass spectrometer for the analysis of mixtures of molecules. The quadrupole ion trap filled with helium serves as both collision cell and MS-2. The quadrupole mass filter may be used either in a mass-selective mode to inject ions of one *m/z* or in a scanning mode to sequentially inject ions into the QITMS. The concept is demonstrated using ions generated from electron ionization of the model compound perfluorotributylamine (FC-43) and utilizing a pulsed Cs^+ source to ionize selected peptides.

4.3 Experimental

The instrument constructed for this work was a hybrid quadrupole mass filter/quadrupole ion trap mass spectrometer (Q/QITMS), a modification of an ion trap mass spectrometer that has been previously described (29). The hybrid instrument was assembled from components of an ITMS quadrupole ion trap mass spectrometer (Finnigan MAT, San Jose, CA, USA) and a TSQ70 triple quadrupole mass spectrometer (Finnigan MAT) as illustrated in Figure 4.1.

Figure 4.1: Diagram of the Q/QITMS. The EI source is easily replaced by a matrix-assisted laser desorption ionization source, a pulsed Cs^+ source, or an electrospray ionization source. Ions were extracted with a 3 kV lens and were detected with a 20 kV collision dynode and an off-axis electron multiplier.

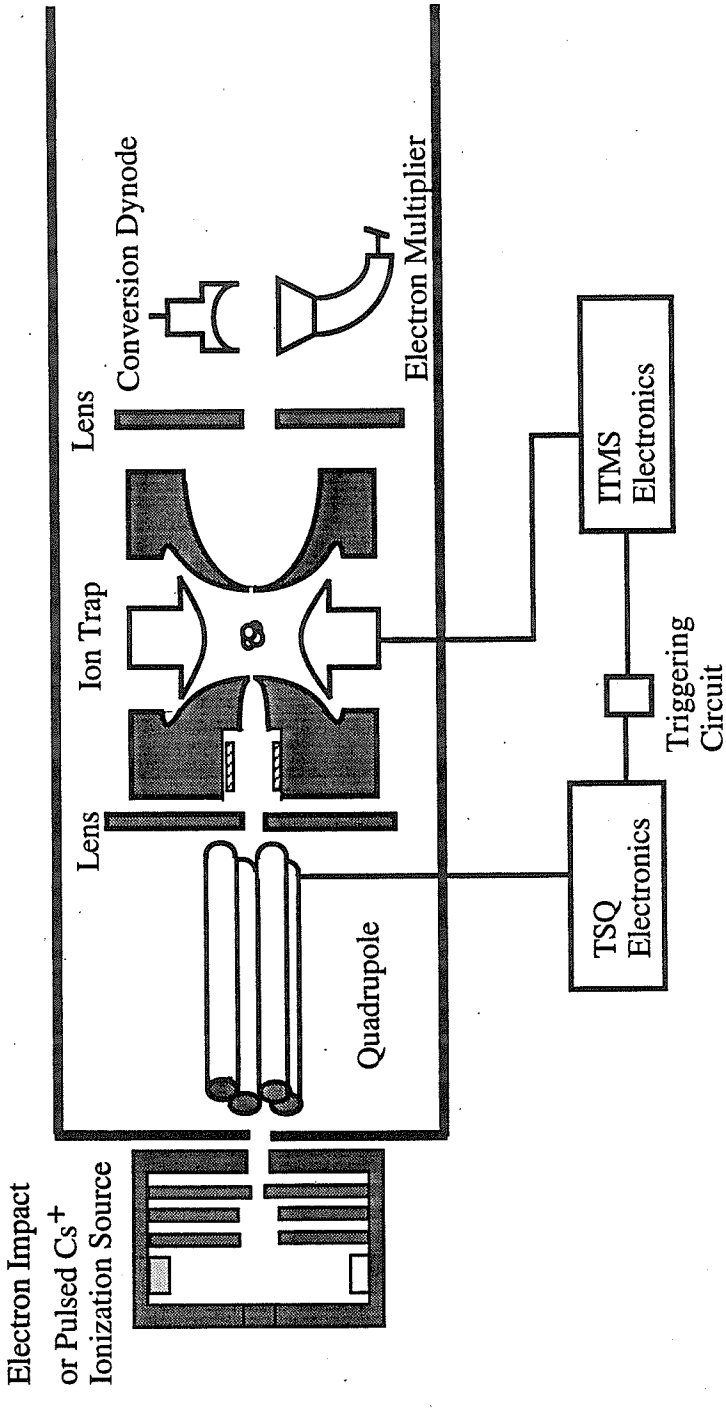
Analyzer Region
Electron Impact
or Pulsed Cs^+
Ionization Source
Lens
Ion Trap
Lens
Conversion Dynode
Electron Multiplier
Quadrupole
TSQ
Electronics
Triggering
Circuit
ITMS
Electronics

4.3.1 Ion Source

An electron impact (EI) ionization source (Finnigan MAT) was interfaced to the Q/QITMS and an electron beam with an energy of 70 eV was used to ionize gas phase molecules produced by FC-43. A modification of this source incorporated a power supply and pulsed injection system to produce a 6 keV cesium ion beam for ionization of samples by liquid secondary ion mass spectrometry (LSIMS) (30). Samples were loaded onto a probe tip held at ground. Ions formed in the differentially pumped ion source region were then focused by an einzel lens into the quadrupole mass filter. Typical lens voltages were -8.4 V, -130.3 V, and -7.5 V, respectively.

4.3.2 Mass Analyzers

The quadrupole mass filter (MS-1), a focusing lens, and the quadrupole ion trap electrodes (MS-2) were aligned on an optical rail located in the low-pressure region of the baffled and differentially pumped vacuum manifold as illustrated in Figure 4.1. The quadrupole rods were hyperbolic high mass rods from a TSQ70 triple quadrupole and had a nominal mass range of 4000 u. A potential of -5 V was applied as an offset to the quadrupole. The focusing lens, held at 4 V, was followed by a gating tube lens (+/- 200 V) and served to focus the exiting ions into the entrance aperture of the ion trap endcap electrode. The ion trap electrode assembly was floated with a variable dc potential to control the ion injection energy, typically set to -10 V for FC-43 and -8 V for peptides. These values correspond to the conditions for maximum ion intensity observed across the mass range. The ion trapping volume was pressurized with helium to an uncorrected

gauge reading of 5.5 x 10^{-4} Torr as measured by a Convectron gauge located on the outside of the vacuum manifold. The rf and dc voltages applied to the quadrupole to establish ion trajectories were controlled by a DECStation 2100 interfaced to the TSQ70 electronics. The application of the rf voltage to the ring electrode of the QITMS has been described previously (29). Sinusoidal auxiliary signals from the ITMS frequency generator were applied to the endcap electrodes to enable resonance ejection and resonance excitation (31).

A typical QITMS scan function used to obtain molecular weight information is shown diagramatically in Figure 4.2 (solid lines), along with a quadrupole scan (dashed lines). The horizontal axis represents time and the vertical axis represents *m/z*. The QITMS scan function consisted of an ionization period, during which the gating tube lens remained in the "open" position to allow ions into the trap for collection, of 10 - 20 ms. The ionization period was followed by a variable cooling time. The mass-selective instability mode of operation for the QITMS (32) was applied to resonantly eject the trapped ions using a supplementary signal at 520,311 Hz and 4 V (peak-to-peak, endcap-to-endcap) for ions generated by EI and a signal at 119,936 Hz and 8.8 V (peak-to-peak, endcap-to-endcap) for ions generated by pulsed Cs^+. Ramping time for ejecting the ions was ~108 ms and was fixed in the ion trap firmware. The amplified signal was displayed on the ITMS Compac 386 PC, then transported to the DECStation 2100 running ICIS software for acquisition and data processing. Resonance excitation was accomplished by reverse-then-forward rf-isolation of the ion of interest followed by a 30 ms excitation time. A variable cooling time was applied prior to mass analysis.

4.3.3 Synchronization

Two different scanning methods were employed to sequentially inject ions into the ion trap and are illustrated in Figure 4.2. Figure 4.2(a) shows the "continuous scanning" method where the quadrupole and ion trap both scan over the same range of *m/z* values. The thick line overlaying the quadrupole scan indicates the range of *m/z* values that were transmitted by the quadrupole during the ionization period of the ion trap. Only these *m/z* values were detected. Depicted in Figure 4.2(b) is the "step scanning" method of operation. A TTL signal from the quadrupole occurring at the beginning of the quadrupole scan was used to trigger operation of the 8086 microprocessor on the SAP board of the ion trap (33). An instrument control language (ICL) procedure was written to scan the quadrupole over a limited mass range, typically 10 u wide bins, then increment the bin center by 10 u. Again, the thick line overlaying the quadrupole scan represents the range of detectable *m/z* values. Sequential *m/z* values may be transmitted to the ion trap for detection, and by a judicious choice of scan bin and step size, every *m/z* can be transmitted into the ion trap and detected. The time axis is slashed to represent the time required for data porting (see below). For both scanning methods, the ion trap electronics were set to display and port one ion trap "microscan" for each quadrupole bin scan. Mass spectra were first displayed on the PC then ported to the DECStation 2100, displayed using a modification of the SPEC data display program, then acquired to the hard disk. The data porting time was on the order of 450 ms (Figure 4.2) as compared with the actual ion trap scan time of ~130 ms. The ITMS microprocessor does not continue with its next instruction until the data from the ITMS have been completely ported to the DECStation 2100; thus the minimum bin scan time, limited by the data porting time, was

Figure 4.2: Diagram of scanning modes investigated for injection of ions into the ion trap. (**a**) "Continuous scanning" method where the quadrupole mass filter and the ion trap both scanned over the same mass range. The time delay between the ion trap scan functions resulted from the data porting and acquisition time. (**b**) "Step scanning" method where the quadrupole was scanned over a narrow mass range (bin) while the ion trap was scanned over the full mass range. Both mass analyzers were synchronized to start scanning at the same time. The quadrupole scan bin was sequentially stepped to higher *m/z* values until the full mass range was covered. The slash in the time axis represents the data porting time delay.

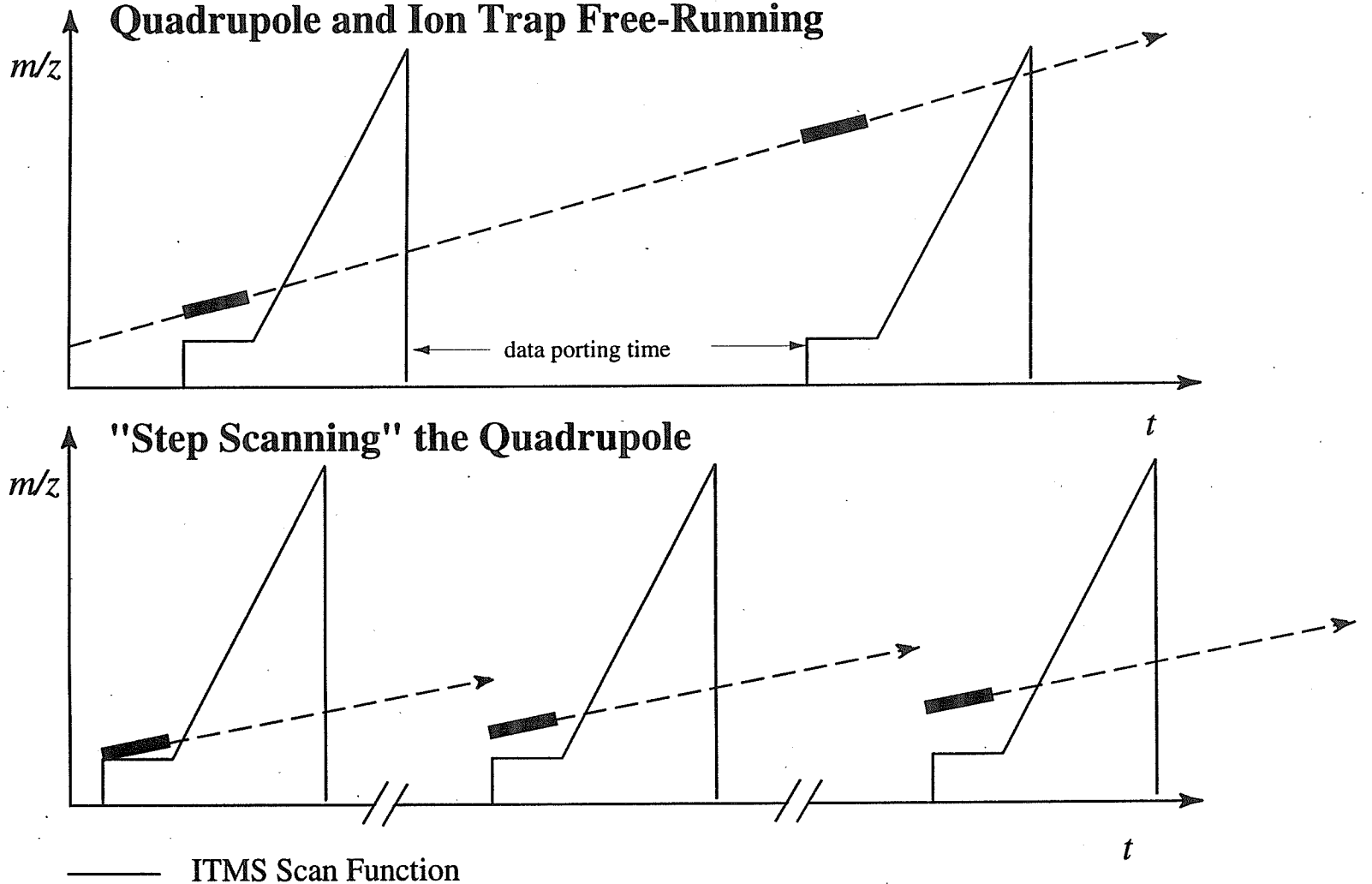
Quadrupole and Ion Trap Free-Running
m/z
data porting time
t
"Step Scanning" the Quadrupole
m/z
t
ITMS Scan Function
Quadrupole Scan
Range of m/z Transmitted by Quadrupole and Injected Into Ion Trap

experimentally determined to be 570 ms. This minimum time required the PC and DECStation display parameters to be set to very narrow windows with no signal displayed so that the spectral display time would be minimized. In addition, the windows on the DECStation representing the status of the instrument (*i.e.*, lens voltages, pressures, etc.) had to be changed to non-updating windows in order to achieve the minimum bin scan time above. The scan times for the experiments ranged from 22.5 (scanning from 1000 u to 1075 u for the case of a mixture of angiotensin II peptides) to 60 s for scanning from 1000 to 2000 u to observe Glu-fibrinopeptide B.

4.3.4 Sample Preparation

Perfluorotributylamine (FC-43) (Ultra Scientific, N. Kingstown, RI) at a pressure of 1 x 10^{-4} Torr (uncorrected) entered the ion source region through a needle valve and was ionized by electron impact ionization using electrons with 70 eV of energy. The peptides [Val^4]angiotensin III (MW 917, Cat. No. A6277, Lot. No. 053F58452), angiotensin II (MW 1046, Cat. No. A9525, Lot No. 13H59001), [Val^5]angiotensin II (MW 1032, Cat. No. A2900, Lot No. 119F58101) and angiotensin I (MW 1296, Cat. No. A9650, Lot No. 13H59101) were purchased from Sigma Chemical Co. (St. Louis, MO, USA) and used without further purification. Peptides were separately dissolved in 0.1% trifluoroacetic acid to a concentration of 25 pmol/μL then mixed together in equal volumes. Approximately 1 μL of 1:1 glycerol:thioglycerol and 0.5 μL of the peptide mixture were co-deposited onto the gold electroplated probe tip. Glu-fibrinopeptide B (MW 1571, Cat. No. F3261, Sigma Chemical Co.) was similarly diluted to a concentration of 5 pmol/μL and applied to the probe tip.

4.4 Results and Discussion

The objective of this work was to study methods for sequential ion injection into the ion trap and the potential for performing "on the fly" tandem mass spectrometry using a hybrid instrument configuration of a quadrupole mass filter and quadrupole ion trap mass spectrometer. Results for the performance of the instrument are reported for FC-43 and selected peptides.

4.4.1 Ion Injection into the Ion Trap

FC-43 typically fragmented in the source region upon electron impact ionization. A simple mixture of singly-charged ions was produced with monoisotopic mass-to-charge ratios of 69 u, 131 u, 264 u, 414 u, 502 u, and 614 u (34). Two different quadrupole scanning methods, continuous and step scanning, were evaluated for sequential injection of this set of ions as diagrammed in Figure 4.2. For the continuous scanning experiment, the quadrupole was scanned continuously from 50 to 650 u with a scan time of 4 s and the ion trap was scanned over the same mass range with a scan time of ~130 ms. Single ion trap microscans were ported to the DECStation 2100 and acquired. The scans of the quadrupole and ion trap were not synchronized. Figure 4.3(a) shows the selected ion chromatograms (SIC) for the above ions with ion intensity plotted against ion trap scan number. Approximately 30 μscans correspond to one quadrupole full-range scan; thus the experiment in Figure 4.3(a) reflects approximately 5-6 scans of the quadrupole mass filter. Signal was observed for all of the selected ion chromatograms over the course of several scans of the quadrupole mass filter, indicating that all of the ions were injected. Not all

Figure 4.3: Selected ion chromatograms resulting from sequential injection of ions generated from perfluorotributylamine. The relative injection energy was 10 eV. The amplitude of the rf voltage on the ion trap ring electrode was set so as to exclude ions with *m/z* less than 40 u from the trapping volume. (**a**) The quadrupole scanned from 50 u - 650 u in 4 seconds while the QITMS scanned over the same mass range in ~150 ms. (**b**) The mass analyzers were synchronized by "step scanning" the quadrupole in 10 u wide bins and triggering QITMS operation after the beginning of the quadrupole scan.

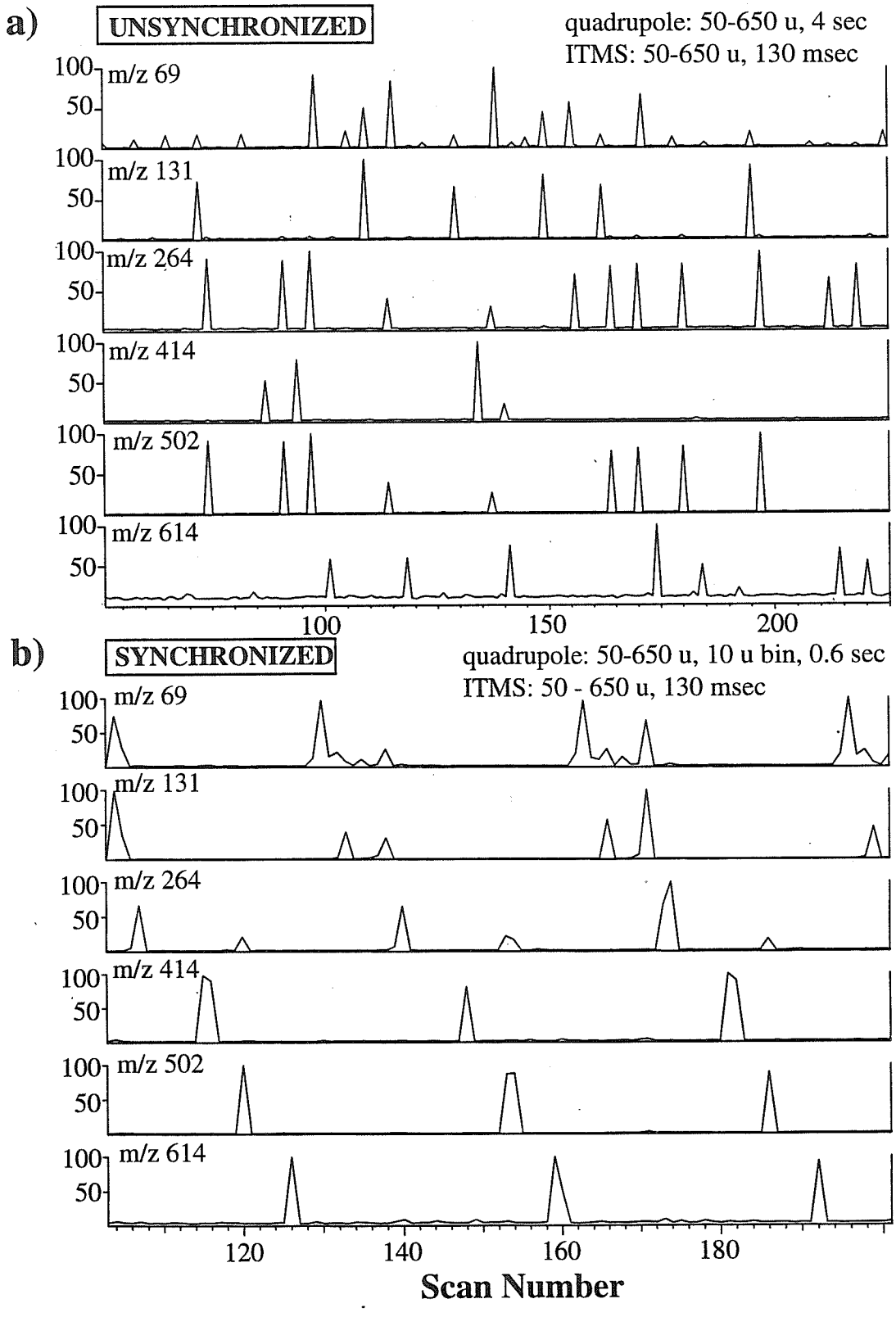
a)
UNSYNCHRONIZED
quadrupole: 50-650 u, 4 sec
ITMS: 50-650 u, 130 msec
m/z 69
m/z 131
m/z 264
m/z 414
m/z 502
m/z 614
100
50
100
150
200
b)
SYNCHRONIZED
quadrupole: 50-650 u, 10 u bin, 0.6 sec
ITMS: 50 - 650 u, 130 msec
m/z 69
m/z 131
m/z 264
m/z 414
m/z 502
m/z 614
120
140
160
180
Scan Number

single scans of the quadrupole mass filter, however, transmitted all of the FC-43 ions. This is particularly evident in the chromatogram for *m/z* 414.

The result of using the step scanning method is shown in Figure 4.3(b). The quadrupole mass filter was set to scan from 50 u to 650 u in 10 u wide mass bins, each bin having a scan time of 600 ms, affording a 36 s scan time over the desired mass range. The lower limit for the bin scan time was the time necessary to port the data from the ITMS to the DECStation (450 ms) and was not a function of the QITMS scanning time (130 ms). If the data porting time were negligible, the scan time over this mass range would be on the order of 9 seconds. Mass spectra from 200 scans of the ion trap were acquired.

The selected ion chromatograms resulting from the synchronization of the mass analyzers, shown in Figure 4.3(b), are strikingly different from those obtained in Figure 4.3(a) where the two mass analyzers were free-running. Using the "step scanning" technique, mass separation of the FC-43 fragmentation products by the quadrupole clearly afforded sequential injection of ions, from low to high *m/z* values, into the ion trap. The peaks of smaller intensity in the chromatogram for *m/z* 264 result from fragmentation of the mass selected *m/z* 502 ion. The ion chromatogram for *m/z* 131 shows a double-peak pattern; the peak at the lower scan number results from mass selection of *m/z* 131 and produces a corresponding fragment ion of *m/z* 69, while the peak at the higher scan number results from dissociation of mass-selected *m/z* 197, producing fragment ions of *m/z* 69 and *m/z* 131. The ion chromatogram for *m/z* 69 shows a quadruple peak pattern deriving from mass selection of *m/z* 69 as well as fragmentation from *m/z* 131, from *m/z* 181, and from *m/z* 197.

As demonstrated by Julian and Cooks, the use of broadband excitation with frequency notches to eject matrix ions from the trap can significantly improve the signal-to-

noise (S/N) ratio for the analyte (28). An analogous experiment illustrated in Figure 4.4 compared S/N ratios for Glu-fibrinopeptide B ions generated by pulsed Cs^+ bombardment and injected into the ion trap using no pre-processing with those obtained using step scanning. As shown in Figure 4.4(a), when an rf-only potential was applied to the quadrupole, the ion trap was quickly filled to the space-charge limit due to the transmission of the ion background generated by desorption of the matrix. The peptide signal was suppressed. Figure 4.4(b) depicts the mass spectrum, with the SIC displayed as an inset, obtained by the step scanning injection of the same peptide. The mass filter was scanned from 1000 to 2000 u in 10 u wide mass bins with a bin scan time of 0.6 s, a 60 s scan over the entire mass range. Matrix suppression effects were dramatically reduced and a S/N ratio of 17.2 was calculated for *m/z* 1572.

Figure 4.5 illustrates the typical performance of the instrument for a mixture of peptides with similar structures. An equimolar mixture of angiotensin I, angiotensin II, [Val^4]angiotensin III and [Val^5]angiotensin II was applied to the probe tip and ionized by Cs^+ bombardment. Depicted in Figure 4.5(a) is the mass spectrum resulting from rf-only transmission of ions through the quadrupole and injection into the ion trap. The appearance of the mass spectrum is similar to that obtained using only the QITMS as a mass analyzer. The mass spectrum is complicated by signals resulting from fragmentation of the precursor ions as well as matrix clusters and adducts. By comparison, Figure 4.5(b) depicts the result of sequential injection of the peptide mixture using the quadrupole in step scanning mode. The quadrupole mass filter was stepped from 850 to 1350 u using 5 u wide bins and a bin scan time of 0.6 s. A total of 110 scans were summed, corresponding to 1 full mass range cycle of the quadrupole. The S/N ratio and resolution of the precursor ions were markedly improved and the chemical background usually detected when a liquid

Figure 4.4: Reduction in signal suppression achieved utilizing mass-selected sequential injection. The QITMS rf exclusion limit was set to exclude ions with *m/z* below 100 u from the trapping volume. The gating time to allow ions into the trap was 80 ms. (**a**) Hybrid operated in rf-transmission mode with all ions above 10 u transmitted through the quadrupole and injected into the ion trap for mass analysis. Complete signal suppression was observed for Glu-fibrinopeptide B. (**b**) Sequential injection by "step scanning" the quadrupole from 1000 u - 2000 u significantly improves the S/N ratio. The selected ion chromatogram is shown as an inset.

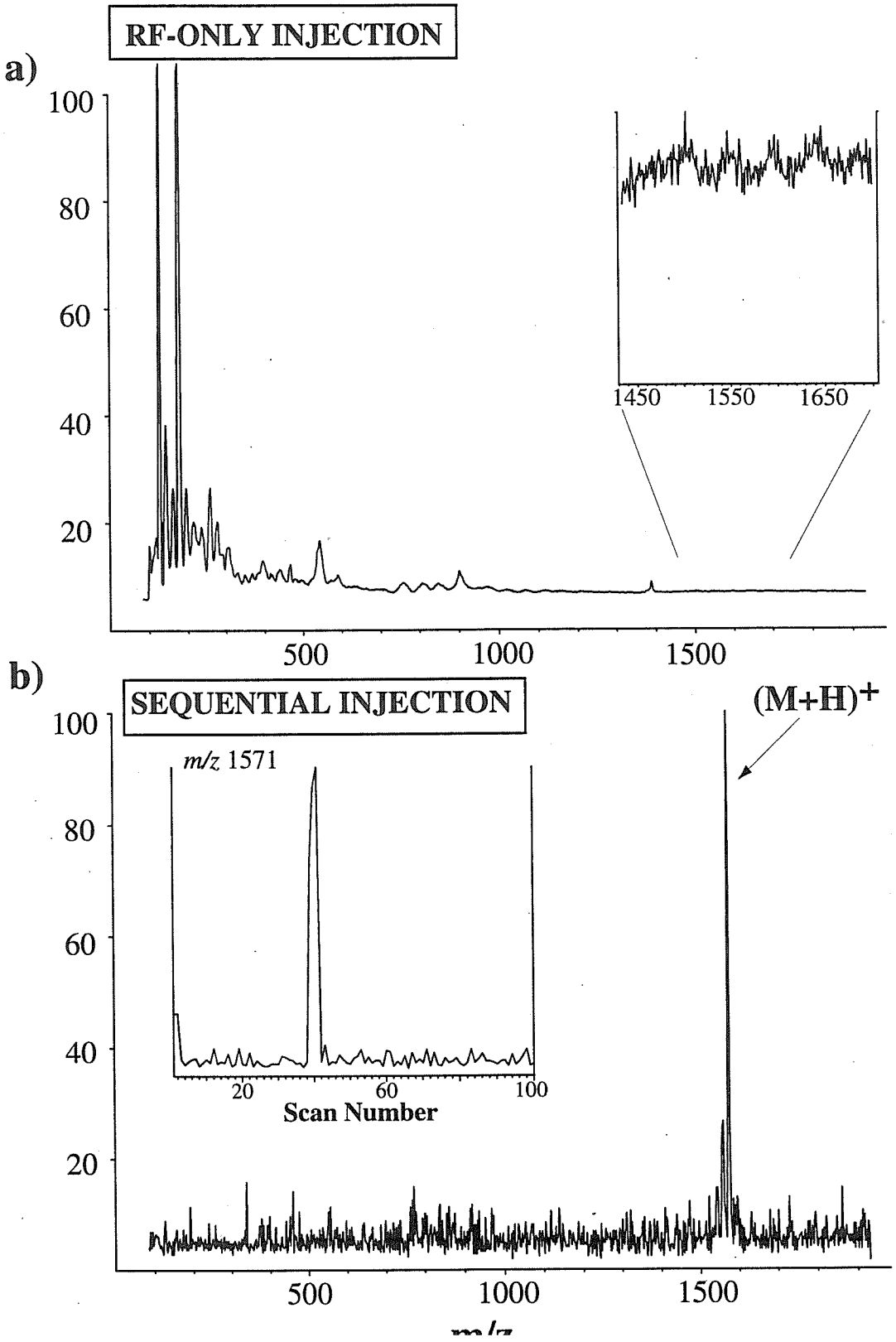
a)
RF-ONLY INJECTION
100
80
60
40
20
500
1000
1500
1450
1550
1650
b)
SEQUENTIAL INJECTION
(M+H)+
m/z 1571
100
80
60
40
20
20
60
100
Scan Number
500
1000
1500
m/z

Figure 4.5: Analysis of a mixture of peptides from the human angiotensin family generated by LSIMS. The QITMS gating time was 20 ms and the rf exclusion limit was 100 u. (**a**) Hybrid operated in rf-transmission mode. (**b**) "Step scanning" the quadrupole from 850 u - 1350 u serves as a mass chromatography stage. 110 scans representing one full mass range cycle of the quadrupole were summed. (**c**) Chromatographic separation of *m/z* 1032 and *m/z* 1046. The quadrupole was stepped from 1000 u to 1075 u in 2 u steps with a bin scan width of 2 u resulting in a 22.5 second scan time over the mass range.

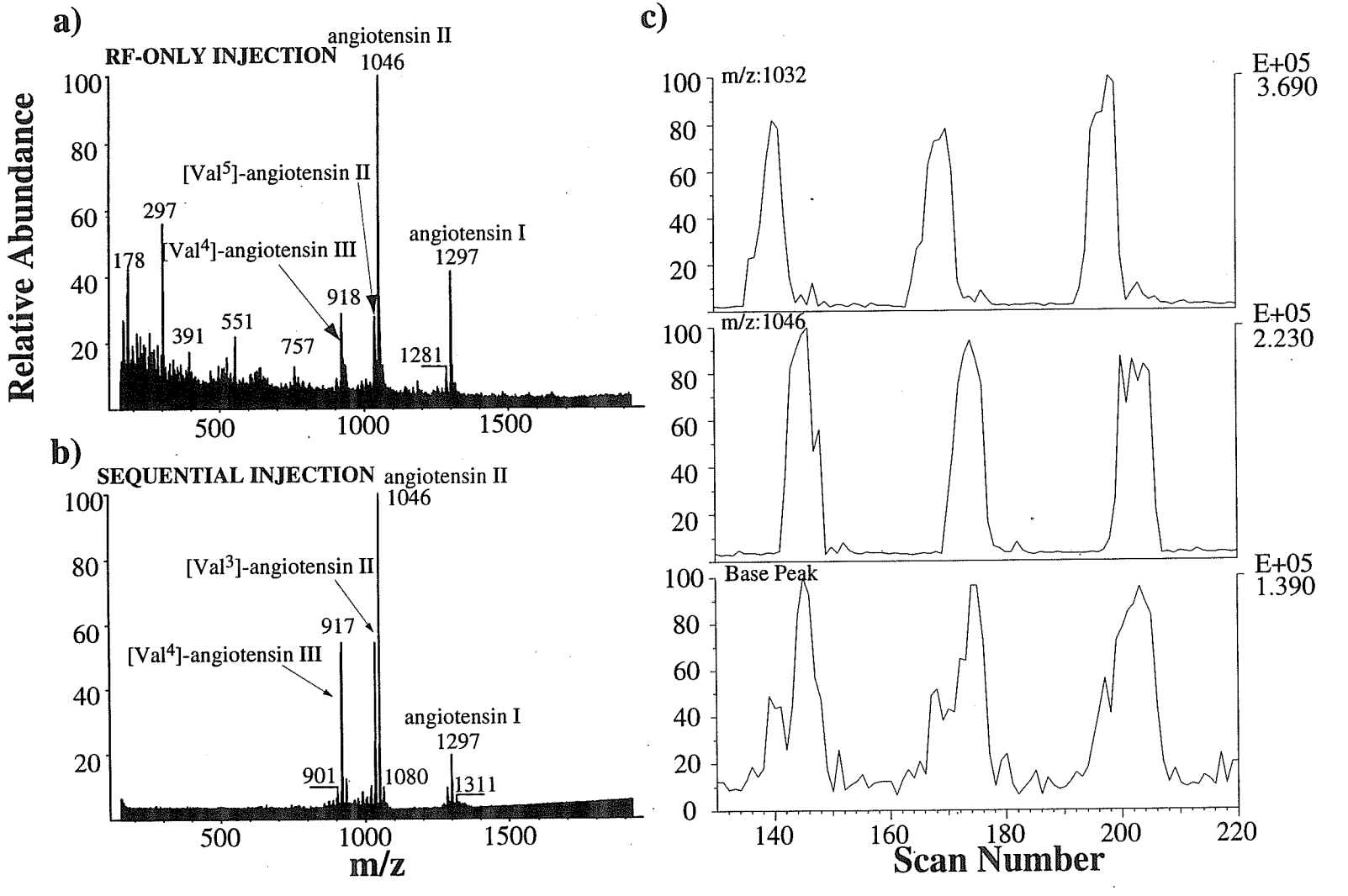
a)
RF-ONLY INJECTION
angiotensin II
1046
[Val5]-angiotensin II
297
[Val4]-angiotensin III
178
angiotensin I
1297
918
551
391
757
1281
Relative Abundance
b)
SEQUENTIAL INJECTION
angiotensin II
1046
[Val3]-angiotensin II
917
[Val4]-angiotensin III
angiotensin I
1297
901
1080
1311
m/z
c)
m/z:1032
E+05
3.690
m/z:1046
E+05
2.230
Base Peak
E+05
1.390
Scan Number

matrix is utilized is not seen. Post-source fragmentation was observed resulting from collision-induced dissociation with the helium bath gas or surface-induced dissociation (35).

Since complex mixtures of ions may contain components with similar mass-to-charge ratios, it was of interest to investigate the separation resolution of the sequential injection technique. Illustrated in Figure 4.5(c) is an example of the mass chromatographic separation of [Val^5]angiotensin II (MW 1032) and angiotensin II (MW 1046). The selected ion chromatograms clearly demonstrate the ability of this technique to mass separate species within a relatively narrow range of *m/z* values. There is a small region of overlap where both ions are being simultaneously transmitted as evidenced in the base peak chromatogram. Increasing the resolution of the quadrupole to narrow the mass transmission window may serve to reduce the extent of simultaneous transmission. Reducing the width of the quadrupole scan bin and decreasing the step size did not reduce the transmission overlap.

4.4.2 Mass Resolution

Space-charge effects typically provide an upper limit for resolution on the QITMS (36) and the primary cause of space-charge is the number of ions in the trap. Selected injection of ions serves to reduce space-charge and improve resolution, especially for components in a mixture. Notch injection using shaped excitation pulses (28), as well as the application of filtered noise fields (27), has been successfully employed to minimize the number of extraneous ions injected into an ITMS. In this work we use the quadrupole

mass filter in selected-ion injection mode to minimize the number of unwanted ions injected into the ion trap.

The high-resolution performance of the Q/QITMS for the analysis of large molecules was investigated with the model peptide angiotensin I (monoisotopic MW 1295.6). The rf exclusion limit of the ion trap was set to 100 u and the quadrupole transmitted ions by scanning a 10 u window around *m/z* 1296. The dc offset controlling the resolution of the quadrupole was set to 20% of the maximum offset. The resolution on the quadrupole cannot be calculated since the peak width is dependent upon the ion trap resolution. Typically, 30 microscans were averaged then ported as one scan to the DECStation. Illustrated in Figure 4.6 is a high resolution mass spectrum for *m/z* 1296 from angiotensin. The spectrum was obtained by slowing the mass scan speed by a factor of 200 employing the technique developed by Schwartz *et al.* (37). The mass spectrum represents data from a single QITMS microscan in which a resolution of 33,220 was calculated. The average resolution obtained for 30 microscans was typically half of this value, resulting from peak shifting that occurs in this type of experiment. The average resolution obtained for 30 microscans utilizing the QITMS was similar to that obtained using the hybrid instrument and mass-selecting ions with the quadrupole. Mass resolution in this range is more than sufficient for most biochemical applications.

The addition of a cooling time prior to mass analysis affords the damping of kinetic energies and trajectories of trapped ions. Compacting the ion cloud near the center of the trapping volume increases the detection efficiency and reduces the amount of time required to eject the ions, leading to improved resolution (38). In a series of experiments, the effect of cooling time on resolution of *m/z* 502 from FC-43 was studied for different modes of operation of the QITMS and hybrid. In the first set of experiments, the quadrupole was

Figure 4.6: High resolution mass spectrum of human angiotensin I (MW 1296 u) obtained by slowing the QITMS acquisition scan speed by a factor of 200 (37). Helium pressure was reduced to 5.0 x 10^{-5} torr (uncorrected) and a resonance ejection signal was applied at 118,936 Hz with an amplitude of 2.4 V (peak-to-peak, endcap-to-endcap) to eject ions from the trapping volume.

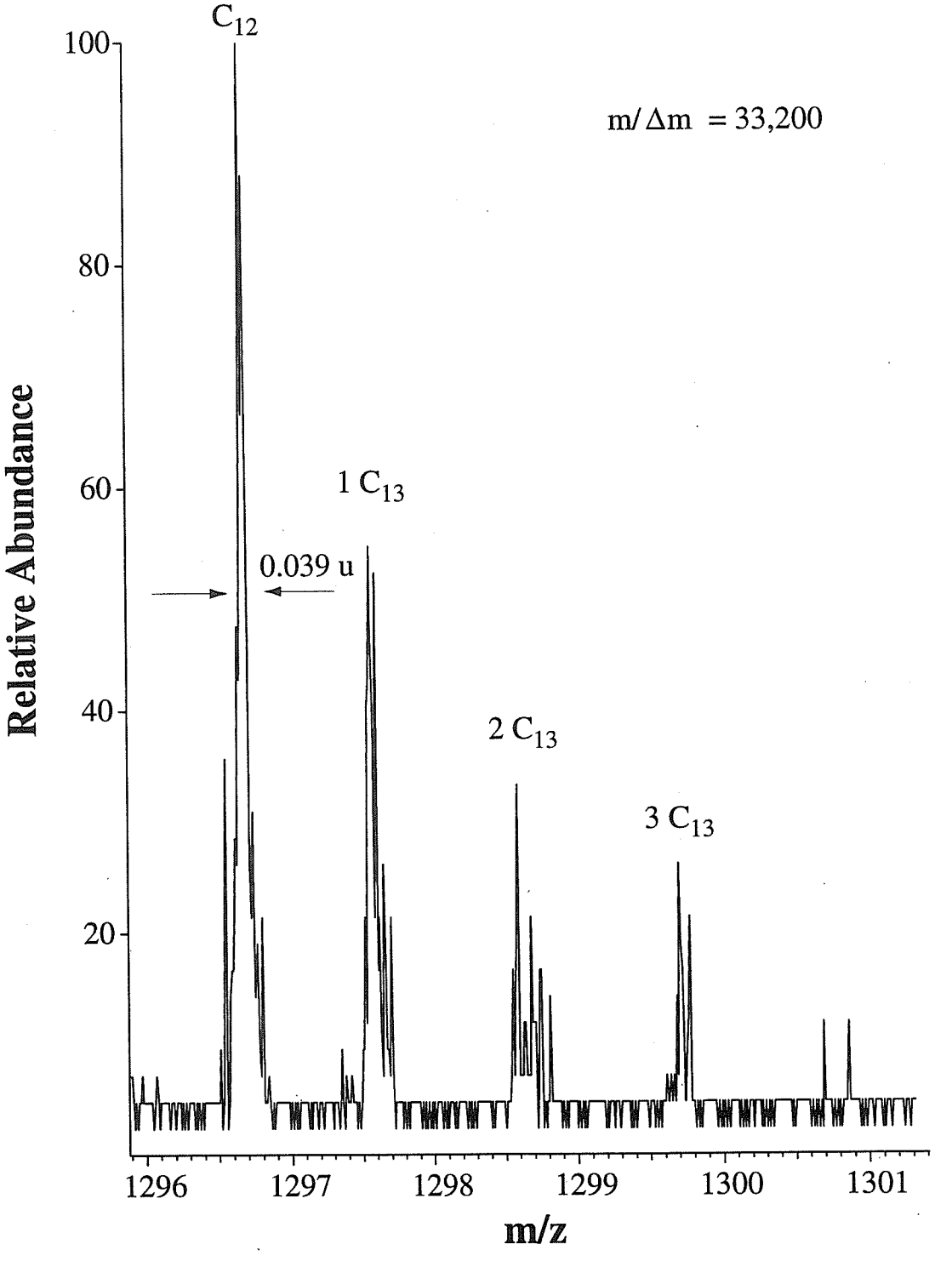
C12
100
80
60
40
20
m/Δm = 33,200
1 C13
0.039 u
2 C13
3 C13
Relative Abundance
1296
1297
1298
1299
1300
1301
m/z

operated in rf-only mode and reverse-then-forward rf-isolation scans were performed in the ion trap. An average resolution of 12,560 was obtained. An average resolution of 12,210 was observed for the QITMS; thus the two modes of operation appear to be analogous, as expected. The quadrupole was subsequently operated in mass-selected injection mode and ions were then rf-isolated in the ion trap. An average mass resolution of 12,820 was calculated. Similar results ($m/\Delta m$=13,640) were achieved when ions were selectively injected but not rf-isolated in the ion trap. Figure 4.7 displays a "least squares fit" linear regression analysis of the mass resolution of *m/z* 502 calculated for each of the modes of operation as a function of cooling time. The original and the regression data show ~10% improvement in resolution obtained by adding the quadrupole and eliminating the rf-isolation step.

Simulations of ion motion inside the trapping volume indicate that initial conditions are crucial to obtain optimal performance (39, 40). It is possible that the ion spatial and velocity distributions at the exit aperture of the quadrupole mass filter provide better initial injection conditions than those obtained using a lens injection system, accounting for the generally improved performance of the hybrid over the QITMS. Data portrayed in Figure 4.7 indicate an enhancement in resolution when ions were not rf-isolated in the QITMS. Nonlinear effects arising from the addition of higher-order fields to the quadrupole trapping field may be a contributing factor to the improved performance of the Q/QITMS when rf-isolation in the trap was not employed. One effect of higher-order fields is to create a shift in the secular frequencies of ions in the ion trap (41). This frequency shifting could cause dispersion of the ion packet during rf-isolation due to the excitation of some of the trajectories of the population of the *m/z* of interest when adjacent ions are resonantly ejected

Figure 4.7: Linear regression analysis of the calculated resolution for *m/z* 502 from FC-43 as a function of cooling time. Cooling time was increased from 0 to 50 ms in 5 ms steps and 30 QITMS microscans were summed and acquired. The high resolution mass spectrum was obtained by slowing the QITMS acquisition scan speed by a factor of 100 (37). ■ indicates mass-selected injection with no rf-isolation in the ion trap, ◆ indicates mass-selected injection with rf-isolation in the ion trap, ▲ indicates QITMS only.

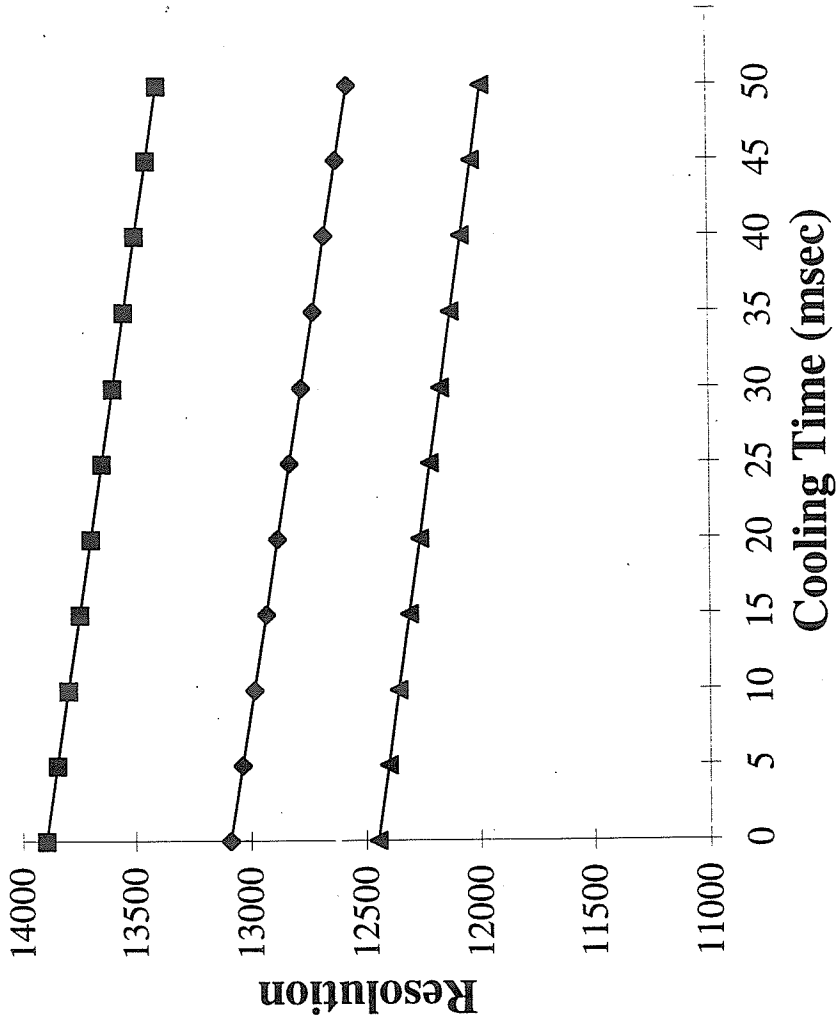
Resolution
14000
13500
13000
12500
12000
11500
11000
0
5
10
15
20
25
30
35
40
45
50
Cooling Time (msec)

(42). Yost *et al.* observed that non-linear effects are intensified as ion storage time is increased (41). The linear decrease in resolution as a function of cooling time for all modes of operation shown in Figure 4.7 corroborates this observation.

4.4.3 Tandem Mass Spectrometry

The next set of studies examined the potential to perform MS/MS analysis "on the fly" during sequential injection of ions into the ion trap. Cooks and Morand demonstrated the use of the ion trap as both collision cell and mass analyzer by adjusting the energy difference between an ion trap and a quadrupole mass filter (22, 23). In a similar experiment, an ICL procedure was written to step the quadrupole from 50 u to 650 u in 10 u steps with a 10 u wide scan window. The value of the dc voltage at which the ion trap electrodes were floated was decremented each time the mass bin was reset to 50 u. As a result, the relative injection energy of the ions from FC-43 was increased. Figure 4.8 portrays signal intensity for the resultant selected ion chromatograms plotted against the trap float voltage. Every group of 60 QITMS scans represents one value of the float voltage. The peaks labeled with circles in the ion chromatogram for *m/z* 264 show the post-source fragmentation produced by the sequential injection of *m/z* 502 into the ion trap. The more intense peaks in the chromatogram result from the sequential injection of *m/z* 264 into the mass spectrometer. The ion injection energy is a parameter that affects the trapping efficiency (23). In this example, *m/z* 502 is trapped most efficiently at a float voltage of -10 V while the optimal trapping voltage for *m/z* 264 is -12 V. Fragmentation for *m/z* 502 is maximized at -11 V. This type of experiment may elucidate the trap float voltage at which the molecules of interest may be optimally trapped as well as the value at

Figure 4.8: "On-the-fly" fragmentation of ions generated from FC-43. Decrementing the trap float voltage increased the relative injection energy, leading to increased fragmentation over a narrow voltage range. Shown are the selected ion chromatograms for *m/z* 502 and *m/z* 264. Each peak corresponds to a different value of the float voltage. Lower intensity peaks in the SIC for *m/z* 264 result from fragmentation of *m/z* 502, and higher intensity peaks result from the sequential injection of *m/z* 264.

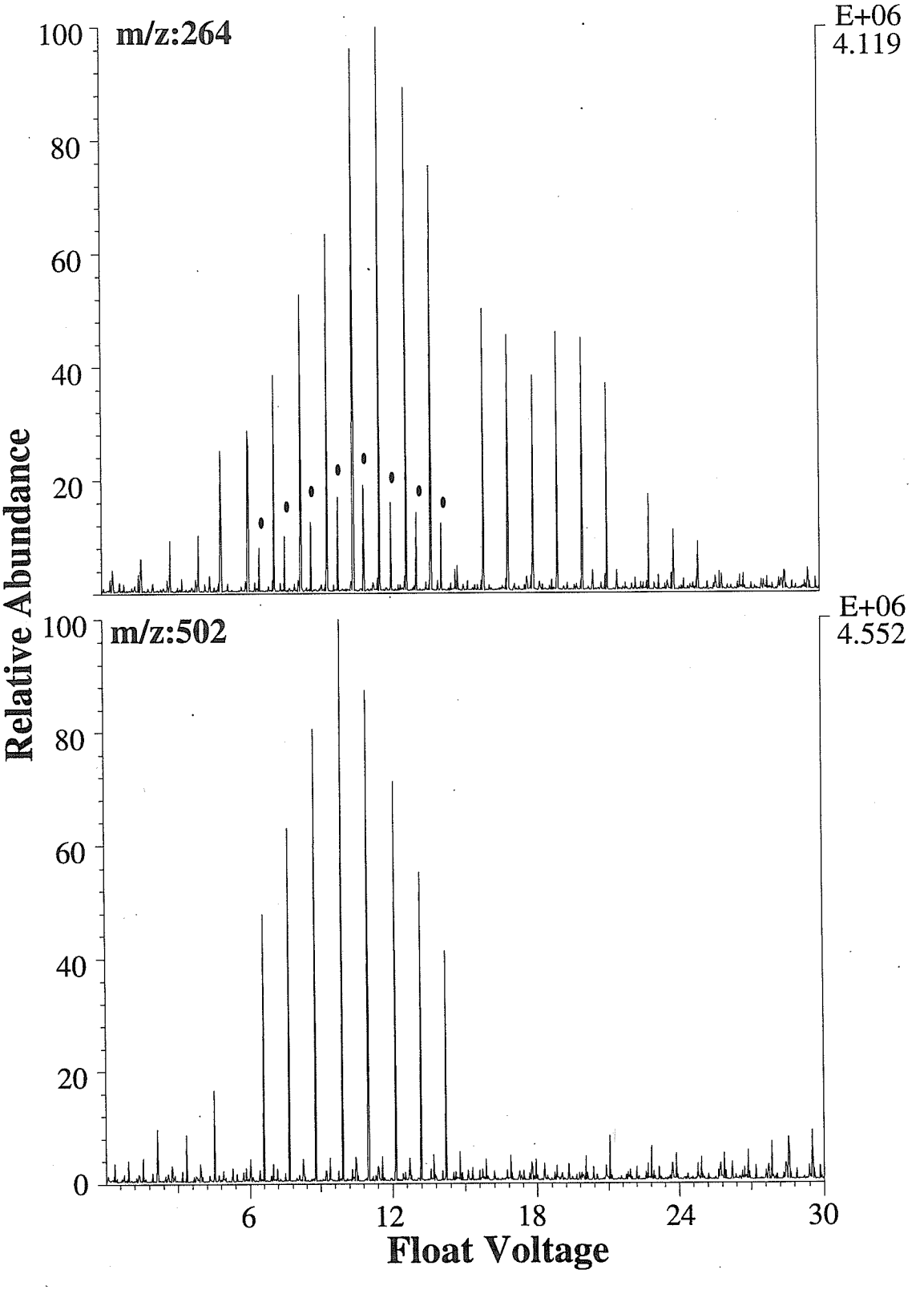
m/z:264
E+06
4.119
m/z:502
E+06
4.552
Relative Abundance
100
80
60
40
20
0
6
12
18
24
30
Float Voltage

which dissociation is most facile. This method did not produce significant dissociation for singly-charged peptides produced by Cs^+ bombardment. The dissociation of these molecules was then investigated using resonance excitation of the trapped ions.

An auxiliary sinusoidal signal is typically placed across the endcap electrodes to induce fragmentation of selected ions by bringing the secular oscillation frequency of the ion into resonance with the frequency of the auxiliary signal (24). Figure 4.9 compares the fragmentation spectrum obtained using the ion trap with that observed on the Q/QITMS when resonance excitation was applied to the molecular ion of human angiotensin I (MW 1296). Angiotensin I was co-deposited with a 1:1 glycerol:thioglycerol matrix onto the probe tip and ions were generated by pulsed Cs^+ bombardment. The molecular ion was isolated by a combination of forward and reverse scans during operation with the QITMS. Utilizing the hybrid instrument, a 10 u wide window was centered around *m/z* 1296. Precursor ions were filtered through the quadrupole mass filter and trapped and then a product mass spectrum was generated by resonance excitation.

The amino acid sequence of the peptide is given in Figure 4.9 with the expected *m/z* values for the sequence ions delineated. Nomenclature is according to that proposed by Roepstorff and Fohlman (43). Observed ions are underlined. An asterisk indicates ions detected using the hybrid but not seen using the QITMS. The nomenclature b_{n-1}+18 is used to represent signal from ions produced via the release by cyclization of the C-terminal amino acid followed by retention of the carboxyl group on the new C-terminus (44). Shown in Figure 4.9(a) is the fragmentation mass spectrum obtained on the QITMS-only instrument. The scale was expanded by a factor of 10 from *m/z* 400 to *m/z* 1170. Some representative fragment ions are labeled. Enough signals were present from high mass b- and y-type ions that the sequence of the peptide could be deduced from the data. The signal

Figure 4.9: MS/MS of human angiotensin I by resonance excitation. The rf level on the ring electrode was set to bring the ion to a q_z value of 0.3 and a signal at 118,111 Hz and 1.44 V (peak-to-peak, endcap-to-endcap) was applied for 30 ms across the endcap electrodes. All ions with *m/z* below 430 were ejected from the trap due to the amplitude of the rf voltage applied to the ring electrode during the excitation period. Ions were cooled for 3 ms before ejection from the ion trap. 14 microscans were summed to provide the mass spectra. The expected peptide sequence masses are shown and observed signals are underlined. An asterisk indicates ions observed utilizing the hybrid and not observed utilizing the QITMS. Ions labeled b_{n-1}+18 presumably result from loss of the C-terminal amino acid with retention of the carboxyl group. (**a**) Ions were rf-isolated in the ion trap for QITMS operation. (**b**) Mass-selected injection was performed by the quadrupole. Ions were not subsequently rf-isolated in the ion trap.

116	272	371	534	647	784	*881	1028	1166	1279	**b-type**
Asp	**Arg**	**Val**	**Tyr**	**Ile**	**His**	**Pro**	**Phe**	**His**	**Leu**	
1297	1182	1026	926	763	650	513	416	269	132	**y-type**
1184	1069	912	813	650	537	400	303	156		**b_{n-1}+18**

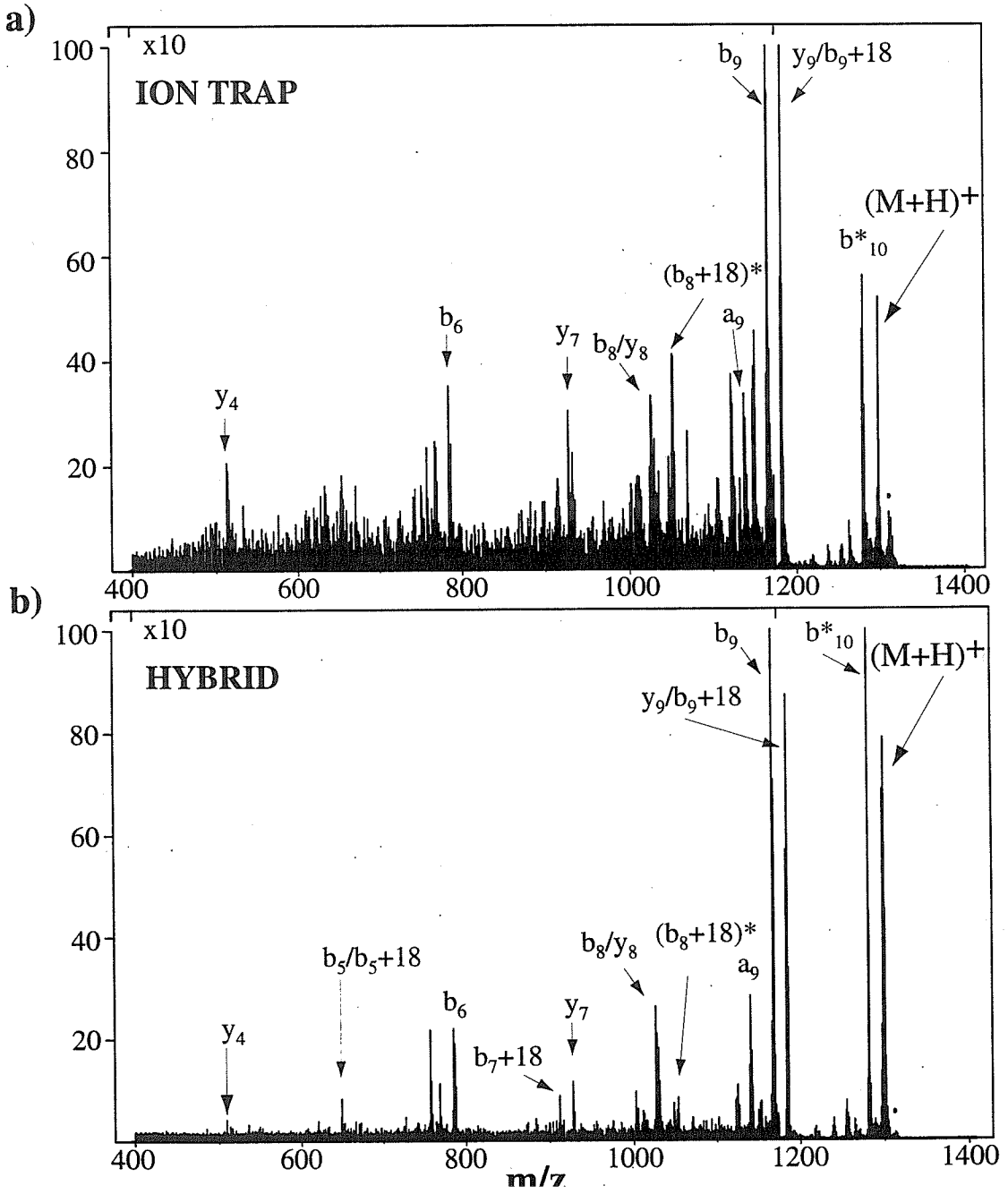

at *m/z* 1309 indicated by a filled circle is thought to result from the creation of adducts due to surface interactions (35). The signal at *m/z* 1051 results from loss of ammonia or water from the b_8+18 ion.

The spectrum in Figure 4.9(b), by comparison, results from mass-selected injection by the quadrupole followed by resonance excitation in the ion trap. The two spectra have many similar features including the number and types of sequence-specific fragment ions observed. A striking difference between the two spectra is the signal-to-noise ratio, far better in the hybrid instrument than when only the QITMS was utilized. In a typical example, the S/N ratio for the b_7+18 ion at *m/z* 912 was 12.3 for the hybrid compared to 5.1 for the QITMS. S/N ratios for *m/z* 1182/1184 were 1212 for the hybrid and 294 for the QITMS. The quality of the mass spectrum was typically better using the Q/QITMS than the ion trap, especially in the low molecular weight region of the spectrum where relative ion abundances were small. Over the course of many experiments, S/N ratios varied for both modes of operation but were typically 20%-30% higher for the hybrid than the QITMS. The most probable explanation for these improvements in the signal quality is the reduction of space-charge and chemical noise. Low-mass matrix ions typically are present in great excess over analyte ions and quickly fill the trap to the space-charge limit. The fundamental rf level during ion injection cannot be set to eject these ions without compromising trapping efficiency for the ions of interest. The mass filtering action of the quadrupole serves to reduce space-charge and chemical noise produced by unwanted ions and improves the quality of the fragmentation mass spectrum for the isolated molecular ion being studied. The improved resolution of the Q/QITMS also affords the observation of a series of b_{n-1}+18 ions that are not clearly noticeable in the ion trap data, providing a mass spectrum rich in sequence information.

The efficiency of fragmentation induced by resonance excitation of angiotensin I was investigated as a function of post-excitation cooling time in the QITMS for the various modes of operation, analogous to experiments performed by March *et al.* on *n*-butylbenzene (45). Cooling time was increased in 1 ms steps from 0 - 15 ms, then in 5 ms steps from 15 - 60 ms. Approximately 12 microscans were acquired for the unattenuated precursor ion, and 30 microscans were acquired for the MS/MS experiment. Calculated peak areas for each microscan were summed and normalized by the number of microscans acquired. The fragmentation efficiency was calculated by dividing the peak area of the unattenuated precursor ion by the sum of the peak areas of the product ions. Linear regression analysis was performed on the resultant data. Results of the regression analysis exhibited similar trends to those observed for the high resolution cooling time experiment shown in Figure 4.7. The performance, measured by the fragmentation efficiency, was improved for the hybrid when compared with the QITMS. The percent improvement in fragmentation efficiency obtained on the hybrid compared to the ion trap was found to increase linearly as a function of cooling time (4% - 30%). Efficiency was maximized when the precursor ion was not rf-isolated in the ion trap. The efficiency difference between the non-rf-isolating mode and the rf-isolating mode of operation was also found to increase linearly as a function of cooling time. Performance dropped overall for long cooling times, unlike the results found by March *et al.* for small molecules (45). Decreased efficiency for long cooling times may be attributed to ion loss due to the effects of nonlinear resonance conditions on the expanded ion cloud (38).

4.5 Conclusion

A quadrupole mass filter/quadrupole ion trap mass spectrometer, an instrument capable of obtaining both molecular weight and structural information for mixtures of molecules, has been assembled. Components from mixtures of gas phase ions were sequentially injected into the ion trap and detected. Improvements in chromatographic resolution of the ion current for a simple mixture of angiotensin II and [Val^5]angiotensin II were demonstrated by increasing the number of data points taken over a limited mass range. This two-dimensional scan mode of operation will be useful for the analysis of complex mixtures. Mass-selective injection was utilized to reduce space-charge induced effects such as signal suppression and decreased resolution. Performance of the hybrid for high-resolution and MS/MS experiments was typically better than that achieved by the QITMS. Eliminating rf-isolation of ions in the ion trap provided the best results, suggesting that step scanning the hybrid is an excellent method of pre-processing the ion population for subsequent analysis. A shortcoming of the Q/QITMS is the bin scan time, limited by the time required to port the data from the PC to the DECStation 2100.

4.6 References

1. Jennings, K. R. (1968) *Int. J. Mass Spectrom. Ion Phys.* **1** 227-235.

2. Mabud, M. A., Dekrey, M. J., and Cooks, R. G. (1985) *Int. J. Mass Spectrom. Ion Phys.* **67** 285-294.

3. Griffiths, I. W., Mukhtar, E. S., March, R. E., Harris, F. M., and Beynon, J. H. (1981) *Int. J. Mass Spectrom. Ion Phys.* **39** 125-132.

4. Louris, J. N., Brodbelt, J. S., Cooks, R. G., Glish, G. L., Van Berkel, G. J., and McLuckey, S. A. (1990) *Int. J. Mass Spectrom. Ion Proc.* **96** 117-137.

5. Yost, R. A., Enke, C. G., McGilvery, D. C., Smith, D., and Morrison, J. D. (1979) *Int. J. Mass Spectrom. Ion Phys.* **30** 127-136.

6. Schey, K., Cooks, R. G., Grix, R., and Wollnick, H. (1987) *Int. J. Mass Spectrom. Ion Proc.* **77** 49-61.

7. Tomer, K. B., Guenat, C. R., and Detering, J. (1988) *Anal. Chem.* **60** 2232-2236.

8. Glish, G. L., McLuckey, S. A., Ridley, T. Y., and Cooks, R. G. (1982) *Int. J. Mass Spectrom. Ion Phys.* **41** 157-177.

9. Gaskell, S. J., Reilly, M. H., and Porter, C. J. (1988) *Rapid Commun. Mass Spectrom.* **2** 142-145.

10. Taylor, L. C. E., and Poulter, L. (1989) *in* Advances in Mass Spectrometry (Longevialle, P., Ed.), **11A**, Elsevier, London, p. 286.

11. Schoen, A. E., Amy, J. W., Ciupek, J. D., Cooks, R. G., Dobberstein, P., and Jung, G. (1985) *Int. J. Mass Spectrom. Ion Proc.* **65** 125-140.

12. Beaugrand, C., Devant, G., Nermag, S. N., and Janoven, D. (1986) *Proc. of the 34th ASMS Conf. on Mass Spectrom. and Allied Topics*, Cincinnatti, OH, American Society for Mass Spectrometry, p. 799.

13. Jennings, K. R. (1983) *Proc. of the 31st ASMS Conf. on Mass Spectrom. and Allied Topics*, Boston, MA, American Society for Mass Spectrometry, p.1.

14. March, R. E., and Hughers, R. J. (1989) *Quadrupole Storage Mass Spectrometry*, (Wineforder, J.D.; Kolthoff, J.M., Eds.) *in* Chemical Analysis: A Series of Monographs on Analytical Chemistry And Its Applications, **V102**, Wiley and Sons, New York, p. 266.

15. Ho, M., Hughes, R. J., Kazdan, E., Matthews, P. J., Young, A. B., and March, R. E. (1984) *Proc. of the 32nd ASMS Conf. on Mass Spectrom. and Allied Topics*, San Antonio, TX, American Society for Mass Spectrometry, p. 513.

16. Suter, M. J.-F., Gfeller, H., and Schlunnegger, U. P. (1989) *Rapid Commun. Mass Spectrom.* **3** 62-66.

17. Schwartz, J. C., Kaiser, R. E., Cooks, R. G., and Savickas, P. J. (1990) *Int. J. Mass Spectrom. Ion Proc.* **98** 209-224.

18. Fraefel, A., and Seibl, J. (1985) *Mass Spectrom. Rev.* **4** 151-221.

19. Yost, R. A., and Enke, C. G. (1983) *in* Tandem Mass Spectrometry (McLafferty, F. W., Ed.) Wiley and Sons, New York, Chapter 8.

20. Kofel, P., Reinhard, H., and Schlunnegger, U. P. (1990) *Proc. of the 38th Conf. on Mass Spectrom. and Allied Topics*, June 3-8, Tucson, AZ, American Society for Mass Spectrometry, p. 1462.

21. Kofel, P., Reinhard, H., and Schlunegger, U. P. (1991) *Org. Mass Spectrom.* **26** 463-467.

22. Cooks, R. G., and Morand, K. L. (1990) *Proc. of the 38th ASMS Conf. on Mass Spectrom. and Allied Topics*, June 3-8, Tucson, AZ, American Society for Mass Spectrometry, p.1460.

23. Morand, K. L., Horning, S. R., and Cooks, R. G. (1991) *Int. J. Mass Spectrom. Ion Proc.* **105** 13-29.

24. Louris, J. N., Cooks, R. G., Syka, J. E. P., Kelley, P. E., Stafford, G. C., Jr., and Todd, J. F. J. (1987) *Anal. Chem.* **59** 1677-1685.

25. Johnson, J. V., Yost, R. A., Kelley, P. E., and Bradford, D. C. (1990) *Anal. Chem.* **62** 2162-2172.

26. Chen, L., Wang, T.-C. L., Ricca, T. L., and Marshall, A. G. (1987) *Anal. Chem.* **59** 449-454.

27. Goeringer, D. E., Asano, K. G., McLuckey, S. A., Hoekman, D., and Stiller, S. W. (1994) *Anal. Chem.* **66** 313-318.

28. Julian, R. K., and Cooks, R. G. (1993) *Anal. Chem.* **65** 1827-1833.

29. Jonscher, K., Currie, G., McCormack, A. L., and Yates, J. R., III (1993) *Rapid Commun. Mass Spectrom.* **7** 20-26.

30. a) Kaiser, R. E., Jr., Louris, J. N., Amy, J. W., and Cooks, R. G. (1989) *Rapid Commun. Mass Spectrom.* **3** 225-229. b) The source was floated at 6 kV. Cesium ions were extracted from the filament region with a grid lens held at -0.5 kV with respect to the high voltage and were pulsed into the sample region utilizing a gating lens pulsing at -381 V (gate open) and +35 V (gate closed) with respect to the high voltage.

31. Kaiser, R. E., Jr., Cooks, R. G., Stafford, G. C., Jr., Syka, J. E. P., and Hemberger, P. H. (1991) *Int. J. Mass Spectrom. Ion Proc.* **106** 79-115.

32. Stafford, G. C., Jr., Kelley, P. E., Syka, J. E. P., Reynolds, W. E., and Todd, J. F. J. (1984) *Int. J. Mass Spectrom. Ion Proc.* **60** 85-98.

33. Steenvoorden, R. (1994) Personal Communication.

34. Schwartz, J. C., Cooks, R. G., Weber-Grabau, M., and Kelley, P. E. (1988) *Proc. of the 36th ASMS Conf. on Mass Spectrom. and Allied Topics*, June 5-10, San Francisco, CA, American Society for Mass Spectrometry, p. 634.

35. a) Bier, M. E., Schwartz, J. C., Schey, K. L., and Cooks, R. G. (1990) *Int. J. Mass Spectrom. Ion Proc.* **103** 1-19. b) The presence of adducts 11 mass units higher than the $(M+H)^+$ ion, often observed with this instrument, may be indicative of surface interactions.

36. Williams, J. D., Cox, K. A., Cooks, R. G., Kaiser, R. E., Jr., and Schwartz, J. C. (1991) *Rapid Commun. Mass Spectrom.* **5** 327-329.

37. Schwartz, J. C., Syka, J. E. P., and Jardine, I. (1991) *J. Am. Soc. Mass Spectrom.* **2** 198-204.

38. Wu, H.-F., and Brodbelt, J. S. (1992) *Int. J. Mass Spectrom. Ion Proc.* **115** 67-81.

39. Reiser, H.-P., Julian, R. K., and Cooks, R. G. (1992) *Int. J. Mass Spectrom. Ion Proc.* **121** 49-63.

40. Julian, R. K., Reiser, H.-P., and Cooks, R. G. (1993) *Int. J. Mass Spectrom. Ion Proc.* **123** 86-96.

41. Eades, D. M., Johnson, J. V., and Yost, R. A. (1993) *J. Am. Soc. Mass Spectrom.* **4** 917-929.

42. Cox, K. A., Williams, J. D., Cooks, R. G., and Kaiser, R. E., Jr. (1992) *Biol. Mass Spectrom.* **21** 226-241.

43. Roepstorff, P., and Fohlman, J. (1984) *Biomed. Mass Spectrom.* **11** 601.

44. Thorne, J. C., Ballard, K. D., and Gaskell, S. J. (1990) *J. Am. Soc. Mass Spectrom.* **1** 249-257.

45. Liere, P., Blasco, T., March, R. E., and Tabet, J.-C. (1994) *Rapid Commun. Mass Spectrom.* **8** 953-956.

Chapter 5

High Sensitivity Peptide Mixture Separation Using Low-Flowrate Electrospray Ionization

5.1 Overview

The use of low-flowrate electrospray ionization (microspray) for the analysis of peptides is described. An ion source was modified and interfaced to a hybrid mass spectrometer that was described in Chapter Four. Phosphopeptides in a tryptic digest of α-casein were identified using a novel method of scanning the hybrid. Two innovative methods of applying voltage to the sample were developed. The first utilized a platinum wire aligned coaxially with a fused silica transfer line and epoxied into a pulled glass micropipette needle. This configuration on the hybrid provided detection of as little as 75 amol of a mixture of angiotensin I and melittin. A platinum wire was also inserted through the sidewall of a piece of Teflon tubing to create a liquid junction. This configuration facilitated connection of the microspray needle to capillary electrophoresis (CE) and HPLC columns as well as to fused silica. One fmol of angiotensin was loaded onto a column and detected by CE-MS on the LCQ ion trap. Crude peptide separations were performed using

step elutions from a pre-concentration membrane. Limits of detection for angiotensin were on the order of 10 fmol loaded onto the membrane. The preliminary data indicate great promise for the development of a sensitive and fast multi-dimensional chromatography technique for the analysis of complex mixtures of peptides.

5.2 Introduction

Liquid chromatography coupled to mass spectrometry (LC-MS) is increasingly becoming the preferred analytical technique for biomedical and biochemical applications. A recent review discusses the application of LC-MS to the analysis of drug metabolites, compounds of pharmacological interest, peptides, proteins, glycoproteins, glycolipids, fatty acids, vitamins, steroids, nucleic acids, drug conjugates, biosynthetic peptides, and recombinant proteins (1). Electrospray ionization (2-5), with flowrates of 1-10 μL/min, has emerged as the primary mode of ionization for the sensitive analysis of mixtures of biomolecules. A series of innovations have decreased the limits of detection of the technique to the femtomole to zeptomole level (6-9). High sensitivity has primarily been achieved by lowering flowrates of effluent directed into the electrospray ionization source by 1-2 orders of magnitude and reducing transfer line, column, and needle sizes (6, 8, 10, 11) in order to increase the effective sample concentration at the needle tip. This typically involves extensively splitting the solvent flowrate of ~160 μL/min from an HPLC, usually done pre-column. The extent of splitting depends upon the size of the column, with smaller ID columns requiring nanoliter to microliter flowrates (6). A limitation of the technique is that lowering the flowrate causes an increase in elution peak widths thus

increasing the concentration limit of detection and decreasing the detectability of low abundance species.

CE-MS (12-16) has been proposed as an alternative to LC-MS for the high sensitivity separation of mixtures. The low flowrates provided by CE afford facile coupling to microspray interfaces and exploit the sensitivity advantage of the technique. A limitation of CE is that separation is poor for relatively complex mixtures. Although high sensitivities are reported, injection of a concentrated sample is required due to the small volumes that are typically injected onto the column. Typical samples of biological interest are generally quite dilute and not compatible with the requirements of CE. A recent refinement provided by Naylor and co-workers is the use of a hydrophobic membrane to concentrate dilute samples prior to injection onto a CE column (17, 18). Dilute solutions (~300 amol/mL) were concentrated and eluted using 100% methanol onto a CE column, affording detection of peptides at low attomole levels. In addition, the membranes were useful for washing samples to remove salts and biological debris prior to CE-MS analysis. This technique increased the utility of CE-MS for the analysis of biological samples.

An electrical contact is required for the establishment of the CE field and the electrospray process. A number of different methods have been employed to create an electrical contact while minimizing the dead volume. CE capillaries and electrospray needles have been coated with gold and connected to a metal surface bearing a potential (8, 12, 19). The process for capillaries involves etching the tips in hydrofluoric acid, coating them with a silanizing solution, then sputter-coating them with gold. Tips produced using this time-consuming process typically last for one day before the gold wears off (20). Mingling the sample with a charged organic coaxial sheath liquid at the needle tip has been

widely used to transfer charge to analytes (14). Careful selection of sheath composition and extensive optimization is required (21). Another widely used approach is the liquid junction design presented by Henion and co-workers (13). A needle and a transfer line or column are placed 10-20 μm away from each other in a liquid reservoir that is charged. Charged liquid flows into the needle while the small gap reduces the possibility of analyte loss. The gap distance is crucial for optimization and is difficult to reproduce, providing a limitation to this technique. A recent innovation by Smith and co-workers is the use of a liquid junction provided by epoxying a length of microdialysis tubing to the needle and CE column and placing the assembly in a reservoir provided by an Eppendorf pipette tip and charged by a piece of copper wire (20). Changing buffer conditions within the reservoir was used to shift the charge-state distribution of bovine carbonic anhydrase II and could be useful in the study of non-covalent interactions. Finally, a metal union is employed to connect the needle and column or transfer line, creating a liquid junction without the use of a large reservoir (6, 11). Chelating interactions of peptides with the metal appears to be a limitation of the technique. A platinum sheath tube inserted in the union and epoxied to the transfer line has been reported to eliminate interaction effects (11).

The work discussed here details the development of a novel microspray ionization source and its application to peptide mixture separations. New needle types and liquid junctions are investigated and a robust, inexpensive, and easy-to-use liquid junction is described. A unique method of mass spectrometric scanning is employed for the identification of phosphopeptides in a mixture. Separation of peptides using step elutions from a hydrophobic membrane with varying ratios of buffer/solvent is proposed as a

means of concentrating and simplifying peptide mixtures prior to CE-MS analysis and preliminary data is presented.

5.3 Experimental

5.3.1 Ion Source

A microspray ionization source was constructed utilizing a lucite sample stage attached to a three-dimensional positioning device (Edmund Scientific Corp., Barrington, NJ, USA). An aluminum plate was recessed into the sample stage and dc voltage (1-2 kV) was applied to the plate. A brass tab was used to anchor the microspray needle to the plate and transfer voltage to the sample *via* the liquid junction. The configuration is diagrammed in Figure 5.1. Sample was typically infused through a length of 365 μm OD x 50 μm ID fused silica (Polymicro Technologies, Phoenix, AZ, USA) using a 10 μL gas-tight syringe (Hamilton Corp., Reno, NV, USA) pushed by a programmable syringe pump (Harvard Apparatus, South Natick, MA). Flowrates ranged from 50 - 200 nL/min for microspray ionization. Conditions for CE experiments are described below.

Figure 5.1 also includes a diagram of an electrospray source that was modified and interfaced to the hybrid mass spectrometer. A heated capillary (Finnigan MAT, San Jose, CA, USA) was inserted with reverse geometry in place of a glass capillary in an electrospray source (Analytica of Branford, Branford, CT, USA). The use of a heated capillary reduces charging problems that may be encountered with glass capillaries (22).

Figure 5.1: Diagram of microspray ionization source. The heated capillary and lensing system were modifications of an existing electrospray ionization source and were used on the hybrid instrument Q/QITMS.

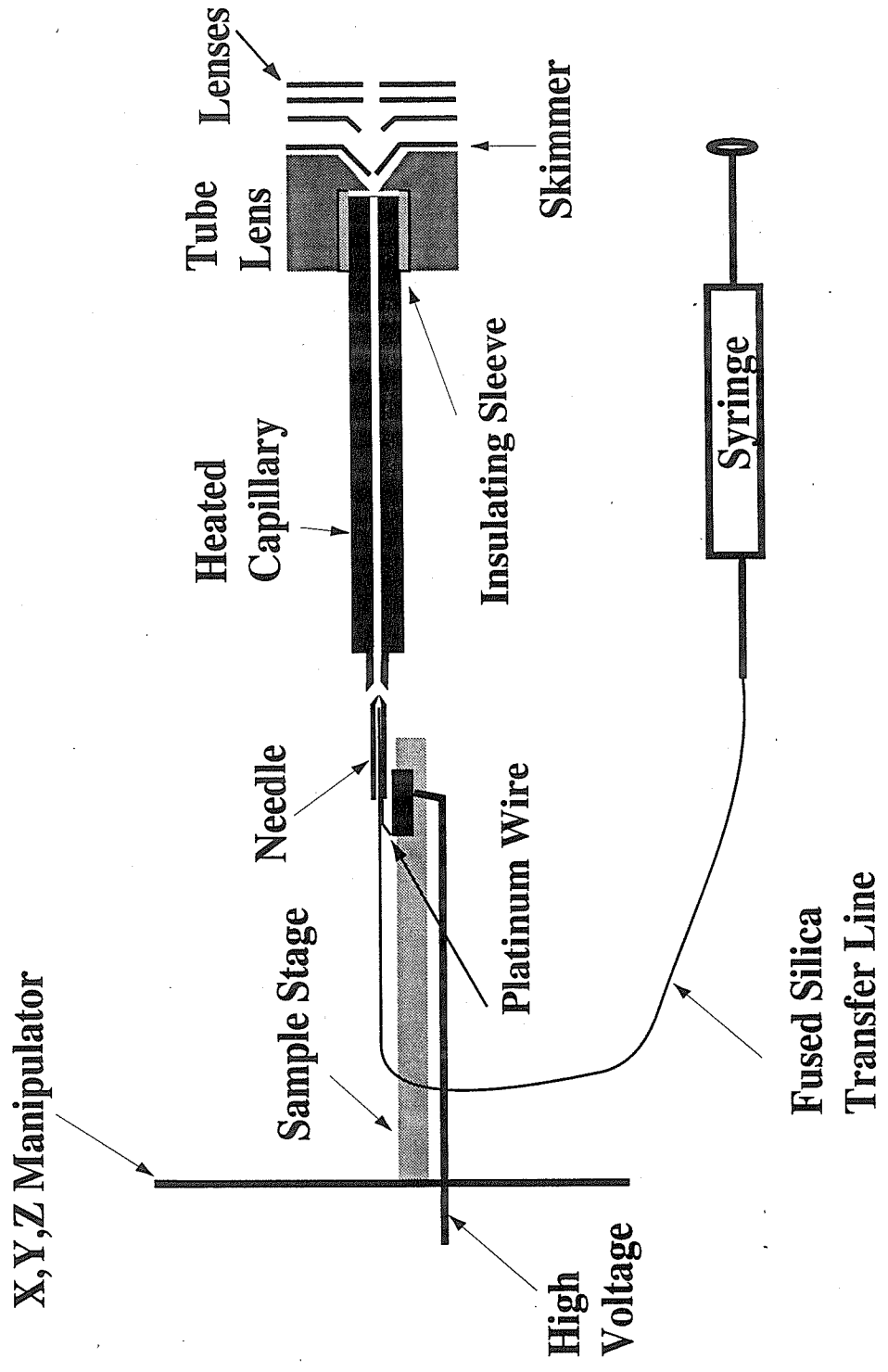
X,Y,Z Manipulator
Sample Stage
Needle
Platinum Wire
High Voltage
Heated Capillary
Tube Lens
Lenses
Skimmer
Insulating Sleeve
Syringe
Fused Silica Transfer Line

The end of the capillary was drilled out to a conical shape to allow the microspray needle to be inserted into the capillary itself and enhances the sensitivity of the technique. Control of the capillary temperature was provided by a programmable temperature controller (Omega Engineering, Inc., Stamford, CT, USA) interfaced to a linear 24 V 2.4 A dc power supply manufactured by Sola and purchased from Newark Electronics (Chicago, IL, USA). Maximum temperature provided by the power supply was 175°C as displayed on the controller LED. A unique tube lens configuration was used to focus ions onto the skimmer and transfer heat from the heated capillary to avoid melting the vespel insulating sleeve. The skimmer and lensing system of the Analytica source were left unmodified and served to further decluster ions and focus them into the acceptance aperture of the quadrupole mass filter. The capillary temperature was typically set to 135°C and the capillary voltage was 15.8 V, with the skimmer held at ground. The tube lens voltage was 23.8 V. Voltages for the three element lensing system were as follows: Lens 1 1.1 V, Lens 2 1.4 V, and Lens 3 -9.4 V.

5.3.2 .Needles and Liquid Junctions

Several types of microspray needles and liquid junctions were investigated and are schematically illustrated in Figure 5.2.

5.3.2.1 Micropipette Needles with Liquid Junction

Needles were made by heating 1 µm OD x 0.5 µm ID borosilicate glass micropipettes (World Precision Instruments, Sarasota, FL, USA) held under tension until they pulled into a needle shape using a PUL-1 puller (World Precision Instruments). The needles were opened by gently touching the tip to the lab bench. Polyimide coating was burned off of the end of a short piece of fused silica transfer line (365-500 µm OD x 50 µm ID). The needle tips were trimmed to a length of ~1 cm and the transfer line was inserted into the tip and epoxied to the glass (EpoTek, Billerica, MA, USA). Liquid junctions were created by inserting a 1.5 cm length of 125 µm diameter platinum wire (Scientific Instrument Services, Inc., Ringoes, NY, USA) coaxially with the transfer line prior to the application of epoxy, illustrated in Figure 5.2(a).

5.3.2.2 Pulled Capillary Needles

Needles were constructed as described by Davis *et al.* (11). A ~30 g weight (large binder clip) was attached to a piece of 365 µm OD x 50 µm ID fused silica taped to the lab bench. The smallest blue flame from a microtorch (Scientific Instrument Services, Inc.) was applied until the capillary began to neck down, then was withdrawn as the fused silica pulled into a needle. A scribe was used to cut the tips of the pulled capillary needles under the microscope to open them. Needle tips used for CE experiments were trimmed so as to keep the ID of the capillary approximately constant while the OD was decreased. Needles were washed with methanol before use to test the patency.

Figure 5.2: Needle and liquid junction configurations used in this work. (**a**) A pulled glass micropipette needle with a fused silica transfer line and a platinum wire inserted coaxially and epoxied. (**b**) A metal union, generally stainless steel tubing epoxied to a fused silica transfer line and a pulled capillary needle. Alternatively, Valco unions with HPLC fittings were used. (**c**) A novel junction made of Teflon tubing and platinum wire with a fused silica transfer line and a pulled capillary needle or a glass micropipette/fused silica needle pushed into the ends.

a)

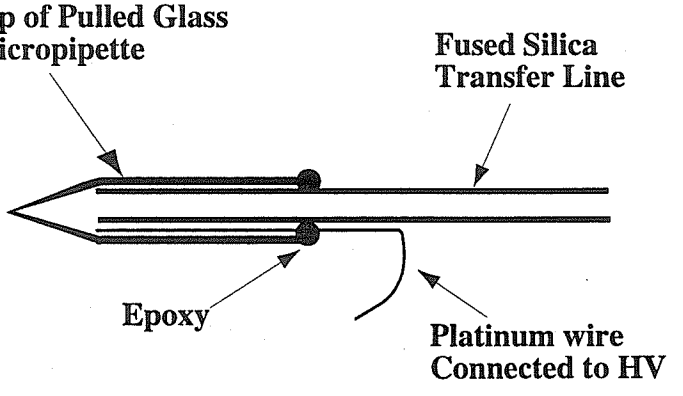
Tip of Pulled Glass
Micropipette
Fused Silica
Transfer Line
Epoxy
Platinum wire
Connected to HV

b)

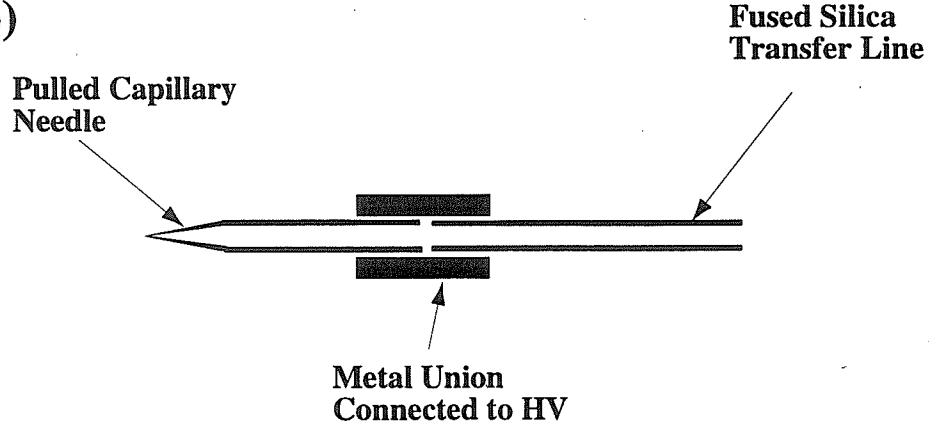
Fused Silica
Transfer Line
Pulled Capillary
Needle
Metal Union
Connected to HV

c)

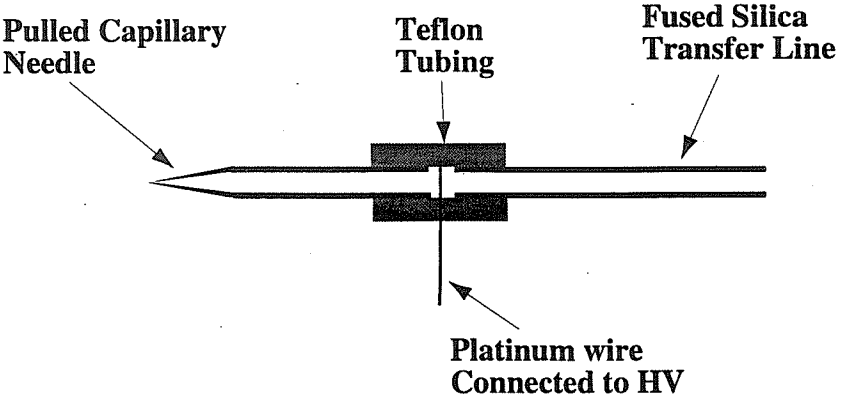
Pulled Capillary
Needle
Teflon
Tubing
Fused Silica
Transfer Line
Platinum wire
Connected to HV

5.3.2.3 Metal Union

Voltage may be applied to a liquid sample by connecting two pieces of fused silica together using a metal union as shown in Figure 5.2(b). Typically, 1.5 cm long pieces of 22 Ga stainless steel tubing were used as the union. Needles were inserted through one end and a transfer line was inserted through the other end until the two ends touched. The fused silica was then epoxied to each end of the tubing. Alternatively, commercially available metal unions were investigated. Fused silica lines and needles were placed in Peek tubing sleeves and butt-connected on either side of a zero dead volume stainless steel union using HPLC fittings.

5.3.2.4 Teflon Junction

A novel liquid junction was developed employing a 1 cm length of 125 μm diameter platinum wire inserted through the sidewall of a ~1 cm long piece of Teflon tubing (250 μm ID x 1.59 mm OD, Upchurch Scientific, WA, USA), through the core and into the other sidewall. Needles and transfer lines were pushed into the ends of the tubing and the Teflon formed a seal about the capillaries. The configuration is shown in Figure 5.2(c). Both pulled micropipette and pulled capillary needles were used with this type of junction. The distance between the fused silica capillaries ranged from 0.6 to 2 mm, providing dead volumes of 30 - 100 nL.

5.3.3 Mass Spectrometry

Two mass spectrometers were employed in the work described here. The hybrid instrument described in Chapter 4 was used to develop the microspray source and investigate the utility of unique mass spectrometric scans available with the quadrupole/ion trap combination for identification of phosphopeptides (discussed below). The quadrupole offset was typically set to -12.8 V and the resolution of the quadrupole set to 50-60% of the maximum attainable value. The electrode assembly was floated at -4.2 V and ions were gated into the trap using a tube lens pulsing from + 200V (gate closed) to -190 V (gate open). The conversion dynode was operated at -10 kV with the electron multiplier set to -1.6 kV.

A newly commercialized ion trap mass spectrometer, the LCQ (Finnigan MAT), was employed for the CE and chromatography experiments. The instrument configuration is shown diagramatically in Figure 5.3. A voltage of 23.5 V was applied to the heated capillary and the temperature was set to 200°C. Two rf-only octopoles were used to transmit ions into the ion trap. The offset of the first octopole was -3.2 V, and that of the second octopole was -6.2 V. Both had an rf voltage amplitude of 400 V_{p-p} applied to the rods. The inter-octopole lens voltage was -26 V. The electrode assembly was floated at a dc offset of -10V and ions were gated into the trap using a tube lens gating from 55 V (gate closed) to -200 V (gate open). Ions were detected using a conversion dynode with the electron multiplier set to -1 kV. Automatic gain control (AGC) was used to maintain a stable number of ions in the trap and eliminate space-charge effects. The AGC target

Figure 5.3: Diagram of the LCQ ion trap mass spectrometer.

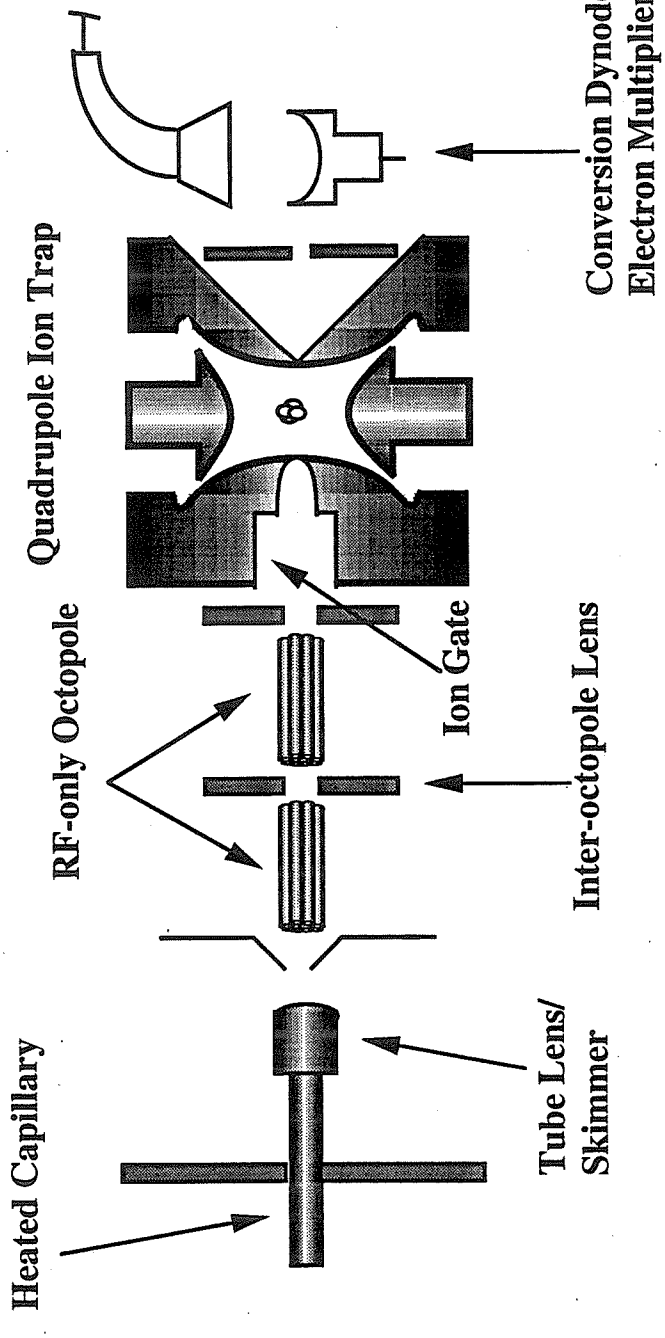
Heated Capillary
Tube Lens/
Skimmer
RF-only Octopole
Inter-octopole Lens
Ion Gate
Quadrupole Ion Trap
Conversion Dynode/
Electron Multiplier

values were 6 x 10^7 ions for full scans, 1 x 10^8 ions for MS^n experiments, and 1 x 10^7 ions for high resolution scans.

5.3.4 Chromatography

5.3.4.1 Capillary Electrophoresis

CE columns were prepared using the protocols of Bruin and co-workers (23) and Thorsteinsdottir and co-workers (24) modified as described by Figeys *et al.* (9). Pressure loading was applied to flow reagents through a 66 cm length of 365 μm OD x 50 μm ID fused silica capillary. Table 5.1 details reagents and reaction times for the preparation. A high voltage supply (Glassman High Voltage, Inc., Whitehouse Station, NJ, USA) with a platinum ribbon (Scientific Instrument Services) soldered to the electrode was used to deliver 25 kV to buffer or sample solutions placed in a microcentrifuge tube inside of a lucite chamber. The CE column was inserted through a Teflon fingertight fitting and was threaded through a holder to ensure the capillary and electrode would stay within the confines of the microcentrifuge tube. At 25 kV applied voltage, the flowrate was measured to be 190 nL/min. Columns were flushed with water and buffer for ~1 hr prior to use.

5.3.4.2 Membrane Chromatography

A ~0.5 cm length of 300 μm ID Teflon tubing (Chromtech, Apple Valley, MN, USA) was opened on the ends using a needle and bored out with a 325 μm diameter piece of stainless steel wire to create a membrane cartridge as illustrated in Figure 5.4. Teflon

Table 5.1: Protocol for preparing CE columns.

Reagent	Reaction Time (hr)	Helium Pressure (psi)
0.5 M NaOH	0.7	500
H_2O	0.2	500
3 M HCl	2.5	300
110°C with He	20	40
10% (v/v) 3-aminopropyltrimethoxysilane in dry toluene	3	100
102°C with He	19	100
dry toluene	0.4	100
acetone	0.3	100

membranes impregnated with poly(styrenedivinylbenzene) coated beads (Empore Extraction Disks with SDB-XC, Lot #710009, 3M, St. Paul, MN, USA) were obtained from Varian (Harbor City, CA, USA) and were prepared in a manner analogous to that presented by Naylor *et al.* (17). A short piece of fused silica (430 μm OD x 320 μm ID) was employed to punch through the membrane disk. The end containing membrane material was placed in the Teflon cartridge. Another piece of fused silica (217 μm OD x 16 μm ID) was used to push the membrane slug into the Teflon cartridge. Fused silica (365 μm OD x 50 μm ID) was placed at either end of the cartridge.

Membranes were activated by washing the membrane in the cartridge with 10 μL of methanol followed by 30 μL of water with 0.5% acetic acid (v/v). Sample was diluted in water with 0.5% acetic acid and 0.5 - 10 μL loaded onto the membrane cartridge. The cartridge was subsequently washed with 10 μL water with 0.5% acetic acid to wash the sample from the walls of the capillary onto the membrane. A short length of fused silica was placed in the Teflon liquid junction and the membrane cartridge placed between the short transfer line on one end and a longer transfer line on the other end that was connected to the syringe and pump. The membrane cartridge was taken off-line and a Teflon connector was used to clean the transfer lines and needles and to fill the lines with elution buffer.

5.3.5 Sample Preparation

Human angiotensin I (MW 1296 Da, Cat. No. A-9650, Lot. No. 13H59101), melittin (MW 2847 Da, Cat. No. M-2272) and bovine α–casein (MW 25 kDa, Cat. No. C-6780, Lot No. 93H9554) were purchased from Sigma Chemical Co. (St. Louis, MO,

Figure 5.4: Diagram of Teflon membrane cartridge used for separation of peptide mixtures.

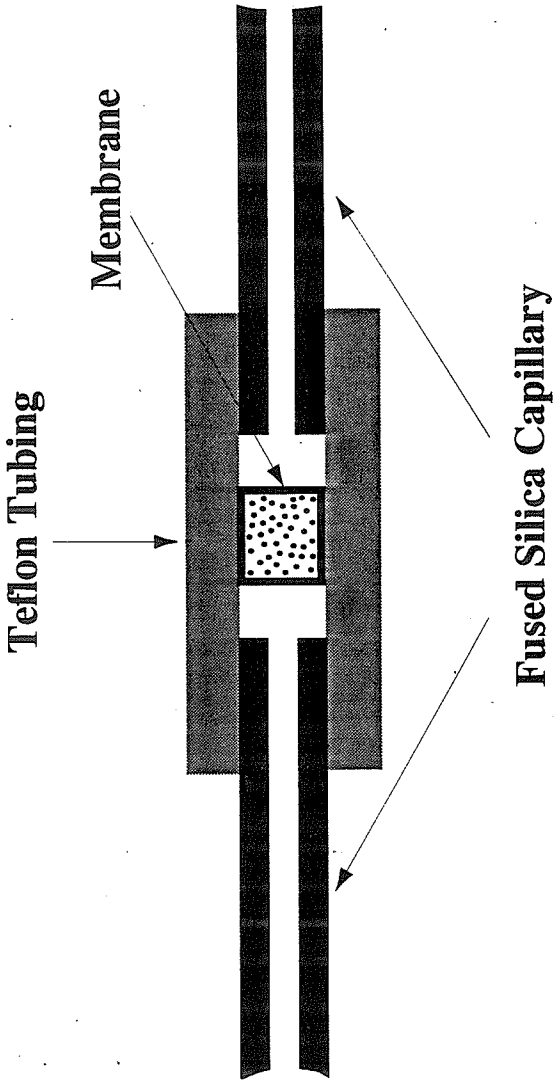
Membrane
Teflon Tubing
Fused Silica Capillary

USA) and used without further purification. TPCK-treated porcine trypsin (Cat. No. V511A, Lot No. 5903801) was purchased from Promega (Madison, WI, USA) and diluted in water to a concentration of 1 μg/μL. Trypsin digestion was performed by diluting ~20 nmol of solid α–casein in 30 μL of 50 mM ammonium bicarbonate, pH 8. Trypsin (8 μg) was added to provide an enzyme to substrate ratio of ~ 1/60 and the mixture was heated at 37°C for 18 hr. The reaction was stopped by adding 5 μL of glacial acetic acid. Sample was subsequently concentrated using a Speed-Vac (Savant Instruments, Farmingdale, NY, USA) and diluted in water with 0.5% acetic acid to a final concentration of ~377 pmol/μL. The stock solution was stored at -20°C. One μL of stock solution was diluted in 377 μL of 0.5% acetic acid to provide the sample. Dilutions from a 1 nmol/μL stock solution of angiotensin I and melittin were similarly prepared to provide a 1 pmol/μL sample in 0.5% acetic acid. Angiotensin and melittin were mixed together to provide an equimolar sample. For high sensitivity experiments, samples were diluted from 1 pmol/μL to 100 fmol/μL or 1 fmol/μL in a microcentrifuge tube. Samples for microspray infusion experiments were further diluted with methanol in a 1:1 mixture.

5.4 Results and Discussion

The objectives of this work were to develop a robust microspray ionization source and to use this source to investigate methods of mixture analysis. Results for the performance of the source are presented for selected peptides. A tryptic digest of α–casein was used to probe various separation techniques.

5.4.1 Microspray Needle Development

Two types of microspray ionization needles are typically in use. The first utilizes either small bore (~6 μm ID) fused silica capillary with an etched tip (6, 10) or fused silica capillary (20-50 μm ID) pulled to a small exit diameter (~2-3 μm ID) (8, 11). The second type of needle developed by Wilm *et al.* utilizes a gold sputter-coated pulled glass micropipette as a needle (~2-3 μm ID exit diameter) (19, 25). The coating apparatus is expensive and the coating does not last long on the needles, even when the glass is derivatized (8, 20). Needle lifetimes are on the order of 3 hrs. Lee and co-workers have reported on the performance of 350 μm OD x 150 μm ID fused silica capillaries pulled to a needle with 150 μm OD x 25 μm ID transfer lines placed inside to minimize the dead volume (11). When a PVDF frit is placed in-line, needle lifetimes are extended significantly to 8-12 hr. Combining these methods, we have inserted a transfer line into a pulled glass micropipette needle as described above. Rather than gold coating, voltage was supplied to the liquid sample either through the use of a stainless steel union epoxied to the needle or *via* a platinum wire inserted into the needle or into a Teflon liquid junction. Needle lifetimes were typically on the order of 3-4 days.

An illustration of the sensitivity of the technique for microspray infusion is shown in Figure 5.5. Serial dilutions of an equimolar mixture of angiotensin I and melittin were used to investigate detection limits on the hybrid quadrupole mass filter/quadrupole ion trap mass spectrometer. A pulled glass needle with an epoxied platinum wire was employed as the liquid junction. A 50 fmol/μL solution was infused into the source at a rate of 50 nL/min. Stable spray was not attainable for less concentrated solutions or lower flowrates.

Figure 5.5: High sensitivity microspray infusion of a mixture of angiotensin I and melittin. The quadrupole mass filter was used in rf-only mode to transmit all ions into the ion trap. The ion gate was opened for 50 msec and all ions above 55 u were stably trapped. Ions were cooled in the trap for 10 msec prior to ejection by ramping the amplitude of the fundamental rf from 450 - 7500 $V_{0\text{-}p}$ with an auxiliary signal at 119,936 Hz and 8.8 V (peak-to-peak, endcap-to-endcap) placed on the endcap electrodes to enable resonance ejection and mass range extension. The mass spectrum is the result of summing 3 microscans, representing the consumption of 75 amol of material.

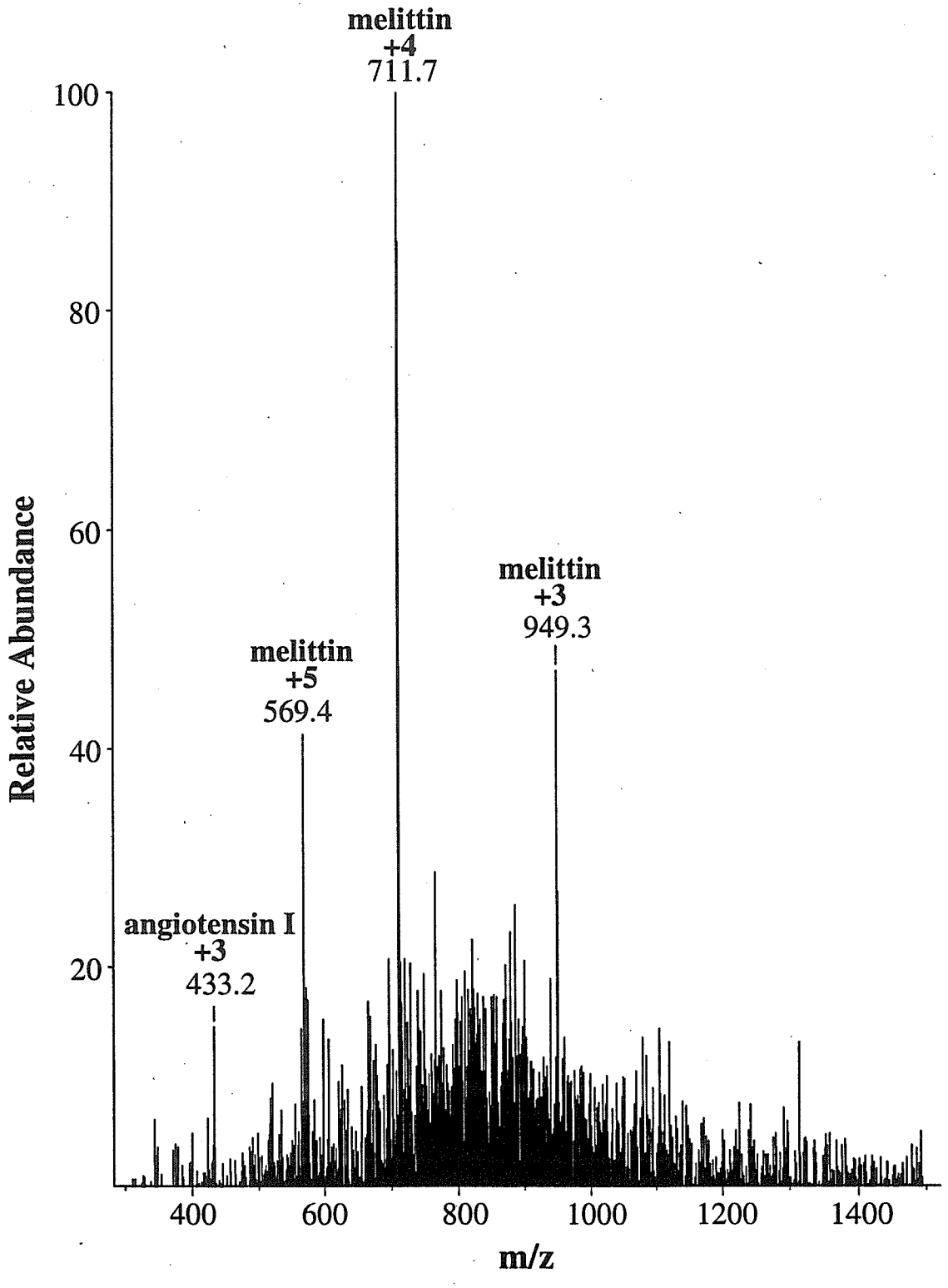
melittin
+4
711.7
melittin
+3
949.3
melittin
+5
569.4
angiotensin I
+3
433.2
Relative Abundance
100
80
60
40
20
400
600
800
1000
1200
1400
m/z

The mass spectrum depicted in Figure 5.5 represents the consumption of 75 amol of material. The signal-to-noise ratio for the quadruply-charged ion from melittin (*m/z* 712) was calculated at 8:1. Calculated detection limits were determined to be in the 5-10 amol range for this experiment (data not shown).

A qualitative comparison of performance between the glass micropipette needles and the pulled capillary needles revealed that the micropipette needles lasted longer without clogging and provided a higher signal-to-noise ratio (although total ion current was generally slightly lower) than did the capillary needles (data not shown). The performance of the needle when the platinum wire was inserted was compromised by depolymerization of the epoxy due to the application of the high voltage. This caused the epoxy to cover the platinum wire and prevented the application of voltage to the liquid in the needle tip. The micropipette needles also required steady solvent flow. Air bubbles in the transfer line caused significant instabilities in the spray. This was a particular problem when the needles were interfaced to the Teflon membrane cartridges, discussed below.

5.4.2 Liquid Junction Development

As discussed above, there are several methods whereby voltage can be applied to a liquid sample for electrospray ionization. Sheath flow sources and reservoir-type liquid junctions are tedious to optimize and result in dilution of the analyte. Metal unions utilizing HPLC fittings can be difficult to troubleshoot at low flowrates because leaks are difficult to find. In addition, changing needles generally requires new ferrules and sleeve fittings and time-consuming leak testing. Metal unions using epoxy must be disposed of when the

needles block, which can be as often as every 1-8 hours (8, 11). In addition, high voltage and/or solvent interactions effect the integrity of the epoxy and lead to an increased background of epoxy peaks. Finally, gold-coated needles have been employed to transfer voltage to a sample. The needles are held at ground and a potential is placed on a glass capillary ~1 mm away. Needles typically last for up to 3 hours (19). When heated capillaries are used, voltage is generally placed on the needle. The gold coating is easily removed when placed either directly in contact with an electrode or close enough to an electrode to induce an arc. This significantly compromises the spray stability.

A unique liquid junction has been designed which incorporates a 125 μm diameter platinum wire pushed through the sidewall of a small length of Teflon tubing, described above. The junction appears to be versatile and robust. Peptides do not interact with the inert material, thus interaction effects are eliminated. Needles and transfer lines can be inserted and removed with ease, facilitating troubleshooting. Removal of epoxy from the system eliminates many of the background signals. Both pulled glass micropipette needles with an epoxied transfer line and pulled capillary needles can be used. Some epoxy background was observed with the micropipette needles; however, it was of low abundance and was virtually eliminated upon optimization of spray conditions (data not shown). Performance of the junctions as measured by spray stability and signal-to-noise of the sample appeared to be equivalent to performance obtained using standard metal unions (data not shown).

5.4.3 Separation of Peptide Mixtures

The analysis of biochemical systems typically involves the analysis of mixtures of molecules. Here we describe a number of approaches used to extract information from peptide mixtures.

5.4.3.1 Neutral Loss Scan

Neutral loss scanning is a technique commonly used on triple quadrupole mass spectrometers (26). The first quadrupole transmits a given *m/z*, collisions occur in the second quadrupole, then the third quadrupole transmits only those ions at a given *m/z* below the precursor ion transmitted by the first quadrupole. For example, when looking for losses of phosphoric acid from a doubly-charged phosphopeptide, the transmission *m/z* of the third quadrupole is offset by *m/z* 49 from the transmission *m/z* of the first quadrupole. This type of experiment cannot easily be done using an ion trap mass spectrometer (27). The hybrid mass spectrometer, described in the preceeding chapter, was employed to develop a new type of neutral loss scan designed to identify the presence of phosphopeptides in a mixture.

Microspray ionization using a pulled glass micropipette tip with a platinum wire epoxied into the tip (Figure 5.2(a)) was used to ionize a tryptic digest of α–casein at a concentration of 3.7 pmol/μL flowing at 100 nL/min. Two peptides from the mixture were investigated, the peptide with *m/z* 693 and that with *m/z* 831. The quadrupole mass

filter was set to transmit ions within a 2 u mass window around 693 and 831, respectively. MS/MS was performed in the ion trap and only the product ions falling within a 60 u mass window below the precursor mass were ejected detected. For example, when analyzing *m/z* 831, only product ions with *m/z* values between *m/z* 750 and *m/z* 810 were ejected from the ion trap and detected. Resultant mass spectra are shown in Figure 5.6. Figure 5.6(a) provides the mass spectrum obtained from analysis of product ions with *m/z* values between *m/z* 615 and *m/z* 675. No signal is present in the spectrum indicating no loss of 49 u from *m/z* 693. Conversely, the peak shown in the mass spectrum in Figure 5.6(b) shows clearly that *m/z* 831 corresponds to a doubly-charged phosphorylated peptide since the peak at *m/z* 781 results from the neutral loss of 49 u from the precursor at *m/z* 831.

5.4.3.2 Separation by Capillary Electrophoresis

CE is a powerful and sensitive technique for analyzing simple mixtures of molecules. Separations can be performed in a shorter time than is possible by liquid chromatographic means and often with higher resolution. Small sample requirements and low flowrates inherent in CE make the technique ideal for interfacing to microspray ionization sources.

Preliminary data is presented here from our first attempts at interfacing CE to a microspray source using the Teflon liquid junction and a pulled capillary needle. The LCQ ion trap was employed for this experiment. The software on the newly commercialized instrument makes it easy to perform relatively complex experiments. For example, Figure

Figure 5.6: Mass spectra arising from neutral loss scanning of the Q/QITMS. Ions were allowed into the ion trap for 100 msec. Ions were cooled for 10 msec then ejected using a supplementary signal at 119,936 Hz with an amplitude of 8.8 V (peak-to-peak, endcap-to-endcap). All ions above *m/z* 55 were trapped. (**a**) The quadrupole injected *m/z* 692-694 into the trap. MS/MS was performed using a q_z value of 0.315, offset by ~5% from the theoretical q_z value of 0.3. The resonance excitation signal was at 118,811 Hz with an amplitude of 24.8 V (peak-to-peak, endcap-to-endcap). The amplitude of the fundamental rf was ramped from 2365 $V_{0\text{-}p}$ to 2596 $V_{0\text{-}p}$ at a resonance frequency chosen to triple the mass range, affording detection of ions between *m/z* 615 and *m/z* 675. The expected neutral loss from a doubly charged phosphopeptide would appear at *m/z* 644. (**b**) The quadrupole injected *m/z* 830-832 into the trap. MS/MS was performed using a q_z value of 0.315, offset by ~5% from the theoretical q_z value of 0.3. The resonance excitation signal was at 118,811 Hz with an amplitude of 28.8 V (peak-to-peak, endcap-to-endcap). The amplitude of the fundamental rf was ramped from 2885 $V_{0\text{-}p}$ to 3115 $V_{0\text{-}p}$ at a resonance frequency chosen to triple the mass range, affording detection of ions between *m/z* 750 and *m/z* 810. The expected neutral loss from a doubly charged phosphopeptide appears at *m/z* 781.5.

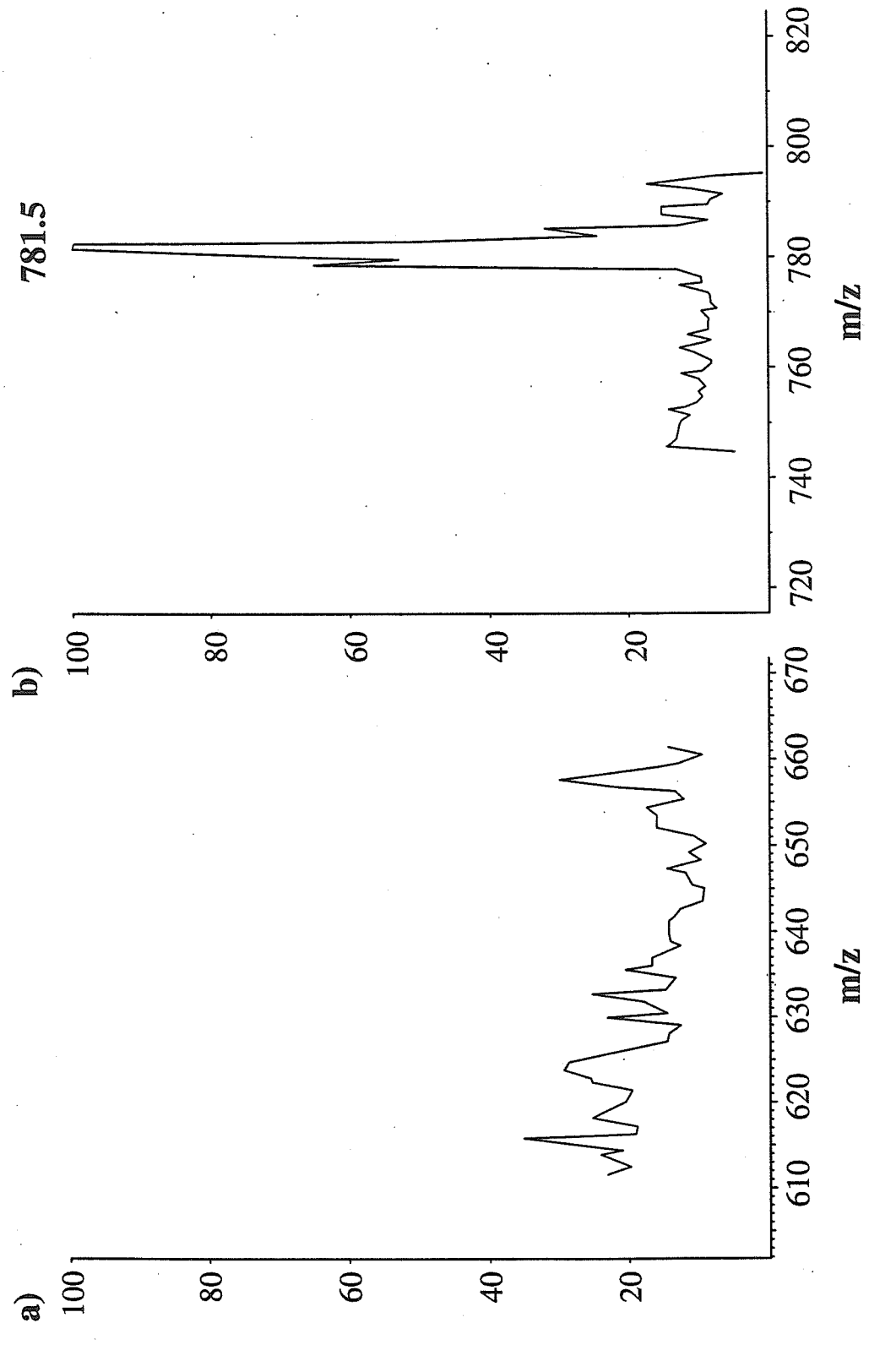
a)
b)
781.5
100
80
60
40
20
610
620
630
640
650
660
670
720
740
760
780
800
820
m/z
m/z

5.7 demonstrates an MS^4 experiment on an ion with *m/z* 880 from a tryptic digest of α-casein. The top panel of Figure 5.7(b) shows the unit resolution full mass-range spectrum of the entire digest. MS/MS on the ion with *m/z* 880 provided the mass spectrum shown in the second panel. Ions below 245 u were ejected upon the application of the resonance excitation pulse. A third stage of mass spectrometry, depicted in the third panel, provides additional low mass sequence ions while the sequence is completed using a fourth stage of mass spectrometry. The amino acid sequence was deduced to be HQGLPQEVLNENLLR. The experiment took approximately 10 min to perform on the LCQ whereas manually tuning all of the parameters would have taken at least 3 hrs on the ITMS ion trap. The following experiments were executed on the LCQ due to the ease of use provided by the upgraded software.

Aminopropyltrimethoxysilane was covalently linked to silane groups on the walls of fused silica capillaries as described above to perform CE experiments. The sensitivity of the technique was investigated using serial dilutions of angiotensin I. A 1 pmol/μL solution of angiotensin I in 0.1% acetic acid was diluted to 50 fmol/μL and injected onto the column using a voltage of -25 kV applied for 6 sec, resulting in the injection of 1 fmol of material onto the column. The column was then placed in buffer solution (10:90 methanol:0.1% acetic acid) and sample was eluted using an applied voltage of -25 kV coupled to a microspray voltage of 1.7 kV. The resultant mass spectrum is depicted in Figure 5.8 with the selected ion chromatogram displayed as an inset. The peptide eluted from the column over ~20 sec time period. Strong signal is observed from the triply-charged and doubly-charged ions with excellent signal-to-noise. Peaks at *m/z* 443, 523, and 579 result from impurities due to solvent filtering. Subsequent experiments have been

Figure 5.7: MS^4 on the doubly-charged ion of *m/z* 880 from a tryptic digest of the model protein α-casein. A 500 fmol/μL sample solution was infused into a microspray ionization source at a flowrate of 200 nL/min. The ionization time was automatically set using automated gain control for the first three stages of mass spectrometry. The AGC was disabled for the fourth stage and the ionization time was set to 400 msec to compensate for the loss in sensitivity due to the performance of multiple stages of mass spectrometry. Ten scans were summed for the MS, MS^2, and MS^3 experiments. Fifteen scans were summed for the MS^4 experiment. (**a**) Mass assignments for sequence ions corresponding to MS^2 of *m/z* 880, MS^3 of *m/z* 436, and MS^4 of *m/z* 266. Observed sequence ions are underlined. (**b**) The precursor ion at *m/z* 880 displayed in the top panel was chosen for fragmentation. The b_4^{+1} fragment ion at *m/z* 436, shown in the second panel, was chosen for a further stage of fragmentation and the resulting mass spectrum is exhibited in the third panel. The b_2^{+1} fragment ion at *m/z* 266 was chosen to obtain the very low mass end of the fragmentation spectrum. Results are displayed in the bottom panel.

a)

MS^2

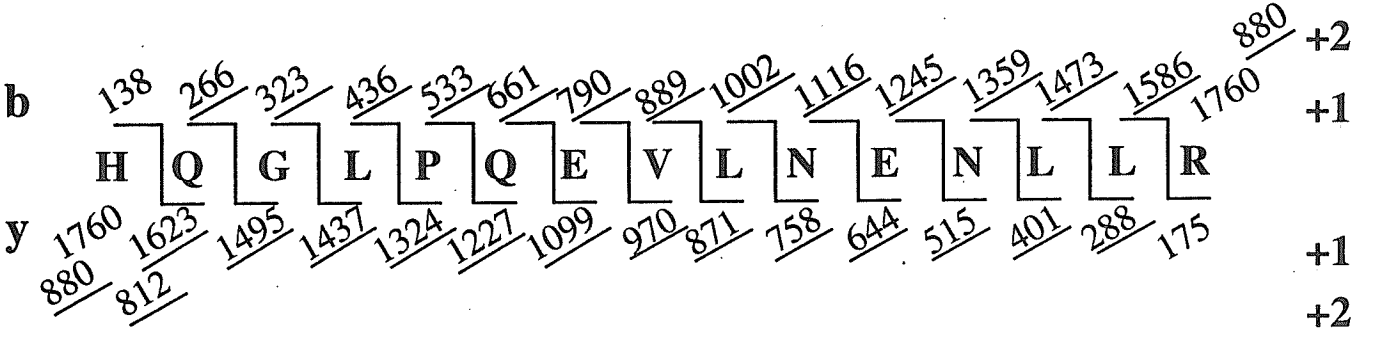
b
138 266 323 436 533 661 790 889 1002 1116 1245 1359 1473 1586 1760
880
+2
+1
H Q G L P Q E V L N E N L L R
y
1760 1623 1495 1437 1324 1227 1099 970 871 758 644 515 401 288 175
880 812
+1
+2

MS^3

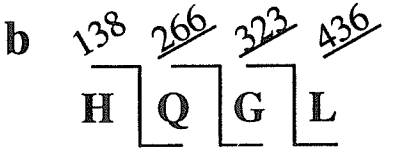
b
138 266 323 436
H Q G L

MS^4

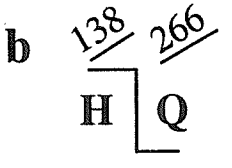
b
138 266
H Q

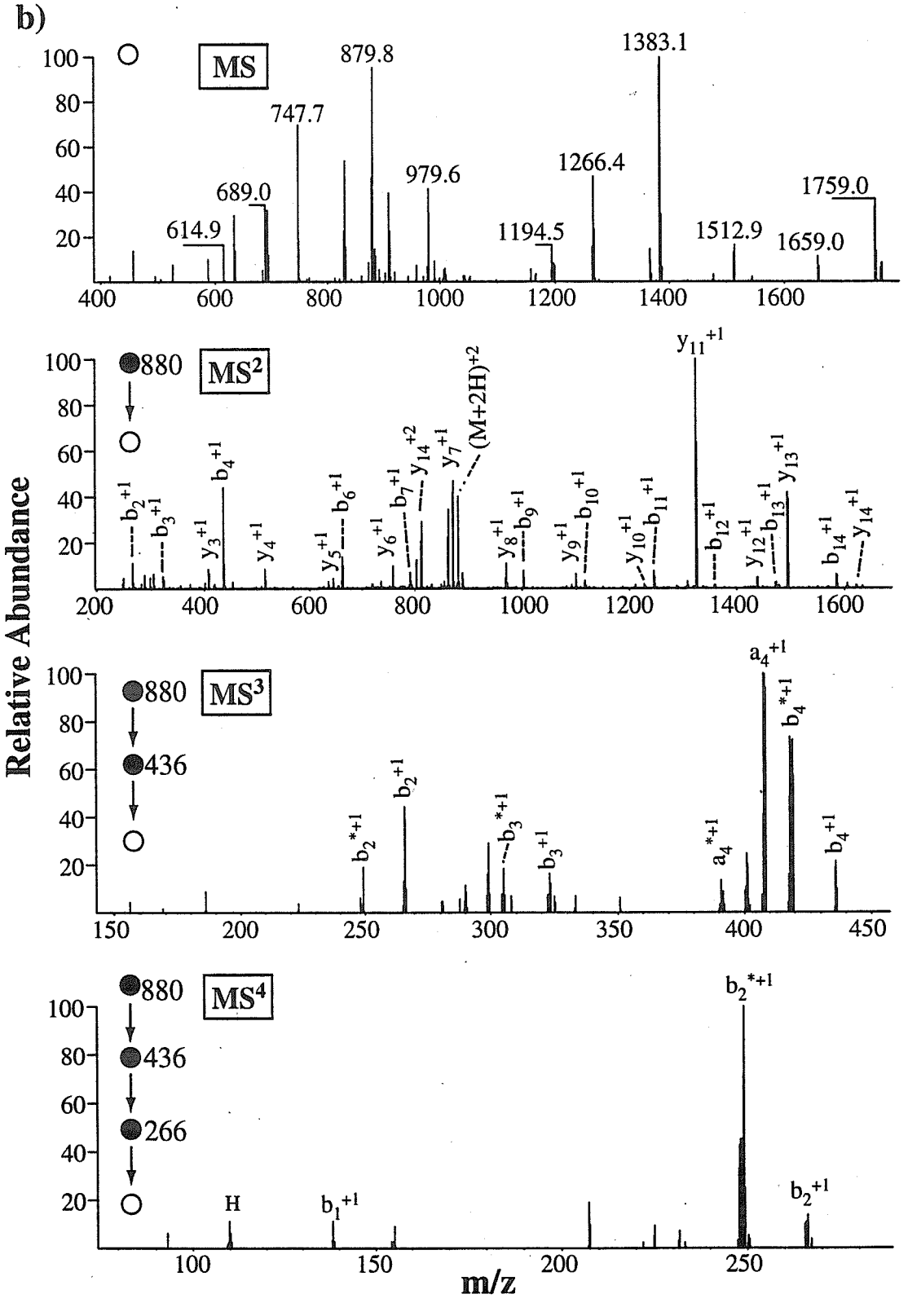
b)
MS
879.8
1383.1
747.7
979.6
1266.4
689.0
1759.0
614.9
1194.5
1512.9
1659.0
MS2
880
(M+2H)+2
MS3
880
436
MS4
880
436
266
H
Relative Abundance
m/z

Figure 5.8: Mass spectrum and selected ion chromatogram resulting from injection of 1 fmol of angiotensin I onto a positively-charged column followed by CE elution at -25 kV. To provide the mass spectrum, 23 scans were summed.

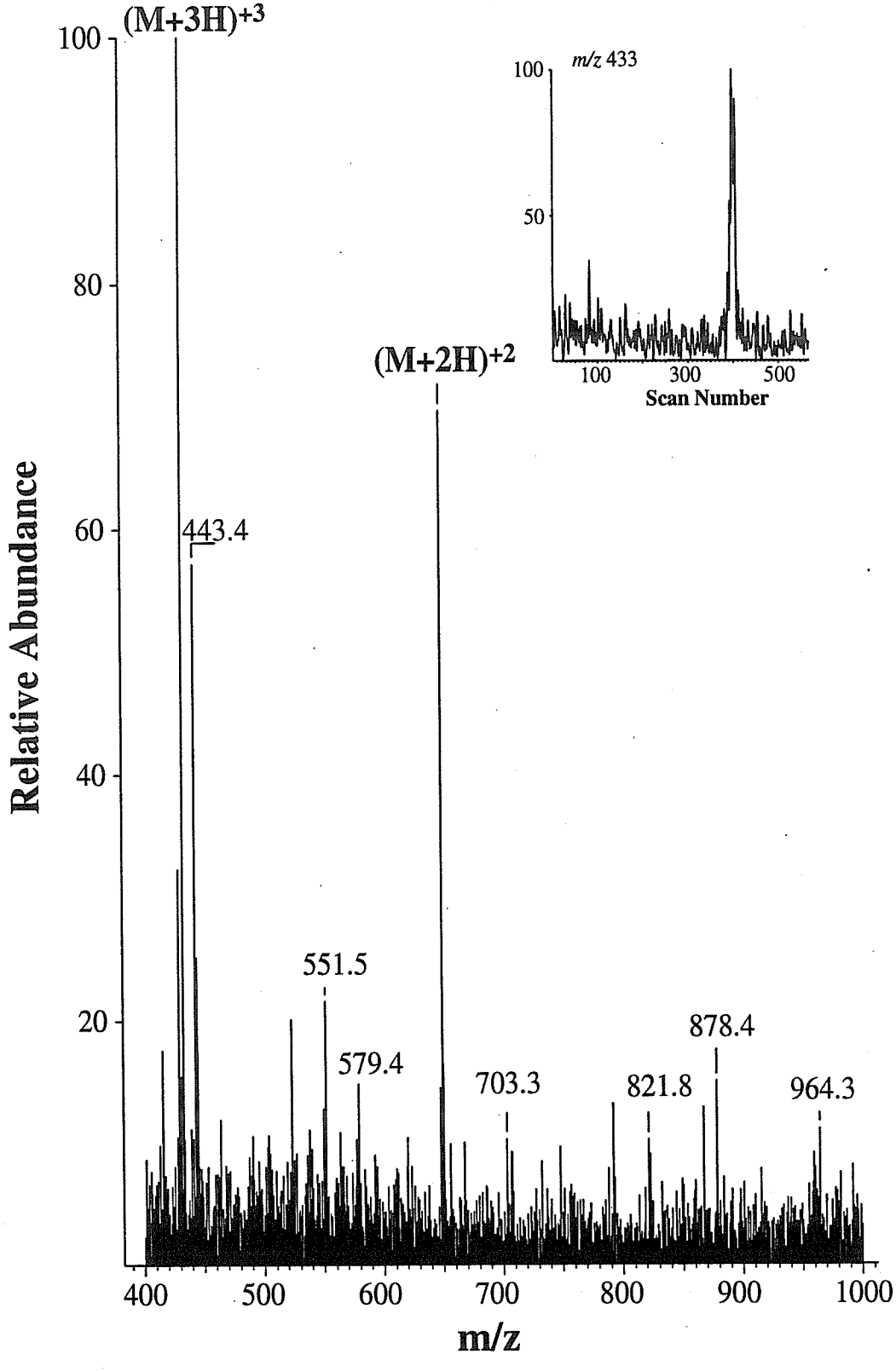
(M+3H)+3
(M+2H)+2
443.4
551.5
579.4
703.3
821.8
878.4
964.3
Relative Abundance
m/z
100
80
60
40
20
400
500
600
700
800
900
1000
m/z 433
100
50
100
300
500
Scan Number

performed without solvent filtering, eliminating this effect. The width of the elution peak is ~2 times greater than is typically observed for CE of peptides. Subsequent use of a commercially available column provided smaller elution bands and stronger signal for the same experiment. A mixture of peptides generated by trypsin digestion of α-casein were only partially separated using this method (data not shown). Separation of the mixture has not been attempted on a commercial column; however, optimization should improve the preliminary results.

5.4.3.3 Separation By Membrane Chromatography

One limitation of CE is that relatively concentrated samples are required. Biological samples are typically quite dilute; therefore, hydrophobic pre-concentration membranes have been used extensively by Naylor *et al.* to concentrate samples prior to injection onto CE columns (17, 18). A second limitation of CE is that the technique is most successful in separating relatively simple mixtures of peptides. Biological samples are typically composed of complex mixtures of molecules; thus it would be useful to develop a concentrating and simplifying procedure to prepare samples for subsequent analysis by CE.

5.4.3.3.1 Sensitivity

Peptides typically bind to hydrophobic surfaces. They can be released from these surfaces by passing an organic solvent over the surface. The solvent and peptides compete for binding and the less hydrophobic peptides are released. Differential release is obtained

by changing the relative amount of organic in the solvent. Most research using pre-concentration membranes has involved elution of all peptides from the membrane with an elution buffer containing 80% methanol and 20% water with acetic acid (17, 18). We investigated the sensitivity of eluting peptides from the membrane interfaced to the Teflon junction with a pulled capillary needle by binding a series of dilutions of angiotensin I to the membrane and eluting using an 80% methanol elution buffer at a flowrate of 200 nL/min. The limit of detection was determined to be 10 fmol of sample loaded onto the membrane from a 1 fmol/μL solution. The corresponding mass spectrum is exhibited in Figure 5.9. The signal-to-noise ratio of the triply-charged ion was calculated to be 6:1 and the elution peak width was ~ 1 min. One minute peak widths correspond to passing one column volume of elution buffer through the membrane. Sample loadings of 100 fmol and 500 fmol of a 100 fmol/μL solution provided signal-to-noise ratios of ~20:1 (data not shown). Graphical representation of the results is shown in Figure 5.10. The best fit to the data was provided by a logarithmic function. In general, S/N ratios decrease in a linear fashion; thus we assume that there are sample losses at low sample concentration causing the apparent logarithmic relationship. The hydrophobicity of angiotensin I can enhance losses to sample tube walls, syringes, and transfer lines; thus a more hydrophilic peptide might provide more sensitive performance.

The calculated limit of detection based upon the logarithmic fit to the data was 1.3 fmol. Signal was observed at the single fmol level from loading 1 μL of a 1 fmol/μL solution; however, there were many background ions of equal intensity. Low abundance signal was also observed for 500 amol loaded onto the membrane from 0.5 μL of a 1 fmol/μL solution. These preliminary results suggest that the hydrophobic membranes

Figure 5.9: Mass spectrum of 10 fmol of angiotensin I obtained from a 10 μL of a 1 fmol/μL solution loaded onto the membrane and eluted using 80:20:0.5 methanol:water:acetic acid (v/v/v). The LCQ ion trap was scanned from 400 u to 1850 u and 20 scans were summed to provide the mass spectrum.

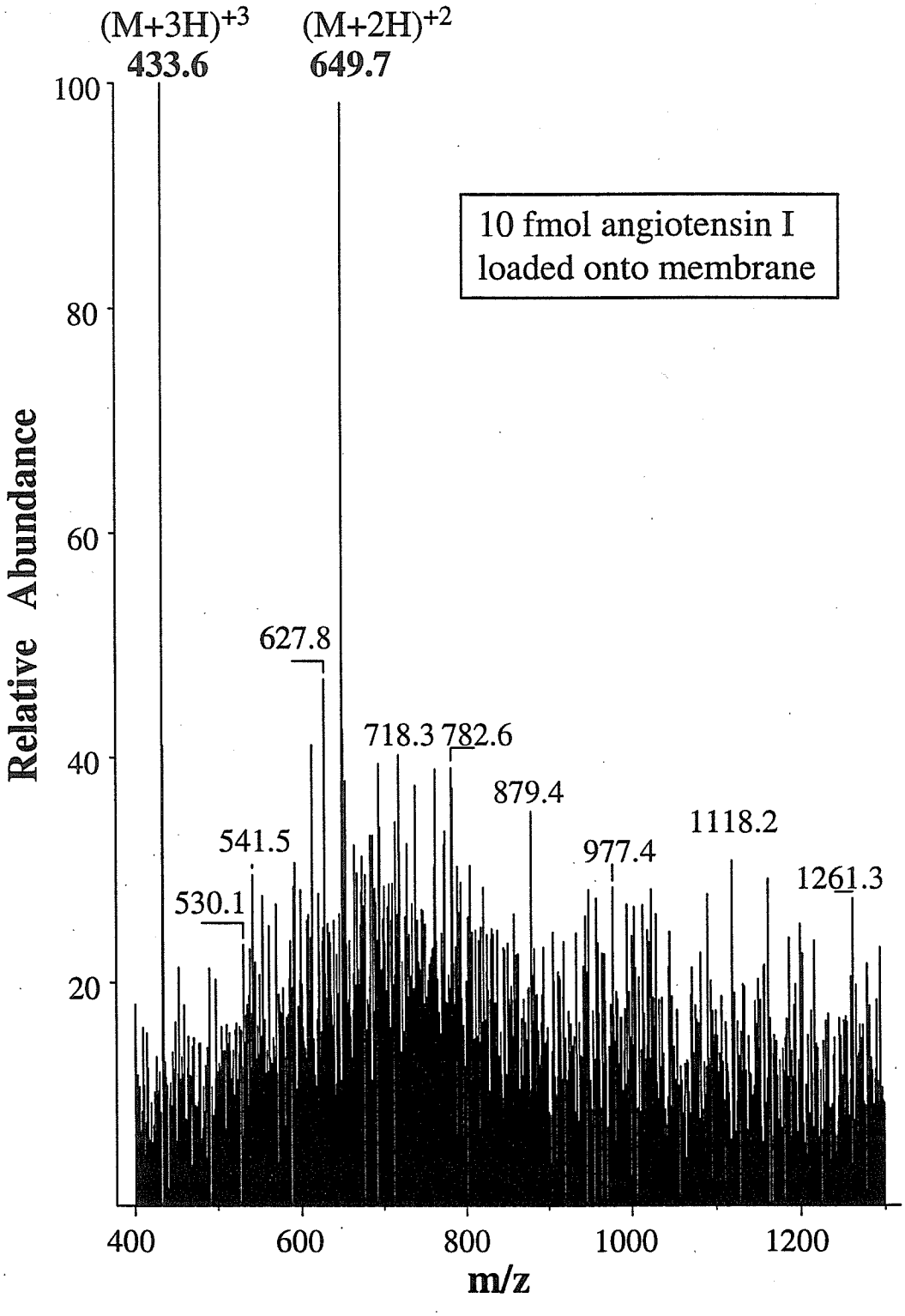
(M+3H)+3
433.6
(M+2H)+2
649.7
10 fmol angiotensin I
loaded onto membrane
Relative Abundance
100
80
60
40
20
627.8
718.3
782.6
879.4
541.5
530.1
977.4
1118.2
1261.3
400
600
800
1000
1200
m/z

Figure 5.10: Calculated signal-to-noise ratio vs. amount of sample loaded onto a hydrophobic membrane. The relationship appears to be logarithmic, suggesting the possibility of sample losses at low sample concentrations.

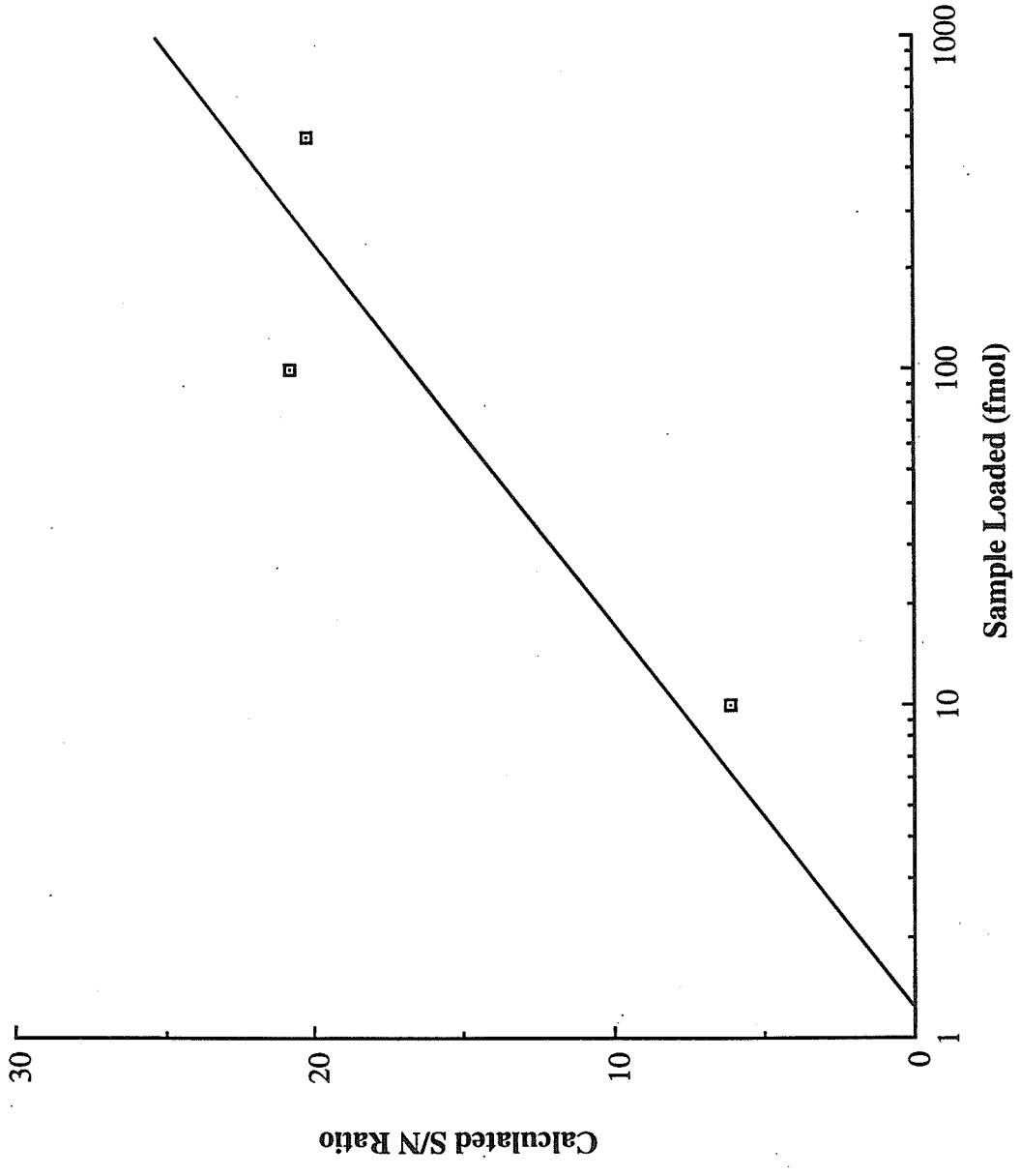
Calculated S/N Ratio
30
20
10
0
1
10
100
1000
Sample Loaded (fmol)

provide a sensitive concentrating device that interfaces well with the Teflon junction system and that further optimization of sample handling should further decrease the limit of detection.

Air bubbles have often been observed forming on the syringe side of the membrane cartridge. The bubbles disrupt the microspray, and pressure must be put on the syringe pump to re-establish the spray. Spray is easily re-established using the pulled capillary needles, but it is much more difficult to re-establish microspray using the micropipette needles. More work must be done to determine how air bubbles can be eliminated before testing the performance of the system using the micropipette needles.

5.4.3.3.2 Mixture Simplification

Peptides obtained from a tryptic digest of α-casein were separated by CE (data not shown). The performance of the column was poor and ion signals from different peptides were not well resolved because the -25 kV applied to the column removed aminopropyltrimethoxysilane from the column walls, preventing efficient separation of the peptides. Additionally, CE is typically most effective at separating peptides in relatively simple mixtures and the column length was too short to effectively resolve the complex mixture investigated. The use of hydrophobic membranes to simplify peptide mixtures prior to CE analysis was investigated. A 0.5 μL aliquant of a 1 pmol/μL solution of the digest was loaded onto the membrane as described above. Peptides were eluted isocratically at 30%, 50%, and 70% methanol in 0.5% acetic acid. Figure 5.11 illustrates the peptides identified. The sample of α-casein obtained from Sigma is contaminated with

Figure 5.11: Amino acid sequences and observed peptides for α–casein. Tryptic peptides identified are denoted by "T." A "P" in the subscript indicates the peptide was phosphorylated. Peptides labeled with a "C" arise from cleavage due to chymotryptic activity. Peptides from both types of casein were identified. High resolution scans were performed to determine charge states and aid in identification of observed ions.

Casein Type 1, MW 24529 u, 214 a.a.

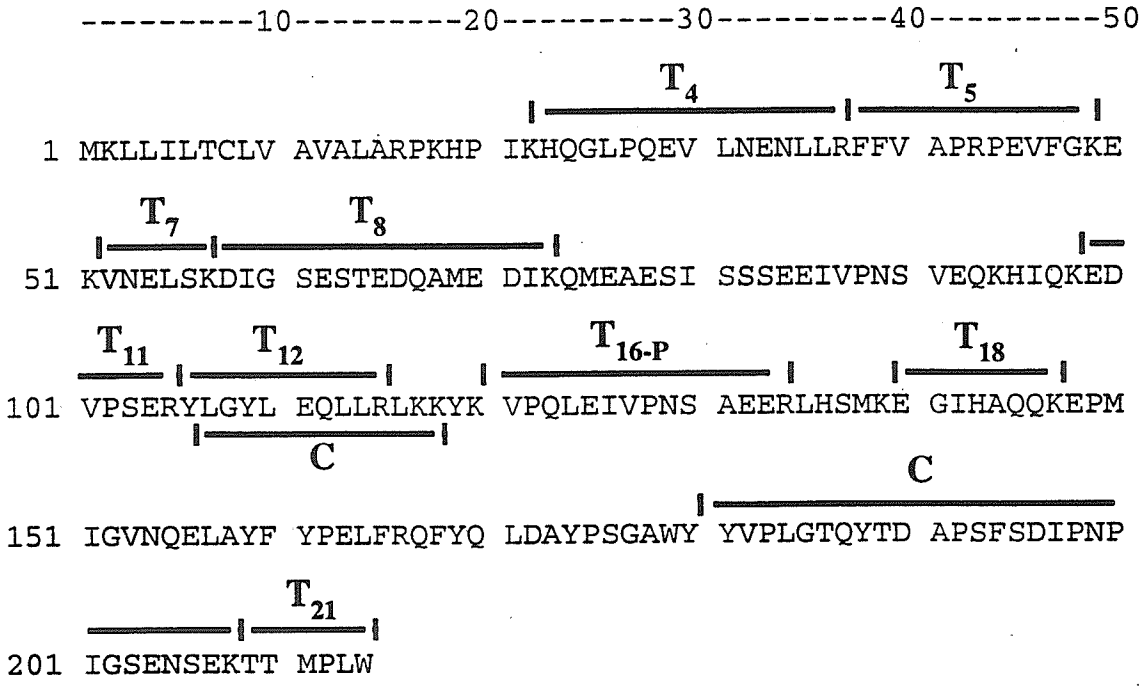

Casein Type 2, MW 26019 u, 222 a.a.

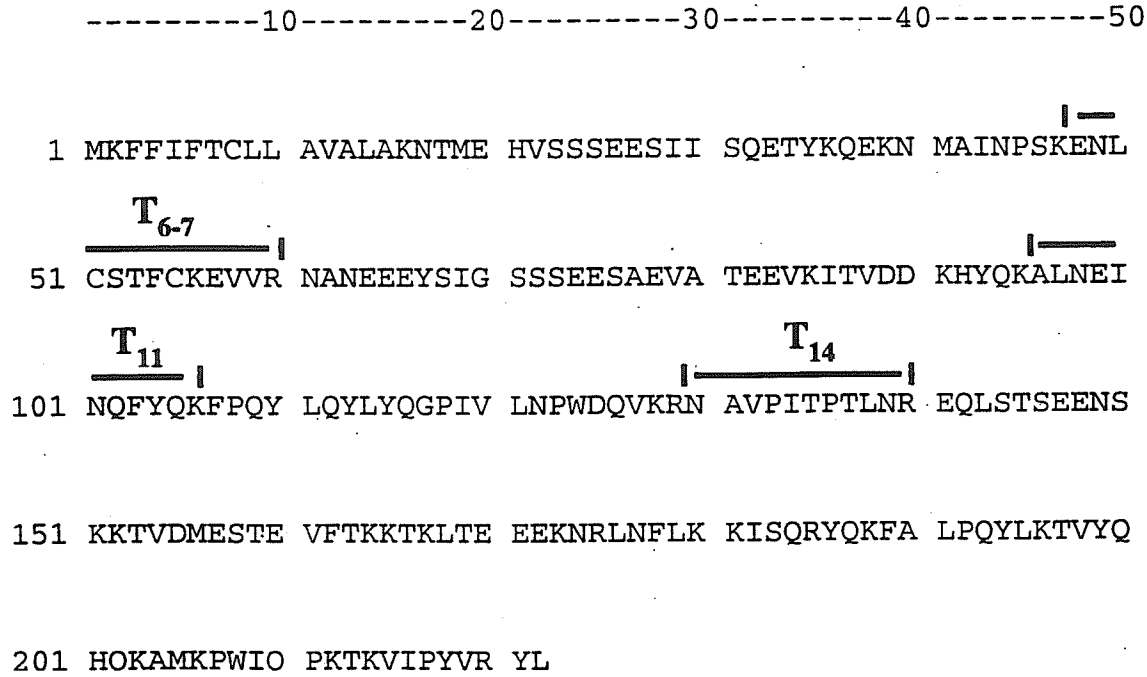

another type of casein, designated here as type 2. Approximately 58% of the amino acids from casein type 1 were identified and 16% of the amino acids from casein type 2 were identified. One phosphopeptide at *m/z* 831 was observed. Casein is known to contain five sites of phosphorylation which have been observed on a triple quadrupole mass spectrometer. We have not yet determined why only one phosphopeptide was observed using the two different ion traps.

Crude separation of peptides at different concentrations of methanol was observed and the data is summarized in Table 5.2. Only two ions, *m/z* 588 and *m/z* 693, appeared in more than one elution. Ions also tended to elute differentially during the course of each elution. An example of the phenomenon is displayed in Table 5.3 where the relative abundances of dominant ions change over elution time. Scans occurring during 30 sec intervals were summed, providing the relative abundances of the ions. Step elution coupled to CE where elution times are ~1-2 min could also provide another dimension of separation. Several CE analyses could be performed during the course of an elution.

5.5 Conclusion

A microspray ionization source has been developed for the high sensitivity analysis of peptides. A novel needle configuration composed of a fused silica transfer line epoxied into a pulled glass micropipette needle tip was tested and provided high sensitivity under infusion conditions. A unique Teflon/platinum liquid junction was designed for ease of

Table 5.2: Dominant ions observed at 30%, 50%, and 70% methanol during step elutions of a casein digest peptide mixture from a hydrophobic membrane.

Percent Methanol	**Observed *m/z***
30	491, 588, 599, 685, 690, 765, 881, 912
50	588, 634, 693, 831, 886, 1010, 1023, 1064, 1267
70	693, 980

Table 5.3: Percent relative abundance of selected ions when eluting a casein digest peptide mixture isocratically from a hydrophobic membrane with 1:1:0.5 methanol:water:acetic acid.

RT Int.*	*m/z* 634	*m/z* 693	*m/z* 748	*m/z* 831	*m/z* 881	*m/z* 980	*m/z* 1267	*m/z* 1384
1	20.3	0	15.72	32.73	100	0	14.49	0
2	66.84	13.72	40.14	34.66	100	0	41.24	0
3	84.81	24.88	71.46	28.1	100	22.06	64.44	0
4	100	53.66	88.72	26.8	46.12	35.26	97.2	26.35
5	100	85.34	53.89	22.31	25.95	47.91	79.16	45.38
6	66.88	100	28.12	24.79	25.07	81.92	63.26	71.69
7	31.84	100	0	15.46	0	55.22	25.92	56.67
8	24.41	100	0	16.6	16.4	62.9	21.37	70.19
9	23.29	100	0	15.87	13.42	49.4	18.97	38.83
10	18.67	100	0	15.88	12.66	64.41	20.4	98.78
11	13.07	73.63	7.36	9.91	11.68	45.39	17.3	100
12	5.5	55.31	0	5.71	5.17	34.67	12.64	100
13	6.0	53.52	0	0	5.81	33.85	11.62	100
14	11.61	68.12	0	7.94	9.6	43.48	14.93	100
15	9.86	100	0	10.05	0	55.13	8.04	78.66
16	0	100	0	0	0	65.65	9.56	90.4

* - RT Int. refers to a 30 second retention time interval beginning at a retention time of 2.5 min. All scans during this interval were summed, providing the relative abundances shown above.

use and to eliminate background derived from interactions of sample with metal and epoxy. The junction gave comparable performance to more traditional liquid junctions and was significantly easier to use. The dead volume in the junction did not significantly impair CE performance as determined by elution peak widths. LC performance using the junction has not yet been investigated.

Neutral loss scanning on a triple quadrupole mass spectrometer is a common means of identifying given components of a mixture; however, this useful technique cannot be implemented easily on a quadrupole ion trap. A neutral loss scan was developed and successfully applied on a hybrid quadrupole mass filter/quadrupole ion trap mass spectrometer to identify phosphopeptides in a mixture.

Hydrophobic membranes have shown great promise as pre-concentration devices fo CE applications. Sensitivity at the 10 fmol level was demonstrated using step elution at low flowrates. The membranes can be used as chromatographic devices in addition to pre-concentration devices. Crude separation of peptide mixtures was accomplished by step eluting peptides at different concentrations of organic. In addition, differential release of peptides during the course of an elution can provide the opportunity of further mixture refinement by performing multiple CE analyses during one elution. Other types of membranes will be investigated to add other chromatographic dimensions.

5.6 References

1. Gelpi, E. (1995) *J. Chromatogr. A* **703** 59-80.

2. Meng, C. K., Mann, M., and Fenn, J. B. (1988) *Z. Phys. D. - Atoms, Mol. Clusters* **10** 361-368.

3. Fenn, J. B., Mann, M., Meng, C. K., Wong, S. F., and Whitehouse, C. M. (1989) *Science* **246** 64-71.

4. Fenn, J. B., Mann, M., Meng, C. K., and Wong, S. F. (1990) *Mass Spec. Rev.* **9** 37-70.

5. Fenn, J. B. (1993) *J. Am. Soc. Mass Spectrom.* **4** 524-535.

6. Emmett, M. R., and Caprioli, R. M. (1994) *J. Am. Soc. Mass Spectrom.* **5** 605-613.

7. Andren, P. E., Emmett, M. R., and Caprioli, R. M. (1994) *J. Am. Soc. Mass Spectrom.* **5** 867-869.

8. Valaskovic, G. A., Kelleher, N. L., Little, D. P., Aaserud, D. J., and McLafferty, F. W. (1995) *Anal. Chem.* **67** 3802-3805.

9. Figeys, D., van Oosteveen, I., Ducret, A., and Aebersold, R. (1996) *Anal. Chem.* **68** 1822-1828.

10. Gale, D. C., and Smith, R. D. (1993) *Rapid Commun. Mass Spectrom.* **7** 1017-1021.

11. Davis, M. T., Stahl, D. C., Hefta, S. A., and Lee, T. D. (1995) *Anal. Chem.* **67** 4549-4556.

12. Olivares, J. A., Nguyen, N. T., Yonker, C. R., and Smith, R. D. (1987) *Anal. Chem.* **59** 1230-1232.

13. Lee, E. D., Mueck, W., Henion, J. D., and Covey, T. R. (1988) *J. Chromatogr.* **458** 313-321.

14. Smith, R. D., Olivares, J. A., Nguyen, N. T., and Udseth, H. R. (1989) *Anal. Chem.* **60** 436-441.

15. Johannson, I. M., Huang, F. C., Henion, J. D., and Zweigenbaum, J. (1991) *J. Chromatogr.* **554** 311-327.

16. Smith, R. D., Wahl, J. A., and Goodlett, D. R. (1993) *Anal. Chem.* **65** 574A-584A.

17. Tomlinson, A. J., and Naylor, S. (1995) *J. Cap. Elec.* **5** 225-233.

18. Tomlinson, A. J., and Naylor, S. (1995) *J. High Resol. Chromatogr.* **18** 384-386.

19. Wilm, M., and Mann, M. (1996) *Anal. Chem.* **68** 1-8.

20. Severs, J. C., Harms, A. C., and Smith, R. D. (1996) *Rapid Commun. Mass Spectrom.* **10** 1175-1178.

21. Foret, F., Thompson, T. J., Vouros, P., Karger, B. L., Gebauer, P., and Bocek, P. (1994) *Anal. Chem.* **66** 4450-4458.

22. Chowdhury, S. K., Katta, V., and Chait, B. T. (1990) *Rapid Commun. Mass Spectrom.* **4** 81-87.

23. Bruin, G. J. M., Huisden, R., Kraak, J. C., and Poppe, H. (1989) *J. Chromatogr.* **480** 339-349.

24. Thorsteinsdottir, M., Isaksson, R., and Westerlund, D. (1995) *Electrophoresis* **16** 557-563.

25. Wilm, M. S., and Mann, M. (1994) *Int. J. Mass Spectrom. Ion Proc.* **136** 167-180.

26. Fetterolf, D. D., and Yost, R. A. (1983) *Mass Spectrom. Rev.* **2** 1-45.

27. Johnson, J. V., Pedder, R. E., and Yost, R. A. (1991) *Int. J. Mass Spectrom. Ion Proc.* **106** 197-212.

Chapter 6

Summary

Presented in this dissertation are a number of approaches investigated for the analysis of molecules of biological origin using a quadrupole ion trap mass spectrometer. Of particular interest was the development of a sensitive methodology with which to analyze peptide mixtures. An "off-line" technique utilizing an HPLC to separate peptide mixtures resulting from enzymatic digests followed by MALDI-ITMS analysis was successfully applied to locate sites of post-translational modification in the P protein from Sendai virus. A hybrid quadrupole mass filter/quadrupole ion trap mass spectrometer was constructed to investigate mixtures by transmitting one value of *m/z* at a time for analysis in an ion trap. Finally, an "on-line" microspray ionization source coupled to a hydrophobic membrane and a capillary electrophoresis interface was applied to explore the utility of peptide mixture separation by high sensitivity multi-dimensional chromatography. A description of these approaches and the results have been discussed in the preceeding chapters. Below is presented future directions for these projects.

6.1 Matrix-Assisted Laser Desorption Ion Trap Mass Spectrometry

A number of innovations have been implemented in MALDI/ion traps since the publication in 1993 of the work described in Chapter Three (1). Sensitivity in the low

femtomole range has been reported for small peptides using an external injection MALDI/FTMS instrument (2) with mass resolutions in excess of 10^6 (3, 4). FTMS has also been employed to detect singly-charged biomolecules with molecular weights up to 157,000 u (5). Emphasis in MALDI/quadrupole ion traps has been placed on improving trapping efficiency, fragmentation efficiency, and ejection efficiency for MALDI-generated peptide ions (6-8). An improved external injection instrument has been utilized to analyze peptide mixtures at high femtomole levels and may serve as the prototype for a commercial instrument in the future (9).

6.2 Hybrid Quadrupole Mass Filter/Quadrupole Ion Trap Mass Spectrometer

The hybrid instrument was shown to provide improved performance both in the quality of the mass spectra and in resolution and fragmentation efficiency. Slow scan times due to the data porting time limited the utility of the approach for continuous ionization techniques. The limitation could be ameliorated by utilizing only the TSQ electronics to analyze and display the signal from the electron multiplier, thus eliminating the need to transfer the data from the ion trap's data system and reducing the bin scan time of the quadrupole mass filter. Similar results could be obtained using tailored waveforms to selectively inject sequential values of *m/z* into an ion trap. The new LCQ ion trap from Finnigan MAT may be employed to investigate the approach.

6.3 Mixture Separation by Low Flowrate Electrospray Ionization

Preliminary data was presented in Chapter Five from a microspray ionization source with unique needle and liquid junction configurations. The source was separately interfaced to capillary electrophoresis and membrane chromatography columns. The low femtomole sensitivity obtained is sufficient for many biological applications and optimization of conditions should further decrease the limit of detection of the technique. Future experiments will entail coupling the hydrophobic membrane cartridge to the CE column to perform two-dimensional chromatography. In addition, ion exchange membranes will be used to obtain a further degree of mixture separation. The combination of pre-concentration of dilute samples, CE, microspray ionization, and quadrupole ion trap mass spectrometry should provide a sensitive, high throughput technique for the simplification and analysis of complex mixtures of peptides generated from the study of biological processes.

6.4 References

1. Jonscher, K. R., Currie, G., McCormack, A. L., and Yates, J. R., III (1993) *Rapid Commun. Mass Spectrom.* **7** 20-26.

2. Li, Y., and McIver, R. T., Jr. (1994) *Rapid Commun. Mass Spectrom.* **8** 743-749.

3. Li, Y., McIver, R. T., Jr., and Hunter, R. L. (1994) *Anal. Chem.* **66** 2077-2083.

4. McIver, R. T., Jr., Li, Y., and Hunter, R. T. (1994) *Proc. Natl. Acad. Sci. USA* **91** 4801-4805.

5. Solouki, T., Gillig, K. J., and Russell, D. H. (1994) *Anal. Chem.* **66** 1583-1587.

6. Doroshenko, V. M., and Cotter, R. J. (1993) *Rapid Commun. Mass Spectrom.* **7** 822-827.

7. Doroshenko, V. M., and Cotter, R. J. (1995) *Anal. Chem.* **67** 2180-2187.

8. Doroshenko, V. M., and Cotter, R. J. (1996) *Rapid Commun. Mass Spectrom.* **10** 65-73.

9. Qin, J., Steenvoorden, R. J. J. M., and Chait, B. T. (1996) *Anal. Chem.* **68,** 10, 1784-1791.

Vita

Karen R. Jonscher was born on March 19, 1959, in Denver, Colorado, to Max and Bobbi Furer. She received her bachelor of science degree in Engineering Physics from the University of Colorado in June, 1989, and graduated with Special Honors. In 1987 she worked as a summer intern at Argonne National Laboratory where she met Peter L. Jonscher. They were married in 1991. Other summer internships were at Martin Marietta Denver Aerospace Mission Operations (1988) and with Drs. Donald Burnett and Thomas Tombrello at the California Institute of Technology (1989). In 1990 Karen joined the research group of Dr. Leroy E. Hood at the California Institute of Technology and worked in the mass spectrometry laboratory under Dr. John R. Yates III. She received a master of science degree in Applied Physics from the California Institute of Technology in June, 1991. Spencer Lucas was born in April of 1992 and shortly thereafter Karen moved to Seattle, Washington, to continue her research with Dr. Hood. In June of 1994 Raleigh Lyle was born. Karen has accepted a post-doctoral position with Dr. Robert C. Murphy at the National Jewish Center for Immunology and Respiratory Medicine in Denver, Colorado, and is expecting the birth of her third child in November of 1996.